Development of a microfluidic protocol for the measurement of basophil activation

By Chloe Rose

UNIVERSITY OF SOUTHAMPTON

ABSTRACT

FACULTY OF ENGINEERING & THE ENVIRONMENT

Bioengineering

A Thesis for the degree of Doctor of Philosophy

Development of a microfluidic protocol for the measurement of basophil activation

Chloe Grace Rose

The prevalence of allergy is increasing worldwide, creating substantial demands on health services in establishing diagnoses and managing patients with allergic sensitivity. The basophil activation test represents a valuable tool for investigation of allergic sensitivity and even for prediction of symptom severity, though practical considerations and the high capital, training and running costs associated with flow cytometry have limited its clinical uptake. In seeking to develop a more rapid and cost effective technology for the diagnosis of allergic disease, we have investigated microfluidic approaches for the efficient enrichment of basophil populations while retaining their functional characteristics to enable basophil activation on a chip.

Acoustofluidic based basophil separation was developed by taking advantage of both the active-force movement of cells and specific surface binding of basophils to anti-CD203c under microfluidic conditions. At flow rates of 30 ml/h, up to 94 % of basophils from whole blood adhered within the acoustofluidic device, as determined by measurements of cell-associated histamine, CD63 expression by flow cytometry and basophil counts based on flow cytometric analysis and confocal microscopy imaging studies. Erythrocyte depletion agents saponin, ammonium chloride and distilled water were evaluated based on their noted affect on basophil viability. The measurement of net histamine release achieved 100% net histamine release upon allergen response and thus was applied to deplete whole blood samples prior to entry into the device. The acoustofluidic platform developed represents a novel way to isolate basophils significantly faster and more efficiently than established methods such as density gradient filtration and negative immunomagnetic separation.

Assays for basophil activation in response to house dust and grass pollen allergens, and to stimuli including anti-IgE antibody and formyl-methionyl-leucyl-phenylalanine (FMLP) peptide, were performed that involved measurement of the release of the granule components histamine (using an enzyme immunoassay) and basogranulin (by dot blotting with monoclonal antibody BB1), or measurement of upregulation of the cell surface marker CD63 (by fluorescence-activated cell sorting: FACS). Concentration response curves for IgE-dependent activation of basophils determined by each of these methods generally followed a bell-shaped curve, though there was considerable inter-subject variation. When the area under the curve was compared between experimental methods, it was found that CD63 expression was strongly correlated with histamine release ($p = <0.0001$, $r = 0.9143$, $n=5$) and basogranulin ($p = 0.0048$, $r = 0.6794$, $n=6$), and fluorescent detection of CD63 was employed as a means for investigating activation status of basophils bound within the device. Promising data has been obtained from the initial imaging studies performed to identify basophils bound within the device. Analysis performed confirmed approximately 23,450 basophils were adhered when using dip pen nanolithography slides and 11,380 using in-house printed slides when compared to controls (445 basophils in the absence of antibody and 56 when no ultrasound was present).

The findings have created a platform for a basophil activation protocol through the implementation of an acoustofluidic device, that could later be further developed as a diagnostic aid to determine allergic sensitivity in clinic.

Conferences & papers

Journal Paper

Rose, Chloe G; Plazonic, Filip; Morgan, Hywel; Eren, Efrem; Zhang, Xunli; *et al*. Journal of Allergy and Clinical Immunology, suppl. S; St. Louis139.2 (Feb 01, 2017): AB125

Klein, O., Ngo-Nyekel, F., Stefanache, T., Torres, R., Salomonsson, M., Hallgren, J., Radinger, M., Bambouskova, M., Campbell, M., Cohen-Mor, S., Dema, B., **Rose, C.G.**, Abrink, M., Charles, N., Ainooson, G., Paivandy, A., Pavlova, V.G., Serrano-Candelas, E., Yu, Y., Hellman, L., Jensen, B.M., Van Anrooij, B., Grootens, J., Gura, H.K., Stylianou, M., Tobio, A., Blank, U., Ohrvik, H. and Maurer, M. (2016) Identification of Biological and Pharmaceutical Mast Cell- and Basophil-Related Targets. *Scandinavian Journal of Immunology*, **83** (6), 465-472.

(A Letter to the Editor resulting from discussion during COST Training School on mast cells and basophils in Uppsala, Sweden, February 2015, for which I had been awarded a scholarship to participate, sponsored by European Mast Cell and Basophil Network (EMBRN).

Presentations

Oral Presentations:

- Rose, C G; Plazonic, F; Morgan, H; Eren, E; Zhang, X L; Carugo, D; Glynne-Jones, P J; Lau, L C K; Hill, M and Walls, A F (2017) Basophil enrichment: how does a microfluidic platform compare to current experimental procedures, *Faculty of Medicine Conference, University of Southampton*
- Rose, C G; Plazonic, F; Morgan, H; Eren, E; Zhang, X L; Carugo, D; Glynne-Jones, P J; Lau, L C K; Hill, M and Walls, A F (2017) Basophil enrichment: how does a microfluidic platform compare to current experimental procedures, *8th EMBRN International Mast Cell & Basophil Meeting, Institute of Molecular Genetics, CAS, Prague, Czech Republic*
- Rose, C G; Morgan, H; Eren, E; Zhang, X L; Lau, L C K and Walls, A F (2016) Rapid diagnosis of allergy to drugs using a microfluidic platform. *University of Aarhus, Denmark*
- Rose, C G; Morgan, H; Eren, E; Zhang, X L; Lau, L C K and Walls, A F (2015) Rapid diagnosis of allergy to drugs using a microfluidic platform. *Faculty of Engineering & the Environment Postgraduate Conference, Southampton*

- Rose, C G; Morgan, H; Eren, E; Zhang, X L; Lau, L C K and Walls, A F (2015) Rapid diagnosis of allergy to drugs using a microfluidic platform. *COST Training School on mast cells and basophils, Uppsala, Sweden*
- Rose, C G; Morgan, H; Eren, E; Zhang, X L; Lau, L C K and Walls, A F (2014) Rapid diagnosis of allergy to drugs using a microfluidic platform. *Microfluidics Away Day, Southampton*

Poster Presentations:

- Rose, C G; Plazonic, F; Morgan, H; Eren, E; Zhang, X L; Carugo, D; Glynne-Jones, P J; Lau, L C K; Hill, M and Walls, A F (2017) Basophil enrichment: How does a microfluidic platform compare to current experimental procedures. *8th EMBRN International Mast Cell & Basophil Meeting, Institute of Molecular Genetics, CAS, Prague, Czech Republic*
- Rose, C G; Plazonic, F; Morgan, H; Eren, E; Zhang, X L; Carugo, D; Glynne-Jones, P J; Lau, L C K; Hill, M and Walls, A F (2017) Development of an acoustofluidic platform for rapid basophil enrichment. *8th European Mast Cell & Basophil Network (EMBRN) Conference, Prague*
- Rose, C G; Morgan, H; Eren, E; Zhang, X L; Lau, L C K and Walls, A F (2016) Can experimental techniques for peripheral blood mononuclear cells affect basophil function? *Faculty of Engineering & the Environment Postgraduate Conference, University of Southampton*
- Rose, C G; Morgan, H; Eren, E; Zhang, X L; Lau, L C K and Walls, A F (2016) Can experimental techniques for peripheral blood mononuclear cell separation effect basophil function? *Faculty of Medicine Conference, University of Southampton*
- Rose, C G; Morgan, H; Eren, E; Zhang, X L; Lau, L C K and Walls, A F (2016) Rapid diagnosis of allergy to drugs using a microfluidic platform. *Bioengineering Seminar, University of Southampton*
- Rose, C G; Morgan, H; Eren, E; Zhang, X L; Lau, L C K and Walls, A F (2015) Can experimental techniques for peripheral blood mononuclear cells affect basophil function? *Institute of Life Sciences poster session in microfluidics, University of Southampton*
- Rose, C G; Morgan, H; Eren, E; Zhang, X L; Lau, L C K and Walls, A F (2015) Separation of peripheral blood mononuclear cells and basophil function. *7th European Mast Cell & Basophil Network Conference, Marseille*

Table of Contents

List of Tables

List of Figures

DECLARATION OF AUTHORSHIP

I, CHLOE GRACE ROSE

declare that this thesis and the work presented in it are my own and have been generated by me as the result of my own original research.

Rapid diagnosis of allergy to drugs using a microfluidic platform

I confirm that:

1. This work was done wholly or mainly while in candidature for a research degree at this University;
2. Where any part of this thesis has previously been submitted for a degree or any other qualification at this University or any other institution, this has been clearly stated;
3. Where I have consulted the published work of others, this is always clearly attributed;
4. Where I have quoted from the work of others, the source is always given. With the exception of such quotations, this thesis is entirely my own work;
5. I have acknowledged all main sources of help;
6. Where the thesis is based on work done by myself jointly with others, I have made clear exactly what was done by others and what I have contributed myself;
7. None of this work has been published before submission [or] Parts of this work have been published as: [please list references below]:

Signed: .....

Date:.....

Acknowledgements

Many thanks to Dr Laurie Lau for teaching me all of the lab techniques I have needed throughout my PhD. I would also like to thank Dr Yuchao Zhao for all of his help working on the microfluidic spiral sorter working long hours to optimise the chip and get to the stage where we could evaluate its abilities in separating blood.

Secondly, I would like to thank my collaborator Filip Plazonic for all of his time spent with me optimising the device and his supervisors, Professor Martyn Hill, Dr Peter Glynne-Jones and Dr Dario Carugo for all of their help and support in the acoustofluidic field and allowing me to further develop their technology for my research goal. In addition, thank you to Sylwia and the Karlsruhe Institute of Technology (KIT) for the grant to print the slides to enable better scientific results.

Thank you to my wonderful husband John for overcoming his needle phobia to aid my experiments and keeping me company in the lab late at night. Thank you to my fantastic friends and family for listening to my ramblings and allowing me to practice venesection on them (as well as donate blood) and I'm so happy that none of you became anaemic during my PhD (just me)! A massive thank you to my family who have supported me entirely throughout this process and proof read my thesis numerous times.

Lastly, would like to thank my supervisors' Dr Xunli Zhang, Dr Andrew Walls, Dr Efrem Eren & Professor Hywel Morgan for their feedback.

“K. B. O.”

Winston Churchill

Definitions and Abbreviations

α-IgE	Anti-Immunoglobulin E
AU	Arbitrary unit
BAL	Bronchoalveolar lavage
β_f	Fluid compressibility
β_p	Particle compressibility
BSA	Bovine serum albumin
Ca^{2+}	Calcium ions
CAST	Cellular allergen stimulation test
CCD	Charge coupled device
CD	Cluster of differentiation
C_L	Lift coefficient of the channel relative to the Reynolds number
CRTH2	Chemoattractant receptor-homologous molecule expressed on Th2 cells
DAG	Diacylglycerol
D_h	Hydraulic diameter
dh_2O	Deionised water
DM	*Dermatophagoides pteronyssinus* (house dust mite)
DPN	Dip pen nanolithography
EDMC	Engineering and Design Manufacturing Centre
EDTA	Ethylene diamine tetra acetic acid
E_{kin}	Averaged kinetic energy density
EIA	Enzyme-linked immunosorbent assay
E-NPP3	Ectonucleotide pyrophosphatase/ phosphodiesterase 3
E_{pot}	Potential energy density
F	Radiation force
FACS	Fluorescence activated cell sorting
FBS	Foetal bovine serum
FcεRI	High affinity Immunoglobulin E receptor
FcϒRI	High affinity Immunoglobulin G receptor
FEIA	Fluorescent enzyme immunoassay
FITC	Fluorescein isothiocyanate

F_L	Net lift force
FMLP	N-Formylmethionine-leucyl-phenylalanine
G	Shear rate of fluid
HRP	Horseradish peroxidase
HW	Half wave resonator
Ig	Immunoglobulin
IH	In-house
IL	Interleukin
kDa	Kilodalton
kHz	Kilohertz
MACS	Magnetic activated cell sorting
MAPK	Mitogen activated kinase
MHC	Major histocompatibility complex
NMBA	Neuromuscular blocking agent
NSAIDS	Non-steroidal anti-inflammatory drug(s)
P	Calculated probability
ρ or p_f	Density of fluid medium
PBMC	Peripheral blood mononuclear cells
PBS	Phosphate buffered saline
PBS-T	Phosphate buffered saline with Tween 20
PDMA	Poly(N, N-dimethylacrylamide)
PDMS	Polydimethylsiloxane
PE	Phycoerythrin
Pg	Picogram
pH	Potential hydrogen
PKC	Protein kinase C
PLC	Phospholipase C
PMD	Piecemeal degranulation
PMMA	Poly (methyl methacrylate)
pN	Piconewtons
p_p	Particle density
PTFE	Polytetrafluoroethylene
PVDF	Polyvinylidene fluoride
PZT	Piezoelectric transducer

R	Coefficient of determination
r	Particle location
r_s	Spearman's coefficient of rank correlation
RBC	Red blood cell (erythrocyte)
RCF	Relative centrifugal force
SCL	Steel carrier layer
SQ-U	Standardised quality units
T_H	T-helper cells
TNF-α	Tumour necrosis factor-α
TR	Thin reflector device
U	Aquagen standardised quality units
U_{max}	Maximum fluid velocity
$\mathcal{V}$	Spherical particle volume
Vpp	Voltage peak to peak

Chapter 1: Introduction

1.1 Background

Tests to measure the activation of basophils, key cells implicated in allergic reactions, are proving useful in the assessment of suspected sensitisation to allergens. Recent studies indicate that such tests cannot only aid in identification of allergic sensitisation, but may also have predictive value in assessing the extent of susceptibility to severe reactions. Thus, for example, basophil activation tests may help to predict the sensitivity of a reaction that may be provoked and allow assessment of the effectiveness of immunotherapy. However, their use has been restricted by the high associated costs and the impracticality of the technology currently available. The advent of microfluidic approaches has opened the way for rapid tests with cells to be conducted with small volumes. The focus of the present studies has been to investigate various methods for performing basophil activation tests and to adapt them to a microfluidic format that could form the basis of an effective diagnostic procedure without the limitations of the methods currently available.

1.2 Basophils and mast cells

Basophils are the least abundant of the white blood cells; with numbers in the circulation much lower than those of lymphocytes, monocytes and neutrophils. Basophils are characterised by their multi-lobed nucleus and granules that may be demonstrated histologically with basic dyes. They were discovered by Paul Ehrlich at the end of the nineteenth century (Erhlich, 1878), and are now known to originate from CD34 positive cells and mature in the bone marrow. In healthy subjects there may be just 45 basophils per μl of blood, and some 200 million in circulation (Grattan, 2001). As a minor constituent of blood, their isolation from whole blood samples can be extremely challenging.

Basophils are likely to be the most important source of histamine in the peripheral blood (Jacobi *et al.*, 2000). Mast cells are inflammatory cells based in the connective tissue, and like basophils, they originate from bone marrow $CD34^+$ cells; though they differentiate in different locations within the human body (Prussin and Metcalfe, 2006). Basophil maturation is triggered by IL-3 and IL-4; whereas mast cell differentiation is activated by stem cell factor. Basophils and mast cells are often considered to be related cell types as they both contain and release histamine and other mediators of allergic inflammation. However, they differ in a number of ways as shown in Table 1. For example, they differ in size, granule contents and the number of granules per cell. Basophils and mast cells both release histamine and a range of mediators upon activation (considered separately in section 1.2.2).

Table 1: Characteristics of human basophils and mast cells Adapted from (Stone *et al.*, 2010)

	Basophils	Mast Cells
Location	Blood	Connective tissue
Origin	$CD34^+$ progenitor	$CD34^+$ progenitor
Life span	60 hours (Ohnmacht and Voehringer, 2009)	Months (Stone *et al.*, 2010)
Differentiation factors	IL-3, IL-4	Stem Cell Factor
Maturation site	Bone marrow	Connective tissue
Size	10-14 µm (Arock *et al.*, 2002)	8-20 µm (Schulman *et al.*, 1983)
Nucleus	Multi-lobed	Single, rounded
Cytoplasmic granule	Heterogeneous	Homogeneous
Staining	Basic dyes	Basic dyes
Number of granules	1000 per cell	80 per cell
Size of granules	0.2 µm	1.2 µm
Granule amines	Histamine	Histamine
Granule proteoglycans	Chondroitin sulphate diB (Katz *et al.*, 1985)	Heparin and chondroitin sulphate A
Granule proteases	Tryptases, chymase, carboxypeptidase A3, cathepsin G (present in much lower quantities than in mast cells)	Tryptases, chymase, carboxypeptidase A3, cathepsin G

1.2.1 Identification of basophils and mast cells

Basic dyes have been widely used histologically to identify basophils and mast cells. In the present studies, Kimura stain has been used for routine identification of basophils (Kimura *et al.*, 1973). This stain was first described in 1973 as an adaption of Kovac's solution and consists of a solution of toluidine blue, light green (Merck) solution and phosphate buffer (Kovacs, 1961). Alcian blue, is also frequently used to identify basophils and mast cells (Gilbert and Ornstein, 1975) where alcian blue competes with cations for binding sites with heparin and nucleic acids.

1.2.2 Products of basophil and mast cell activation

A range of mediators are released in IgE-mediated allergic responses; and measurement of their release from basophils *in vitro* provides a way of determining allergic sensitivity. Basophil mediators include proteoglycans, cytokines, lipid mediators, proteases and basic proteins (Figure 1). They may be categorised into those that are pre-formed, newly generated or those that are both pre-formed and newly generated.

1.2.2.1 Preformed Mediators

A well established basophil and mast cell mediator is histamine. Basophils contain 1 – 2 pg/cell of histamine, which is synthesised *via* the decarboxylation of histidine by L-histidine decarboxylase (Sabroe *et al.*, 1998b). In anaphylaxis circulating levels of histamine peak 5 – 10 minutes' post exposure of the allergen, though levels return to baseline shortly after as it is rapidly metabolised. Histamine is metabolised by two major pathways prior to excretion (97%); the first being the two-part metabolism into M- methyl imidazole acetic acid (Abe *et al.*, 1993) shown below:

$$Histamine \xrightarrow{Histamine\ N-methyl-transferase} N-methyl\ histamine \xrightarrow{monoamine\ oxidase} M-methylimidazole\ \ acetic\ acid$$

The second pathway results in 15 – 30% of histamine being oxidised into imidazole acetic acid by diamine oxidase. Despite its rapid breakdown *in vivo*, histamine can be measured in basophil supernatants *in vitro* following cell activation by allergens. In addition, histamine can be measured indirectly through the measurement of diamine oxidase within the basophils through the application of flow cytometry (Ebo *et al.*, 2012). Shamji *et al* hypothesised and verified that fluorescently labelled DAO within the basophil would decrease immediately after *ex vivo* allergen stimulation in those with grass pollen allergy in comparison to non-atopic subjects (Shamji *et al.*, 2015). Histamine is bound in the acidic granules as a complex with other preformed mediators such as proteoglycans. Histamine

is a vasoactive amine and can act on the blood vessels to induce their dilation, as observed in the skin as a wheal and flare response (Berroa *et al.*, 2014). The measurement of histamine as means of measuring basophil activation are found to be time consuming, complex and poorly reproducible.

Proteases are present in trace amounts in basophils in comparison to mast cells, which contain much larger quantities of proteases such as tryptase, chymase and carboxypeptidase A3. These proteases have come to be regarded as reliable markers of mast cell degranulation and due to their content, mast cells are classified into two types in humans.

Tryptase is a major neutral protease and comprises 15 - 40% of the total granular protein of mast cells. Tryptase is present in quantities of 6 – 19 ug per 10^6 mast cells (Schwartz *et al.*, 1987). Basophils may only contain 1/500th of this amount (Jogie-Brahim *et al.*, 2004). Tryptase is a tetramer consisting of subunits each containing an enzymatic active site and it exists in two major forms - α (αI and αII) and β (βI, βII, and βIII). Less well studied forms are γ (a membrane anchored tryptase), and δ-tryptases, which were initially named mouse mast cell protease-7-like tryptases due to exon 5 of this protein being closely related to that of mouse mast cell protease 7 (Pallaoro *et al.*, 1999). Tryptase has been reported to play a key role in degrading human C3 into C3a and C3b anaphylatoxin. Tryptase can be measured in the blood to determine how many mast cells are present by measuring how much pro-tryptase there is and subtracting mature tryptase from the total tryptase measurement. Pro-tryptase is when tryptase is dissociated from heparin in blood and is spontaneously degraded into monomeric subunits, which are enzymatically inactive. Both α and β pro-tryptase are spontaneously secreted from mast cells, however the rationale for this is currently unclear. One theory is that through its high affinity association with heparin proteoglycan it is able to be translocated to the secretory granules (Schwartz *et al.*, 2003). β-tryptase in pro-tryptase form has a lower affinity for heparin proteoglycan than mature β-tryptase. This is optimally processed to mature β-tryptase in an acidic pH and when the –R3 terminal is catalytically cleaved; and pro-dipeptide is removed by dipeptidyl peptidase I. This process increases tryptase's affinity to bound heparin (Schwartz, 2006). Mature tryptase is considered a measurement of mast cell activation as it is only secreted upon degranulation of activated mast cells. Mature β-tryptase can be converted to its enzymatically inactive form when stored at neutral pH. This allows tryptase to be measured using a non-competitive B-12 and G5 based enzyme immunoassay. The immunoassay uses monoclonal antibody B12 for capture and mAb G5 for detection. G5 binds to a linear epitope only present on mature β-tryptase and α tryptase. β-tryptase in serum can be used to measure anaphylaxis. For healthy individuals, mature tryptase levels are < 1 ng/ml; *those* with > 1 ng/ml are considered to have mast cell activation. It has been reported that bodies post mortem whose cause of death is suspected to be due to an allergic reaction (which have >10 ng/ml of mature tryptase), are reported to be

caused by anaphylaxis (Hamilton, 2016). One advantage is the half-life of tryptase is 1.5 – 2.5 hours (Schwartz *et al.*, 1989a), which is much longer than histamine (5 minutes), which allows an accurate measurement after suspected anaphylactic incident.

Chymase, like β-tryptase is synthesised as an inactive enzyme and converted to its active form as a pro-enzyme in the secretory granules of the mast cell by dipeptidyl peptidase I. In MC_{TC} there is approximately 5 pg/cell of chymase and 12 pg/cell of cathepsin G. Chymase is a 30 kDa serine protease stored alongside heparin in secretory granules. It is released by the MC_{TC} subset of mast cells upon activation >3ng/ml and encoded on chromosome 14 (Jogie-Brahim *et al.*, 2004). Chymase's chymotryptic activity is responsible for the degradation of neurotensin, angiontensin I and cleaving type IV collagen, which is specific to tissue remodelling in asthma. Chymase is known for its major role in producing angiotensin II through its activity as a non-angiotensin-converting enzyme (ACE) as well as its responsibility in generating endothelin-I as a non-endothelin converting-enzyme (ECE). Based on its characteristics chymase has a role in the modulation of numerous inflammatory responses. In respiratory diseases and inflammation, chymase contributes to the cleaving of IL-13 to IL-3, the degradation of IL-4 and submucosal gland stimulation (Church and Levi-Schaffer, 1997). However, despite its established roles within inflammation, an assay to measure chymase has not yet been developed.

There are two isotypes of mast cell; $MC_{T,}$ defines mast cells that contain only tryptase, MC_{TC}, for mast cells that contain tryptase, chymase and carboxypeptidase A3. MC_T due to their role in host defence are considered to be immune system related, whereas MC_{TC} are considered to be non-immune system related. Chymotryptic mast cell proteases present in MC_{TC} form include chymase and cathepsin G and are expressed predominantly in the dermis of the skin.

Carboxypeptidase A3 is a metalloexoprotease contained within the secretory granules of mast cells with a molecular weight of 36 kDa. It is contained in the MC_{TC} mast cell subpopulation and is present at 15 pg/cell. This exopeptidase is responsible for cleaving aromatic amino acid substrates or the carboxyl-terminal aliphatic terminal of proteins. Carboxypeptidase A3 is bound to acidically charged proteoglycans within the granules of the mast cell; upon release this complex can be measured to determine mast cell activation (Reynolds *et al.*, 1989). In systemic mastocytosis, carboxypeptidase A3 was identified as one of the ten genes overexpressed in the mononuclear cells of the bone marrow (D'Ambrosio *et al.*, 2003). Mast cells containing carboxypeptidase are reported to be associated with allergic diseases of the upper and lower airways (Takabayashi *et al.*, 2012). Despite their simultaneous release, carboxypeptidase levels in serum of patients with reported anaphylaxis do not correlate with those of tryptase. In addition, serum levels of individuals with anaphylaxis were elevated in carboxypeptidase A3, in the absence of elevated tryptase levels (Simons *et al.*, 2007a).

Both basophil and mast cell granule matrix is formed of negatively charged proteoglycans. These contain a core protein and differ based on the number of covalently attached glycosaminoglycan (GAG) chains and the cellular location (responsible for determining their classification. Proteoglycans are negatively charged due to their sulphate and uronic acid groups. There is only one intracellular proteoglycan, serglycin, which forms its own unique class of proteoglycan. Serglycin is present in mast cells, and is the only proteoglycan to be covalently substituted with heparin, and acts as a glue by electrostatically binding to other proteases and basic proteins within the secretory granules (Lozzo and Schaefer, 2015). This is evident in the the consistencies between the defects in the formation of mast cells taken from serglycin deficient mice and those that lack the enzyme responsible for the sulphation of heparin (N-deactelyase/N-sulfotransferase 2) (Douaiher *et al.*, 2014). Heparin has a molecular weight of 60 kDa and approximately 5 ug is present per 10^6 human lung and skin mast cells. Heparin is released in response to immunological stimulant and modulates tryptase activity (as mentioned earlier). Heparin is present in human basophils however in much lower quantities; the most predominant proteoglycans present in human basophils are chondroitin sulphates (2 – 5 pg per 10^6 cells). In basophils, the main proteoglycan identified is chondroitin sulphate A in patients with myelogenous leukaemia (Metcalfe *et al.*, 1984), whereas in mast cells both heparin and chondroitin sulphate have been purified (Stevens *et al.*, 1988). Chondroitin sulphates possess a molecular weight of 30 kDa and like heparin bind histamine, but on a much lower level (1/5 of that of heparin) (Wasserman, 1983).

β-Hexosaminidase is an enzyme prominent in mast cell granules and thus can be measured as a mediator of activation. Mast cells contain 3.8 U of β Hexosaminidase per 10^6 cells. This enzyme is an exoglycosidase responsible for removing the terminal glycosamine residues (Schwartz *et al.*, 1981).

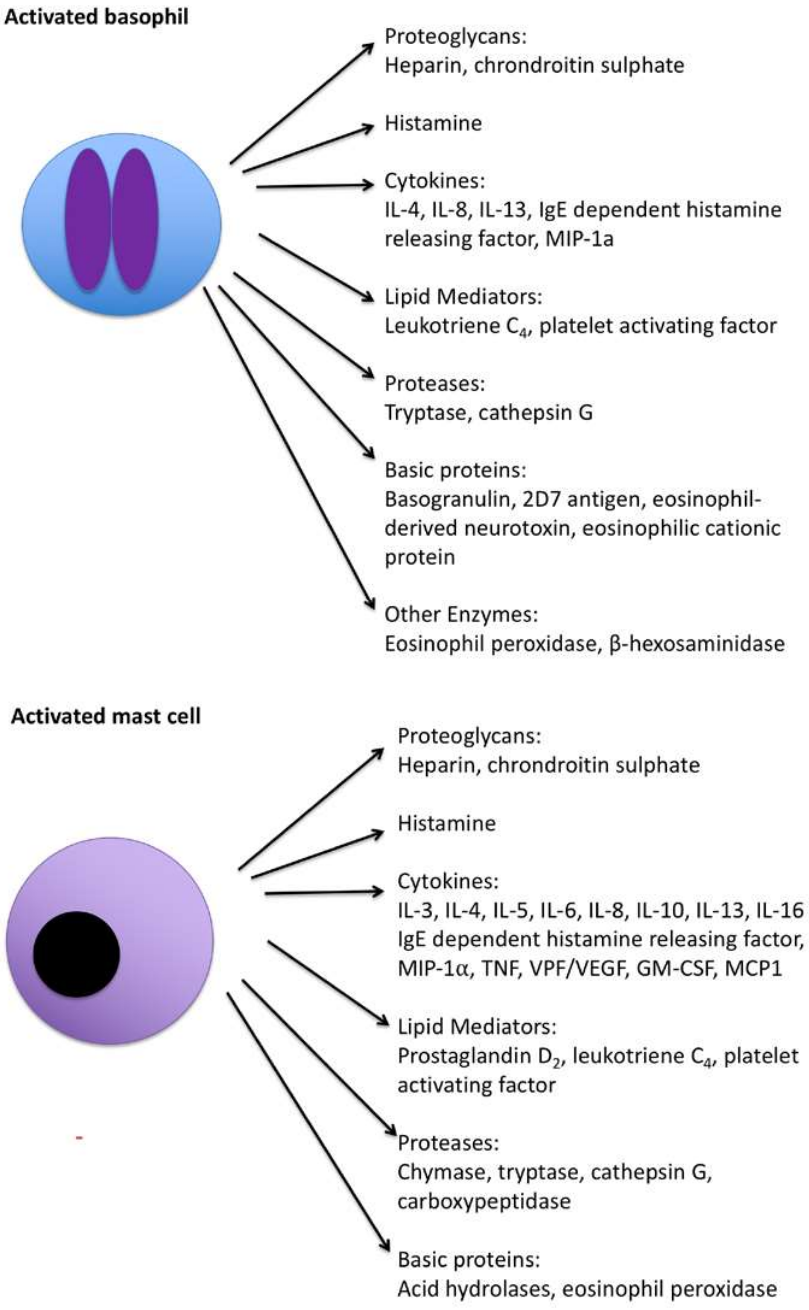

Figure 1: Comparison of secretory mediators released during the activation of basophils and mast cells (Adapted from (Simons *et al.*, 2007b)

1.2.2.2 Newly generated mediators

Whereas both basophils and mast cells can generate leukotriene C_4, only mast cells are able to generate prostaglandin D_2 (PGD_2). Upon mast cell activation, arachidonic acid is oxidised by the enzyme cyclooxygenase into prostaglandin D_2. Alternatively, arachidonic acid may be oxidised by 5-lipoxygenase to form leukotriene C_4. Leukotriene C_4 in the lungs can contribute to inflammation of the respiratory tract and bronchoconstriction. PGD_2 is released upon mast cell stimulation and is also a potent bronchoconstrictor playing roles in both vascular permeability and the enhancement of basophil release (Church and Levi-Schaffer, 1997).

1.2.2.3 Both preformed and newly generated mediators

Cytokines fall into both categories as preformed and newly synthesised mediators. Although many are listed in Figure 1; the main focus will be on cytokines relevant to both basophils and mast cells. For example, IL-4 and IL-13, one of their roles is to stimulate IgE production in B-lymphocytes. This was first demonstrated, when IL-4 was produced by basophils cultured in IL-3 upon IgE stimulation (Brunner *et al.*, 1993). These cytokines regulate leukocyte adhesion, secretion, and contribute to the T_H2 differentiation pathway and increase bronchial responsiveness to allergens. IL-3 is able to prime basophils for degranulation; therefore, this is often present in the stimulation buffer for basophil activation measurement. IL-4 in the presence of stem cell factor has been identified to prime cultured mast cells in the production and release of IL-3, IL-5 and IL-13; when compared to those cultured in stem cell factor alone (Lorentz *et al.*, 2005). .IL-4, IL-6 and IL-13 have a protective effect on the mast cells and basophils (IL-6 mast cells only) by preventing apoptosis (Kalesnikoff *et al.*, 2001).

1.2.3 Monoclonal antibodies for basophil identification

Monoclonal antibody BSP-1 (Basophil-1) is an IgM class antibody developed in 1987 (Bodger *et al.*, 1987) which binds to an unknown 45 kDa antigen on the basophil cell surface (Bodger *et al.*, 1989). Another example of basophil specific antibody was first described in 1995 known as 2D7. This is an IgG1 *K* antibody located in the secretory granules whose high sensitivity makes it a reliable marker of basophils (Irani *et al.*, 1998; Idoate *et al.*, 2013). Despite this, 2D7 is yet to be implemented in protocols other than immunohistochemistry. Both BSP-1 and 2D7 are unable to be measured in bodily fluids, which has prevented their implementation in clinic to measure basophil activation.

BB1 is an antibody originally described as binding to the cytosolic granules of basophils. This monoclonal antibody of the IgG2a subclass was later found to identify a murine proteoglycan, later

given the name basogranulin. This has been reported to be released in parallel with histamine upon basophil activation (Mochizuki *et al.*, 2003a). Thus, its measurement *in vitro* can allow assessment of IgE-mediated activation of basophils. In addition, basogranulin has been localised by immunoelectron microscopy to the cytosolic granules. BB1 can be integrated into several protocols such as for the detection secretion of basogranulin in fluids, (utilised to do so using a dot blotting procedure), in addition to identification of basophils *via* immunohistochemistry.

Basophils may be identified by monoclonal antibodies that bind to their surface expression markers using flow cytometry. For example, CD63 is a lysosome-associated protein (LAMP-3) and is a member of the tetraspanin family. CD63 is anchored to intracellular granules and its expression is rapidly up-regulated (Ebo *et al.*, 2008) on the surface of basophils upon granule release. In addition, CD203 is up regulated upon basophil granule release. This neural surface differentiation antigen is also known as E-NPP3 and is responsible for the catalysis and hydrolysis reactions that occur in oligonucleotides, nucleoside phosphates and NAD (Ebo *et al.*, 2008).

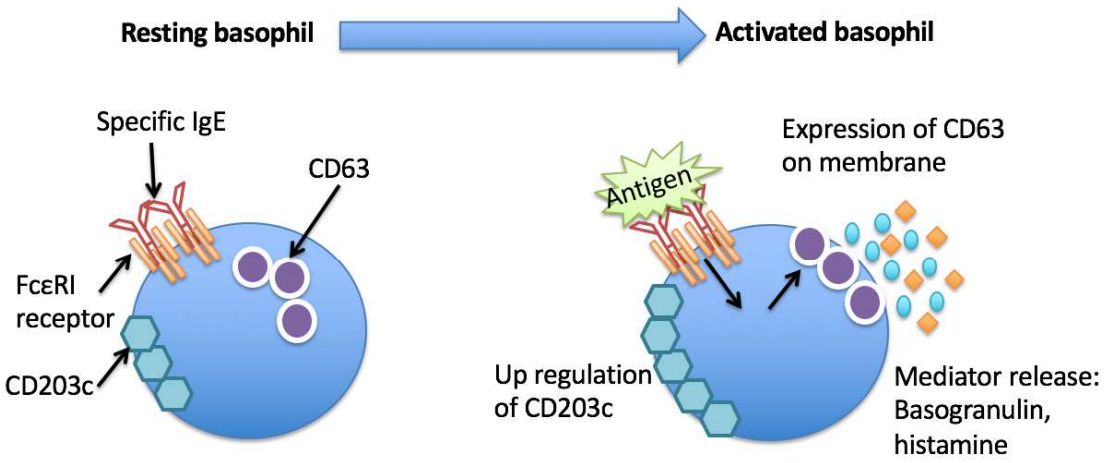

Figure 2: Comparison of basophil surface marker presentation when resting, and the up-regulation of markers upon stimulation

IgE cross links with membrane bound FcεRI and causes up-regulation of the expression of activation markers such as CD63 and CD203c. (Adapted from Haussmann *et al* (2009))

1.3 Allergy

The prevalence of allergy is increasing dramatically worldwide. In a survey conducted by the World Allergy Organisation based on population samples taken as a representative of 1.39 billion people, it was reported that 22% of the world's population may be affected by allergy (Warner *et al.*, 2006). The United Kingdom was in the top five countries with the highest prevalence of allergy. Allergic diseases represent the most common cause of chronic problems in developed countries and the broad spectrum of symptoms that may be provoked vary in severity from urticarial hives and hay fever to severe bronchoconstriction and life threatening anaphylaxis. Common allergens include foods, dust mite, grass pollen and drug molecules.

The term 'allergy' was first determined by Nobel laureate Baron Clemens von Pirquet in 1906, following observations that re-exposure to a substance can induce a change that could be harmful (allergy) or protective (immunity). Pirquet defined allergy as 'acquired, specific, altered capacity to react to a stimulus' (Von Pirquet, 1906). This was originally observed when treating patients with anti-serum who responded with symptoms such as fever, skin rash, inflammation of joints and lymph node swelling. Such symptoms had been observed previously when patients received tetanus anti-sera and thus it was concluded that the anti-sera could be both protective (create immunity) and elicit hypersensitivity reactions in patients. Over the years, the term 'allergy' is restricted in clinic, as it refers specifically to hypersensitivity reactions rather than the wide spectrum of immunological disorders. Healthcare facilities currently available in most countries appear to be unable to meet the need for caring for allergic patients, despite increases in allergy training facilities and staff. Basophil activation tests are able to distinguish the difference between allergic and sensitised patients. This has been investigated particularly to evaluate activation in peanut allergic diagnosed, peanut sensitised and non-allergic patients (Santos *et al.*, 2014). Such tests enable the reduced need for oral food challenges in children that have not yet been diagnosed with peanut allergy and can accurately discriminate between allergic and sensitised cases. This is certainly an advantage to current provocation testing which require re exposing the patient to the allergen in question. The basophil activation test's capability to predict allergic sensitisation will be explored in this thesis.

1.3.1 Mechanisms of allergy

The underlying mechanisms of hypersensitivity reactions have been classified into four groups I-IV, described below in Table 2 (Gell and Coombs, 1963). Type I hypersensitivity was first described by the observation of symptoms such as sneezing watering eyes congestion and in severe cases

anaphylaxis. Anaphylaxis, a condition rapid in onset, known as the most serious form of allergy. When an allergen is introduced directly into the blood stream it can cause anaphylaxis, resulting widespread histamine release and decreased vascular permeability throughout the body; that leads to decreased blood pressure, airway constriction and suffocation (Tsujimura *et al.*, 2008).

Type I reactions refer to reactions that are the consequence of the generation of specific IgE secreting plasma and memory cells formed in response to allergen specific T_H2 cells. In the initial sensitisation phase; the allergen is taken up by dendritic cells and major histocompatibility complex II, which presents the allergen to Th2 cells (Figure 3). Th2 cells are activated thus beginning the cascade of B-cells that differentiate and proliferate into IgE-secreting plasma cells specific to the allergen originally presented. The second phase of IgE-mediated allergy is the sensitisation phase, that allows allergens to cross-link with FcεRI bound IgE on basophils/mast cells, resulting in their activation. In Type I hypersensitivity reactions the allergen binds to IgE on the high affinity receptor FcεRI present on mast cells or basophils. FcεRI on basophils have been calculated to have a binding affinity of 10^{10} M^{-1} for IgE. The receptor consists of a 45 kDa α subunit, a 33 kDa β subunit and two 9 kDa γ subunits. The IgE receptor functions by the Fc fragment binding to α chain, and β chain is associated with Lyn, a tyrosine kinase receptor which phosphorylates the ϒ chain (Liu *et al.*, 2013) immunoreceptor tyrosine-based activation motif (ITAM) leading to its activation. Immediate reactions occur when IgE activates mast cells and/or basophils through crosslinking and leads to the release of histamine and prostaglandins. Antigen crosslinking with IgE receptors activates a signalling cascade including the phosphorylation of phospholipase C (PLC) and, protein kinase C (PKC), while the activation of inositol 1-3 trisphosphate (IP_3) and diacylglycerol (DAG) leads to the release of calcium (Ca^{2+}) from intracellular calcium stores. Furthermore, the release of calcium leads to degranulation and the release of histamine into the blood stream as well as the synthesis of leukotrienes, prostaglandins and cytokines. In addition to antigens, basophils can be activated by bacterial and viral peptides which recruit basophils *via* their formyl-peptide receptors (Gibbs, 2005). This includes N-formyl-methionyl-leucyl-phenylalanine (FMLP) (Auslander *et al.*, 2014) that can stimulate CD203c up-regulation and is CD63 independent (Chirumbolo, 2011), and calcium ionophore (A23187) which bypasses the downstream phosphorylation cascade and is often used as a positive control in basophil activation testing. Inflammatory mediators such as leukotriene C_4 and PGD_2 increase vascular permeability causing oedema and airway narrowing due to the constriction of smooth muscle. Histamine *via* its H_1 receptors additionally acts on nerve endings causing vasodilation of arterioles leading to the reddening of skin known as a wheel and flare reaction around the site of allergen exposure (Kindt *et al.*, 2007).

Table 2: Allergic mechanism categorisation (Adapted from (Gell and Coombs, 1963))

Type	Effector mechanism	Conditions associated
I	IgE-mediated	Anaphylaxis, hay fever, asthma
II	IgG and IgM antibody mediated reaction	Graves disease, myasthenia gravis, polyarthritis nodosa
III	Drug-antibody mediated reaction	Immune complex disease, systemic lupus erythematosus,
IV	Delayed hypersensitivity reaction	Contact dermatitis, rheumatoid arthritis,

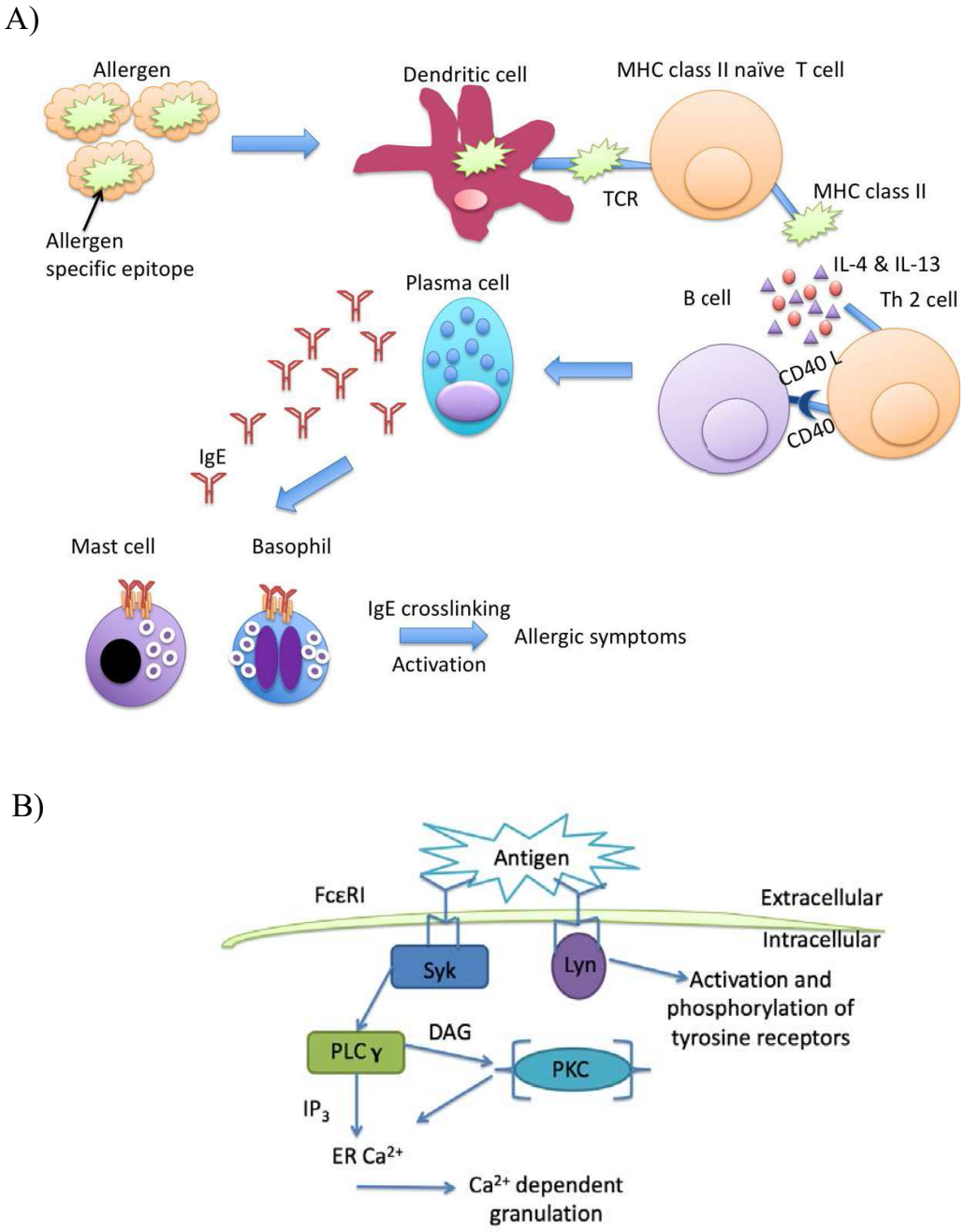

Figure 3: Type I IgE-mediated reaction

A) Type I IgE-mediated reaction adapted from Broekman *et al* (2015)

B) Lyn/Syk downstream phosphorylation pathway starting with the crosslinking of IgE on IgE the surface of basophils or mast cells adapted from Liu *et al,* (2003)

Type II hypersensitivity results in antibody-mediated destruction of cells mediated by IgG and IgM in a cytotoxic reaction. For example, in aplastic anaemia causes the destruction of the subject's own erythrocytes. Type II hypersensitivity can be mediated through three different mechanisms: complement mediated cell lysis, antibody dependent cell mediated cytotoxicity or opsonisation. In complement mediated cell lysis; the lytic enzyme usually inactive in blood, is activated when the antigen binds the antibody to form a complex. Upon binding the complement system is activated resulting in a cascade that results in the lysis of the cell. Antibody dependent cell mediated cytotoxicity is where a CD4 positive cell binds the Fab portion of an antibody-antigen complex. However, due to this binding position the Fc region of the antibody is therefore free to crosslink with natural killer cells and promote cell destruction. In this scenario, the antibody mediates cell destruction through the presentation of an antigen to the cytotoxic cell. Natural killer cells store hydrolytic and digestive enzymes, which are released upon binding to destroy the CD4 positive cell. An example of this is the production of anti-drug antibodies. In this occurrence, the drug is recognised *via* a cell bound antibody (usually IgG) is then removed from the circulation by tissue macrophages in the spleen. Antibiotics adsorb onto the surface of platelet proteins in drug-induced haemolytic anaemia. This creates a hapten-like complex, which can induce the production of antibodies causing complement mediated lysis and anaemia. Interestingly this process is fully reversible and can be cured by withdrawal of the drug in question e.g. penicillin. In this reaction, penicillin is able to chemically couple to host proteins *via* its β lactam ring enabling it to form covalent conjugates through the formation of amide linkages capable of mounting its antigenic activity. This occurs due to the instability of the ring, which allows 95% of penicillin molecules to bind in this manner. This antigenic component, benzyl penicilloyl conjugates formed with self-proteins, which in turn provokes T_H2 response and additionally is able to bind B cells, activating them to produce IgE antibodies against penicillin hapten (Gruchalla, 2003). The third mechanism of type II hypersensitivity reactions is oponisation; this mechanism is somewhat similar to antibody dependent cell mediated cytotoxicity. In both mechanisms, the antibody binds the Fab region of the antigen, leaving the Fc region free. They differ in the receptor bound; instead of cytotoxic cells binding to the Fc region, phagocytic cells such neutrophils and macrophages can bind through their FcεRI receptor. The antibody then binds the antigen (red blood cell / target cell) resulting in the activation of its attached phagocytic cell and the phagocytosis of the target cell.

Type III reactions occur when there is a large accumulation of immune complexes that are caused by inefficient clearance. The deposition of these complexes in the tissue result in the recruitment of neutrophils to the tissue. Neutrophils bind C3b immune complex triggering exocytosis of lytic enzymes to induce phagocytosis of the immune complex. However, due to the complex being on the basement membrane, this process is impeded, leading to further release of lytic enzymes leading to

the destruction of the tissue. Examples where there may be inefficient clearance of immune complexes include systemic lupus erythematosus, serum sickness and rheumatoid arthritis. (Uzzaman and Cho, 2012)

Type IV hypersensitivity reactions are classified into two basic types: delayed-type hypersensitivity mediated by CD4 positive T-cells and T-cell mediated cytotoxicity mediated by CD8 positive T cells. Delayed type hypersensitivity occurs when cytokines secreted by activated T_H1 cells cause localised inflammatory reaction. The clonal expansion of T_H1 cells occurs during the sensitisation phase approximately 1-2 weeks after contact with the antigen. Exposure to the antigen leads to an effector phase where T_H1-MHC II complexes secrete non- specific inflammatory cells, cytokines and macrophages leading further inflammatory activation (Kindt *et al.*, 2007). These reactions occur *via* the continuous production of inflammatory mediators *via* mast cells. In T-cell mediated cytotoxicity; self-reactive cytotoxic CD8 positive T cells that have not been effectively eliminated during development target host cells displaying host antigens. These cells recognise host MHC I complexes, which result in the destruction of host cells leading to immune mediated injury (Murphy *et al.*, 2008).

1.3.2 Forms of allergic disease

Allergic disease has been studied at length with new meta analyses and epidemiological reports being produced each year. Despite extensive investigation to try and identify key cells, genetic and environmental factors to aid diagnosis and management, gaps in knowledge are often identified. In particular, the role of basophils and mast cells in allergic disease. For many allergic diseases such as asthma, allergic rhinitis and urticaria, basophils and mast cells have a suggested involvement. However, this has not been proven.

1.3.2.1 Asthma and allergic rhinitis

Asthma affects over 300 million people worldwide (Cho *et al.*, 2016). Allergic asthma is characterised by the production of cytokines depicted (Figure 4) such as IL-4, IL-5 and IL-13 from T_H2 CD4 cells which directly contribute to increasing IgE levels (Hanania *et al.*, 2013) responsible for symptoms such as eosinophilic airway inflammation, mucus hyper secretion and airway hyper responsiveness (Cho *et al.*, 2016). Mast cell activation and contribution to allergic asthma is well characterised by measuring histamine levels in bronchoalveolar lavage (BAL). In comparison to healthy subjects (non-atopic), asthmatics have more degranulation. Mast cell degranulation results in the release of tryptase, which can contribute to the remodelling of airways of asthmatics and results in smooth

muscle hypertrophy and hyper secretion of mucus. More recently, induced sputum samples have been taken from different asthmatic phenotypes to measure basophils. It was observed that there was an increased population in patients with asthma's sputum than the healthy controls. Such experiments have led to the association of increased sputum basophils to eosinophilic asthma (Brooks *et al.*, 2017). Basophil numbers in asthma are significantly elevated in comparison to healthy controls at baseline, this number is reported to increase upon exacerbation. Due to their production of cytokine IL-4, basophils are thought to contribute to the late phase asthmatic response after allergen inhalation responsible for increased IgE receptor up-regulation on mast cells and basophils and hyper secretion of mucus. In a bronchoprovocation study, basophil activation testing using flow cytometric methods observed the differences between subjects with asthma and dual-responses to those with asthma and early isolated responses by comparing the activation of basophils at baseline and post provocation challenge. Dual-responders had much higher population of activated basophils than isolated early responders. Such results correlated with the subjects' forced expiratory volume performed at baseline (Salter *et al.*, 2016). Results propose that basophil activation tests could essentially be used to predict airway challenge results and determine the occurrence of late asthmatic responses.

Based on the role of mast cells and basophils exacerbating the symptoms of asthma, therapies have been formed based on their current mechanisms of action. Patient responses to current anti-IgE therapies cannot be predicted in readily available tests to measure serum IgE, and presently the levels of cytokines of interest are low and thus cannot be measured accurately in blood (Miyara *et al.*, 2009). Therefore, basophil activation tests have been utilised in studies to predict the efficacy of allergic response when treated with anti-IgE therapies such as omalizumab (Nopp *et al.*, 2006; Hoffmann *et al.*, 2015). For example, in double blind, placebo controlled trial in omalizumab, whereby basophil activation tests were combined with oral immunotherapy for the treatment of cow's milk allergy to measure the efficacy of the immunotherapies used. This study involved 52 patients who received either placebo or omalizumab over a 48-month period. Basophil activation tests were performed measuring CD63+ cells in flow cytometry at baseline and months 4, 16, 22, 30 and 32. At month 28, basophil activation in response to milk stimulation demonstrated that the activated basophil population was lower in patients taking omalizumab than those taking placebo (Wood *et al.*, 2016). Results of this trial demonstrated that patients could be desensitised to milk whilst taking omalizumab. Asthma is associated with up to 75% of those with allergic rhinitis, as indicated in Figure 4, the mechanism of action for allergic rhinitis affects the upper airways, whilst asthma affects the lower airways when an allergen is introduced to the respiratory tract.

Rhinitis is present in two forms, both allergic and non-allergic rhinitis. The condition 'rhinitis' is characterised by nasal congestion, sneezing and rhinorrhoea (Settipane and Charnock, 2006). Allergic rhinitis is increasing in prevalence in the UK affecting more than 20% of the population, thus presenting a problem in primary care (Lipworth *et al.*, 2017). In allergic rhinitis, an allergen provokes inflammation inside the nose resulting in cold like symptoms such as rhinorrhoea, sneezing and itchiness of the nose. Despite presenting mild symptoms, allergic rhinitis is associated with morbidity, decreased quality of life and both direct and indirect health costs to the NHS. According to a study conducted in 2017, up to 80% of patients reported that the condition had resulted in insomnia, depression, irritability and adversely influence work attendance and performance due to inability to concentrate (Lipworth *et al.*, 2017). Mast cells are typically associated with rhinitis due to their release of pro inflammatory mediators such as histamine, PGD_2 and leukotriene C_4. Basophils have additionally been found to play a part in this disease; found in nasal washes of patients with allergic rhinitis (Siracusa *et al.*, 2013). These cells are suggested to be the main source of histamine in late phase responses and produce LTC_4, thus current therapeutic strategies have moved towards targeting histamine and leukotrienes derived from basophils.

For diagnosis, a clinical history is taken and skin prick tests and/or provocation tests can be advised as a means to identify or exclude an allergic trigger that could influence management of the condition e.g. aeroallergen avoidance. Diagnosis of allergic rhinitis is conducted either *via* skin prick testing or via total specific IgE. Skin prick testing is preferred as it is cheaper with immediate feedback for the patient. Basophil activation tests could be a more sensitive and time saving technique in the distinguishing between patients who have either allergic rhinitis, non-allergic rhinitis and those with local allergic rhinitis. Currently local allergic rhinitis' diagnosis is determined either by nasal provocation tests or by non-invasive specific serum IgE tests in combination with positive skin prick tests and the patient medical history. Nasal provocation tests are easily reproducible and have a high sensitivity. However, each test has their disadvantages; nasal provocation tests are time consuming and require trained personnel, whereas serum IgE testing has low sensitivity, which can result in the misdiagnosis of local allergic rhinitis. Healthy volunteers' basophil activation was tested in comparison to those with allergic rhinitis, local allergic rhinitis and non-allergic rhinitis in a pilot study by Gomez *et al.* Results indicated that the basophil activation test using D pteronyssinus was able to diagnose more than 50% of local allergic rhinitis (Gómez *et al.*, 2013). In addition, these tests were more sensitive than nasal specific IgE and required less time to perform than nasal provocation tests.

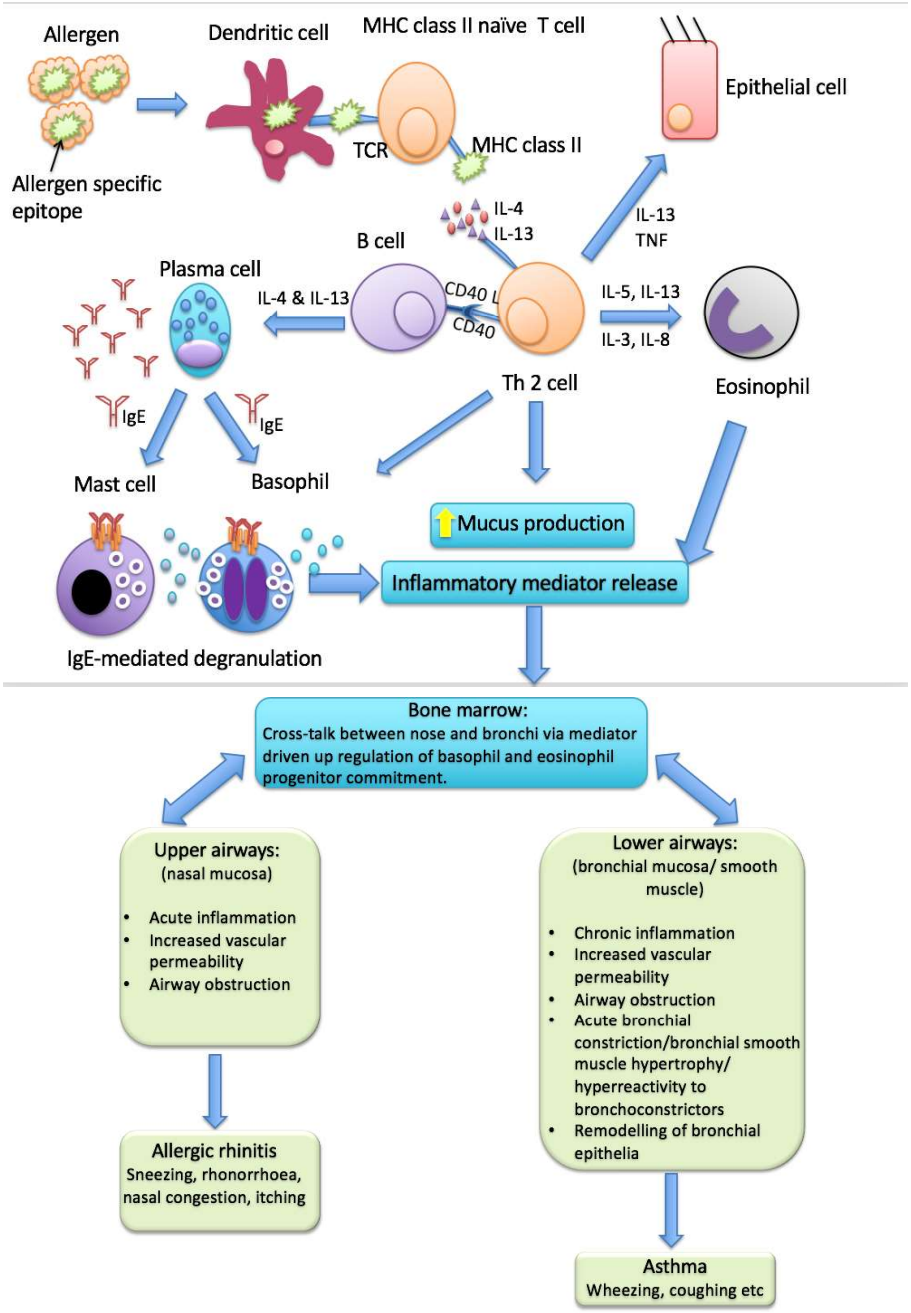

Figure 4: Allergic mechanisms involved in asthma and allergic rhinitis (Adapted from (Gandhi *et al.*, 2016)

The allergen is presented to T helper cells, that in turn *via* IL-4 result in the clonal expansion of Th2 cells and differentiation into Th2 cells resulting in production of cytokines. A result of this is eosinophilia driven by the differentiation of eosinophils by IL-5 in the bone marrow and circulated to the tissues resulting in inflammatory infiltrate and eosinophil rich nasal polyps. IL-13 is responsible for effects on the endothelial tissue cells causing mucus secretion (airway obstruction) and smooth muscle contraction (bronchoconstriction).

1.3.2.2 Urticaria

Urticaria is characterised by the rapid onset of red wheals on the skin and itchiness. Urticaria is exhibited in four different forms. The first is spontaneous urticaria, this is divided into subtypes chronic and acute. Chronic urticaria is a recurrent skin disorder that is characterised by erythematous wheals that present for a minimum of 6 weeks, whereas acute urticarial is present for less than 6 weeks. Basophils play a role in urticaria in 35 - 40 % of patients who possess a IgG autoantibody for the α subunit of their FcεRI receptor (high affinity type I IgE receptor) and an additional 5 - 10 % have anti-IgE (Kikuchi and Kaplan, 2001). These autoantibodies are able to activate histamine release from basophils and dermal mast cells *in vitro* (Sabroe *et al.*, 1998a). In a study by Sabroe *et al* basophil numbers were reduced in chronic urticaria, and more pronounced basopenia was demonstrated in patients with autoantibodies (1 basophil per 2000 leukocytes). Based on blood basophil numbers and histamine measurement assays run, patients who had basophils with autoantibodies had the same amount of histamine per cell as the control, however the autoantibodies were found to play a role not only in desensitising these basophils (unresponsive to FcεRI stimulation) but also removing them from circulation (Sabroe *et al.*, 1998a). When comparing patients with or without autoantibodies, those with had more severe symptoms in terms of number of wheals ($p = 0.05$), itch score ($p = 0.002$), lower serum IgE levels ($p < 0.0005$) and a larger distribution of wheals ($p = 0.009$) than patients without autoantibodies (Sabroe *et al.*, 1999).

In several studies for the diagnosis of chronic urticaria, the basophil activation test was proposed as a safer non-invasive, sensitive alternative to autologous serum skin testing (Konstantinou *et al.*, 2009). The autologous serum skin testing is non-specific and most commonly used in the diagnosis of urticarial and evaluates the presence of histamine releasing factors. The basophil activation test represents a safer alternative by lowering the risk of skin infections from carrying out autologous serum skin testing and could potentially provide a more sensitive *in vivo* alternative to current testing. In chronic urticaria, the density of FcεRI receptors on basophils and mast cells are thought to play a key role in the determination in the effectiveness of its treatment. In a double blind, randomised, placebo controlled study in the effectiveness of using omalizumab in chronic urticaria using patient serum as the allergen. Despite leading to a significant reduction in FcεRI receptors as early as one week into treatment; basophil releasability and activation tests were unchanged by this treatment (Jörg *et al.*, 2018).

1.3.2.3 Food allergy

The most common food allergies that result in hospitalizations and deaths in the United Kingdom are peanuts, tree nuts and seafood (Koplina *et al.*, 2011). The prevalence of peanut allergy in the UK and westernised countries has doubled in the past 10 years from 1.4 - 3.0 % (Du Toit *et al.*, 2015). Originally, UK guidelines suggested avoidance in high-risk infants in early life, and thus diagnosis is particularly important to diagnose infant's allergic sensitivity to potential allergens. The diagnosis to allergy sensitivity of allergens is currently an unmet need, and the the availability of basophil activation tests to predict infant's allergic sensitivity is urgently required. Realistically, if basophil activation tests were to be standardised, oral food challenges could be avoided as a diagnosis method. In addition, basophil activation tests could be used to determine a patient's response to immuno-modulatory treatments for food allergy.

1.3.2.4 Drug allergy

As drug allergy poses a significant challenge to determine patients' sensitivity to specific stimuli. Drug allergy is of particular interest as in extreme reactions, anaphylaxis can lead to withdrawal of drugs from the market, and additionally can result in death (Demoly *et al.*, 2014). According to a World Allergy Organisation report (2011), adverse drug reactions (ADRs) may affect up to 1/10 of the world's population (WAO, 2011). ADRs are responsible for 5% of all hospital admissions and affect 10-20% of hospital inpatients (Pirmohamed *et al.*, 1998). Factors that contribute to drug allergy can be directly related to either the drug or the host. For example, drugs with a similar chemical structure to a confirmed drug allergy are equally likely mount an allergic response (Thong and Tan, 2011). In the Liew *et al* study that observed the Australian population over a 8 year period, drug-induced anaphylaxis admissions increased over 150% (Liew *et al.*, 2009). In addition to the increased demand for drug allergy identification and diagnosis, an alternative for serum IgE testing is required; since many drugs cannot be produced in solid state for binding and are unable to be tested (Mayorga *et al.*, 2010). There is a substantial need for a standardised basophil activation test is required for diagnosis as not only does it offer a safer, more sensitive alternative, but in some cases it is the only option to diagnose drug allergy and to determine safe drug alternatives for patients.

Type I IgE-mediated hypersensitivity reactions account for 60-70% of adverse reactions that occur when anaesthesia is administered (Mertes *et al.*, 2012). This percentage has increased rapidly over the past 25 years as anaesthesia is being used in both doctorial and dental surgery. In a meta-analysis it has been reported that neuromuscular blockers account for 63% of these reactions, latex 14%, hypnotics 7%, antibiotics 6%, plasma substitutes 3% and morphine like substances 2% (Mertes *et al.*,

2011). Allergy to general anaesthetics is of particular interest as cross reactivity has previously been reported. Thus, when testing patients who have previously had general anaesthesia induced anaphylaxis; they have additionally been tested for numerous drug compounds to determine a safe alternative for any future procedures (which can be kept in their patient notes for future reference).

1.3.2.5 Diagnosis of allergic diseases

Allergy can elicit a wide spectrum of symptoms and therefore to diagnose the allergy a detailed clinical history must be taken. Both IgE and non-IgE based testing must be performed to eliminate possible causes to diagnose the allergy correctly. Although not standardised, IgE and skin prick tests are scientifically validated. By performing both tests, it can enable an accurate interpretation of the results; for example, those with very high IgE levels can be associated with multiple positive skin prick tests that may not be clinically relevant as they have high baseline IgE measurement. By performing both tests, it can confirm result or rule out IgE-mediated hypersensitivity; as these tests are used to determine sensitivity to allergens. These tests cannot differentiate between desensitisation, tolerance and clinically relevant allergy; and further review is required dependent on the type of allergy being investigated i.e. food allergy, re exposure to the allergen in question by using an oral challenge.

The most commonly used methods for the determination of specific allergens responsible for allergic sensitisation are skin prick testing and intradermal testing without skin prick testing. Skin prick testing involves scratching the surface of the skin with a needle that has been dipped into an allergen solution on the volar aspect of the forearm (Brockow *et al.*, 2002). This uses a positive control, often histamine, which will induce a wheal and flare response on the skin, with saline is used as a negative test (Muraro *et al.*, 2014). However, if the allergen is unstable, false-negative reactions may occur. For subjects that test negative, often an intradermal skin testing is carried out in the same location on the other arm to determine allergy; this is conducted by testing serial dilutions of the allergen in question. The weakest dilution is tested first. The allergens are injected in between the subcutaneous layers of the skin to form a 'blip'; which is drawn around in pen. These are left for 15 minutes and if no response is seen then the test is repeated in increasing concentrations of the allergen until a response is shown (if any). The method involves intradermal injections of 0.02-0.05 ml allergen (Brockow *et al.*, 2002). Intradermal testing is generally more sensitive than direct exposure, yet it is not as safe nor as reliable, often leading to a false positive reaction and potentially may provoke anaphylaxis. A further disadvantage is its limitations in patients whom take antihistamines or those displaying a rash (Khan *et al.*, 2012).

Provocation tests are the current gold standard for determining type I hypersensitivity reactions in patients when other tests have given a negative response (Demoly *et al.*, 2014). This testing generally uses the same route of administration of the allergen that caused the reaction initially; oral administration is preferable based on severe reactions in IV administration. It is frequently used for hypersensitivity testing to antibiotics, non-steroidal anti-inflammatory drugs (NSAIDs) and local anaesthetics, allowing either the confirmation of hypersensitivity or its exclusion from patient diagnosis. Despite provocation tests being the current *in vivo* gold standard there are numerous pitfalls with this technique. For example, patients are hesitant at being re-exposed, while stress itself can contribute to allergic reaction. Re exposure, testing needs to be performed in a controlled setting with trained medical staff on hand to act in case of a severe reaction. In addition, provocation tests are contraindicated in severe hypersensitivity reactions.

Serum IgE levels in response to allergen can be measured using a fluorescent immunoabsorbant assay. It has been observed that prognosis is poor for those with higher early serum IgE levels than those with lower early serum IgE levels due to their decreased measurement over time, thus reflecting desensitisation over time (Neuman-Sunshine *et al.*, 2012). Serum IgE immunoassays are considered less predictive than skin prick tests (<50%) (Sampson, 1999). A positive sIgE test is indicative that the patient is sensitised to the allergen it was tested against; if the patient has presented with clinical symptoms typically of IgE-mediated allergy, a positive test is interpreted as clinical allergy. It has been reported that the misinterpretation of these tests by wrongfully correlating allergen specific IgE level with the probability/severity of the patient reacting to the allergen (Fleischer, 2015).

Basophil activation testing typically runs using fluorescent activated cell sorting (FACS), a simple protocol yet one that requires extensive training to use the technology required. Tests need to be performed within 24 hours of blood taking and thus careful organisation is required to ensure trained lab staff are available, and a flow cytometer is free to run the blood samples through, as in hospitals this technology is a shared facility. Thus, basophil activation tests are not widely employed in clinical practice on account of the technological impediments of this technique (Tanno *et al.*, 2016). Confirmatory laboratory tests would be useful as *in vivo* diagnostic tests have the potential to be unreliable with the ability to produce either false negative and false positive results. Currently, basophil activation tests *in vitro* additionally have the capability of exposing small blood samples to increased doses of allergen, in addition to running positive and negative controls. These tests only require one needle prick for venesection instead of several hours of needle insertion into the patients' skin that are necessary to conduct skin prick tests and intradermal testing. Basophil activation tests are confirmatory tests in the diagnosis of milk, egg and peanut allergy (Sato *et al.*,

2010). These tests demonstrate higher specificity and more accurate negative predictive value than current tests used to confirm negative skin prick tests such as serum IgE testing. In addition, basophil activation tests are able to diagnose sensitivity to allergens without losing any positive predictive value. In conclusion, *in vitro* basophil activation tests are expensive, time consuming and require specific training and expensive facilities in order to conduct. There is an urgent unmet need to develop advanced technologies for a rapid, reliable, cost effective diagnostic test of allergy to drugs.

1.3.3 Basophil purification for basophil activation testing

With basophils accounting for less than 0.5% of the leukocyte population, their efficient isolation has long presented a challenge. Currently, the main isolation techniques employed for basophils are magnetic activated cell sorting using *negative* selection, in combination with an initial density gradient centrifugation. Briefly, leukocytes are incubated with an antibody cocktail, which is then mixed with micro-sized magnetic beads, which are coated with antibodies specific for the cell surface antigens: CD2, CD3, CD14, CD15, CD16, CD19, CD24, CD34, CD36, CD45RA, CD56 and glycophorin A. Cells other than basophils become bound to the surface of the beads enabling negative selection of basophils when run through either a magnetic column or entered into a large hollowed magnet. Commercially available procedures are available for this procedure, such as magnetic activated cell sorting (MACS) (MACS, Miltenyi Biotec, Tetero, Germany and EasySep, Stemcell Technologies, Vancouver, Canada), but are costly and can take up to 3 hours for each run. In addition, confirmation of the separation can be made either by counting or by a more accurate determination of the percentage purity *via* flow cytometric analysis, extending the length of the procedure and cost further. Therefore, there is a clear need to develop advanced methodologies to address the above challenges. In addition, current techniques require large quantities of blood for separation; by introducing a microfluidic device it would implement a downscaling of materials required to perform the isolation and therefore less blood would be required.

1.4 Microfluidics

Microfluidics are defined as 'devices and methods for controlling and manipulating fluid flows with length scales less than a millimetre' (Stone *et al.*, 2004). Of particular relevance to allergy testing, the advantages of this technology include the ability to provide high sensitivity screening and a short analysis time using only a small volume of samples (Lim and Zhang, 2007), as current techniques for basophil activation testing have proven lengthy. For some basophil activation testing, blood separation is required to improve accuracy, and the protocols for this in their current form would add hours to the process time.

Microfluidic platforms are often applied to biochemical processes to enable a consistent way of miniaturising and automating a process. Key characteristics that make these devices so attractive to scientists and industry include their ability to be high throughput i.e. process a large number of samples/assays a day. In addition, these devices can be produced at a low cost (dependent upon the material) and due to their size are able to minimise turnaround time and reagent consumption, which keep costs fairly low. These devices are programmable and thus there is flexibility in their design to adapt to other liquid handling protocols, which removes the necessity of redesigning or fabricating a new device. Microfluidic systems can be classified according to their main liquid propulsion principle. There are five major groups these devices fall into: capillary, pressure driven, centrifugal, electrokinetic and acoustic (Mark *et al.*, 2010). In this research, we will be focussing on two groups: capillary (spiral sorter 1.4.3) and acoustic devices (described in section 1.4.5). For both of these groups, buoyant polymer particles are used to mimic cell suspensions in blood to try and characterise the devices. Particles are useful in visualising the focusing in acoustofluidic devices and the size based separation in the channels of capillary based devices. This enables the user to predict what size particles will be separated from the main suspension and determine if your cell of interest will be isolated. This methodology is particularly useful as it eliminates cost, and removes the inconvenience of using biological samples at the characterisation phase of the research. Therefore, the user has already created optimal settings prior to using the real sample.

The use of a microfluidic device to isolate basophils could noticeably improve the process time in comparison to the commonly used bead-based magnetic cell isolation, or magnetic-activated cell sorting (MACS) for basophil isolation (Haisch *et al.*, 1999; Shiratori, 2005). Furthermore, integrating multi-purpose microfluidic devices could be adapted to provide a cost effective (potential to be mass-produced), high throughput-screening device to determine allergy in patients.

1.4.1 Fabrication materials

In the early stages of microfluidic technology, silicon has been used for microfluidic device fabrication. However, its opaque structure prevents optical detection while its surface can potentially adsorb biological molecules resulting in inaccurate measurement (Yu *et al.*, 2010). Glass based devices avoid silicon's failings yet fabrication complexity is considered a disadvantage (Whitesides, 2006).

Polymers are now the material of choice for many biological applications (Becker and Locascio, 2002; Boone *et al.*, 2002; Fiorini and Chiu, 2005; Sollier *et al.*, 2011). Unlike glass, polymers are easy to fabricate and can additionally have their surfaces modified to improve efficiency of the device. Polydimethylsiloxane (PDMS) is currently the preferred polymer due to its flexibility (Lim and Zhang, 2007), cost effectiveness and transparency, which enables it to be vital in optical detection. PDMS is additionally biocompatible, non-toxic to cells and can easily be bonded to other surfaces (Lim and Zhang, 2007). The porosity of PDMS can be advantageous when functional permeability is required, which can be disadvantageous as it may enhance surface attachment of biological molecules. Polymethyl methacrylate (PMMA) also known as acrylic or acrylic glass has similar optical property with PDMS but is more rigid with sufficient mechanical stability. At present, polymers such as PDMS and PMMA are commonly used in biological applications, which can also be candidates for developing microdevices for allergy testing.

1.4.2 Passive separation of microparticles

Manipulation of microparticles has been developed as a useful tool for cell-based analysis in order to sort, enrich and/or separate different cell types, in particular rare cells from a cell population. In general, there are two groups of cell separation methods, namely, passive and active separation. Passive separation utilises hydrodynamic forces generated by fluid flow to separate particles by manipulating flow *via* channel geometry (Gossett *et al.*, 2010). These techniques can potentially reach a high throughput, are easier to fabricate and cost effective due to their ability to operate continuously. A disadvantage is that it has lower resolution and can only distinguish particle size (Gossett *et al.*, 2010). Channels can be designed to identify cells based on their characteristics such as weight and size. An example is using human peripheral blood samples where the cells were sorted based on their sizes: red blood cells are 6 to 8 µm in diameter, neutrophils and eosinophils 10 µm, basophils 12 µm and monocytes 21 µm (Chatterjee, 2011).

1.4.3 Spiral sorters

As an example of passive separation, spiral sorters have been frequently used for separating microparticles including blood cells according to size. In a typical design, a spiral sorter consists of an Archimedean spiral with a 500 μm x 100 μm channel cross section and consist of 3 – 4 outlets. In principle, when particles in suspension flow along the spiral channel they are subject to forces of inertial lift and Dean drag resulting in a net lift force (Nivedita and Papautsky, 2013). Therefore, spiral sorters depend upon the balance of hydrodynamic forces, Dean drag from the secondary flows and the curvature of the spiral sorter, that is known as Dean coupled inertial migration (Nivedita and Papautsky, 2013). This balance of forces results in an equilibrium shift towards the inner wall of the microchannel, thus particles are focused here. The ratio of inertial lift and Dean drag forces determine when particles equilibrate. As the particles migrate towards the wall, their rotational wake is disturbed and thus the particles are directed away from the wall due to the net lift force (F_L) (Chatterjee, 2011). Net lift force can be calculated using the following equation:

$$F_L = \rho G^2 C_L \alpha_\rho^4 \qquad \text{(Equation 1)}$$

Where ρ is the density of fluid medium, α is the particle diameter, G is shear rate of fluid given by $G = U_{max}/D_h$ and U_{max} is the maximum fluid velocity and D_h is the hydraulic diameter and is calculated by $D_h = \frac{2hw}{(h+w)}$. In this equation h is representative of height and w = width. C_L is the lift coefficient relative to the channel cross section and Reynolds's number $C_L = \frac{F_L H^2}{pV^2\alpha^4}$. $\mathcal{V}$ = spherical particle volume.

In the study conducted by Chatterjee, the device consisted of 5-loop Archimedean spiral with two inlets and eight outlets at equidistance to each other. The channel itself was 40 cm long in order for the experiment to be feasible with 87% efficiency on average across the eight outlets (Chatterjee, 2011). Spiral structure of the device manipulated Dean drag force and thus disrupts particle equilibration, forcing particles to align along the inner channel of the microchannel wall. As explained previously smaller particles migrate further away from the wall and thus can be separated by size (Chatterjee, 2011). This suggests that this technique can potentially be employed for basophil separation from whole blood.

1.4.4 Active separation of microparticles

Active separation is achieved by using an external source to create a drive to manipulate the particles/cells in the microchannel. There are numerous ways to enforce this such as micro motors, magnetic separation, electrophoresis, dielectrophoresis or optical fractionation (Zhang and Andreas Manz, 2003; Doh and Cho, 2005; Xia *et al.*, 2006; Lee *et al.*, 2011; Balachandar *et al.*, 2016). A disadvantage is that when using electrical fields, damage can be caused to the cells. Compared to passive techniques these forms of separation produce high efficiency and resolution, such as acoustic based microparticle manipulation, which is examined in more detail below.

1.4.5 Acoustic based microparticle manipulation

Acoustic based microparticle manipulation normally employs ultrasonic standing waves to manipulate particles purely depending on their acoustophysical properties. It offers a non-contact separation approach in a continuous flow based system independent of other properties such as ionic strength, pH or surface charge (Lenshof *et al.*, 2012); thus making this an attractive method for cell separation.

Acoustic based microfluidics, also referred to as acoustofluidics has recently been used as a way of separating particles on a micron-scale level (Glynne-Jones *et al.*, 2012). Such forces can be generated by two different methods. Standing waves are generated by the non-linear interaction between the standing wave and the scattered acoustic field created by the particle of interest (Glynne-Jones *et al.*, 2012). The averaged radiation forces $F(\boldsymbol{r})$ can be determined by the following equation(Gor'kov;, 1962):

$$F(r) = \mathcal{V}\nabla\left(\frac{3(p_p - p_f)}{(2p_p + p_f)}E_{kin}(\boldsymbol{r})\right) - \left(1 - \frac{\beta_p}{\beta_f}\right)E_{pot}(\boldsymbol{r}) \qquad \text{(Equation 2)}$$

$\mathcal{V}$ = spherical particle volume, $\boldsymbol{r}$= particle location, E_{kin}= averaged kinetic energy densities, E_{pot}= potential energy densities, p_p= particle density, p_f= fluid density, β_p= particle compressibility, β_f = fluid compressibility. If particles of interest are less dense and less compressible than the fluid which they are suspended in, these can then be manipulated towards the acoustic pressure node and the acoustic velocity antinode (Glynne-Jones *et al.*, 2012). Compressibility is determined by the equation, which takes into account c = speed of sound:

$$\beta = \frac{1}{\rho c^2} \qquad \text{(Equation 3)}$$

In addition, the particle contrast factor ($\emptyset$) can be calculated; this determines whether the particle will move towards the pressure node or the antinode in the acoustic standing wave. If the value is positive, the particle will move towards the pressure node; if the contrast factor is negative, the particle will migrate towards the antinode. The contrast factor ($\emptyset$) can be calculated using the following equation:

$$\emptyset = \frac{\rho_p + \frac{2}{3}(\rho_p - \rho_0)}{2\rho_p + \rho_0} - \frac{1}{3}\frac{\rho_o c_0^2}{\rho_p c_p^2} \qquad \text{(Equation 4)}$$

Whereby ρ_p and ρ_0 represent the densities of the particle and fluid. Speed of sound in the particle material and fluid are represented by c_p and c_0.

One of the most straightforward approaches in acoustofluidics is to use a planar, layered resonant device as depicted in its 1D format in Figure 5. Classification of these devices is based on the number of wavelengths and the type of transducers used i.e. position of the pressure nodes within the various layers (Glynne-Jones *et al.*, 2012). The generation of the ultrasonic standing wave within the fluid layer is known as acoustic streaming (Lighthill, 1978).

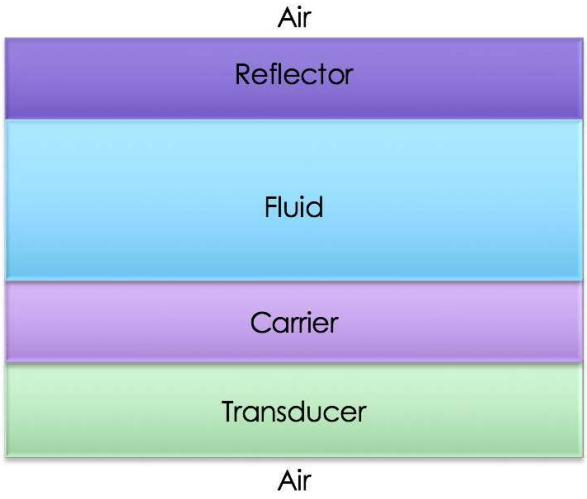

Figure 5: Layered components of a planar resonator (Adapted from (Glynne-Jones *et al.*, 2012))

The Figure illustrates a one-dimensional simplified diagram of a planar resonator. It comprises of 4 layers with air boundaries either side. The transducer is piezoceramic and the type of transducer used determines location of pressure node. The carrier layer is responsible for coupling energy to subsequent layers. The fluid layer is where the particle manipulation occurs (Carugo *et al.*, 2014). Finally, the reflector is responsible for reflecting energy back into the device to create a standing wave and to maintain the resonant operations.

The acoustic radiation forces create standing wave fields inside the channel to manipulate cells to a specific place. There are two types of layered device that will be explored – half wave resonator (HW) and thin reflector device (TR).

1.4.5.1 Half wave resonator

Half wave resonators were first described by (Mandralis *et al.*, 1990), and are described as "resonators in which the fluid channel is close to a half wavelength in thickness" (Lenshof *et al.*, 2012). Based on this description the constitutive layers are as follows: $2n\lambda/4$ (carrier layer), $\lambda/2$ (fluid layer) and $(2n+1)\,\lambda/4$ (reflector layer) (Glynne-Jones *et al.*, 2012). Due to its design, this results in higher acoustic impedance in the reflector than the fluid layer and thus creates pressure maxima at the channel walls and the pressure minima close to the channel centre, as depicted in Figure 6 (A).

1.4.5.2 Thin reflector resonator

Glynne-Jones *et al* in 2009 first described the thin reflector resonator (Glynne-Jones *et al.*, 2009). In this device particles are directed towards the reflector layer by placing the pressure node in the air boundary above the reflector layer (B). This is achieved by designing a device where all layers are thin in comparison to the wavelength. If the surface of the reflector layer is pre-coated with proteins (e.g. antibodies) which can selectively bind cells (e.g. basophils), that can facilitate attachment of selected cells to the reflector surface under optimised microfluidic conditions, leading to capture of such cells of interest. That forms the key principle for basophil separation in this project. With comparison to traditional laboratory techniques for basophil separation and activation this new development can be further evaluated in terms of efficiency and cost effectiveness.

Acoustofluidic technology has been extensively studied in the groups of Professor Martyn Hill, Dr Peter Glynne-Jones and Dr Dario Carugo within the Bioengineering Laboratory, and the acoustofluidics aspect of the present studies has been carried out in close collaboration with those groups and their PhD researcher Filip Plazonic, to enable the adaption of this technology more effectively for basophil separation from whole blood.

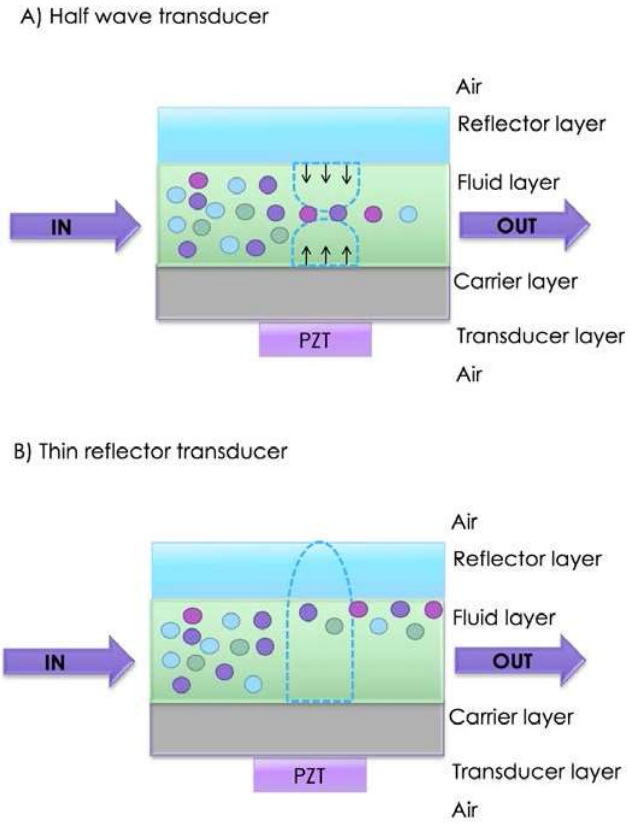

Figure 6: Cross sections of acoustofluidic devices with A) half wave transducer, B) Thin reflector transducer

The blue dotted line indicates the wave and the origin of the pressure node and its location within the boundaries of the acoustofluidic devices. As depicted, in half-wave devices the pressure minima are in the centre of the device and the pressure maxima are at the walls as indicated by the arrows. For the thin reflector device, the pressure node is found in the reflector layer and thus particles are moved up towards the reflector layer.

1.4.5.3 Current application of microfluidics to basophil research

The world of microfluidics is continually expanding, microfluidics centred around basophil research has begun and articles have already been published. For example, label-free measurement of basophils in blood has been achieved by cells passed through a microfluidic device and the application of digital holography and light scattering and quantitive phase imaging (Dannhauser *et al.*, 2017).

The measurement of basophil activation for allergen testing has also been of interest. Currently, there are two devices that have been reported to date. The first is a polymer based centrifugal microfluidic device designed to detect multiple allergens *in vitro* through the measurement of acridine orange release from the granules of KU812 human cell line (Chen *et al.*, 2010). For this experiment, cells were incubated with 0.5 μg/ml acridine orange and later loaded into four reservoirs. Cells that were labelled by released stain during degranulation moved away from the centre and entered the first detection chamber at a low speed (620 rpm). As speed increased, KU812 incubated with acridine orange, patient serum IgE and allergen were released into reaction chamber five. The mixture of the three materials resulted in cell-IgE-Ag complexes and result in acridine orange released into the medium, which will enter the final chamber. Cells labelled will produce fluorescence and thus signify an allergy-positive result. The second microfluidic device employed an electrochemical cell, which measured histamine as a basis for positive basophil activation from RBL-2H3 cells (Kurita *et al.*, 2002). The device contained two electrodes, one coated with Os-polyvinylpyridine mediator with horseradish peroxidase (OS-gel-HRP, containing histamine oxidase), the other was coated with OS-gel-HRP. The electrode containing histamine oxidase was used for the differential measurement of histamine release when RBL-2H3 line became activated and degranulation occurred, the second electrode was used as a reference. The current was measured to determine histamine release to 25 nM.

Current basophil separation and activation has been measured in cell lines and not human blood. In this thesis, a microfluidic device was employed to perform such actions in whole blood.

1.5 Aims & Objectives

Application of a microfluidic platform for the isolation of basophils from whole blood has not been studied, although there have been attempts to separate other rare cells such as circulating tumour cells from larger cell populations (Holmes *et al.*, 2009a). Thus, the aim of is to explore the potential of microfluidic technology for reducing both the complexity of the protocol and the time required for basophil isolation.

In seeking to identify the most appropriate means to carry out basophil isolation with a microfluidic platform for assessing basophil activation *in vitro*, it was necessary to meet the main objectives:

1. Develop a protocol for a novel basophil isolation method for extracting basophils from whole blood
2. Assess and acquire means for determining the extent of basophil activation *in vitro*
3. Develop protocols for measuring basophil activation within a microfluidic device

Chapter 2: Methods

2.1 Basophil purification

With basophils accounting for less than 0.5% of the leukocyte population, their efficient isolation has long presented a challenge. Currently, the main isolation techniques employed for basophils are MACS sorting using *negative* selection, in combination with an initial density gradient centrifugation. Briefly, leukocytes are incubated with an antibody cocktail, which is then mixed with micro-sized magnetic beads, which are coated with antibodies specific for the cell surface antigens: CD2, CD3, CD14, CD15, CD16, CD19, CD24, CD34, CD36, CD45RA, CD56 and glycophorin A. Cells other than basophils become bound to the surface of the beads enabling negative selection of basophils when run through either a magnetic column or entered into a large hollowed magnet. Commercially available procedures are available for this procedure (MACS, Miltenyi Biotec, Tetero, Germany and EasySep, Stemcell Technologies, Vancouver, Canada), but are costly and can take up to 3 hours for each run. In addition, confirmation of the separation can be made either by counting or by a more accurate determination of the percentage purity *via* flow cytometric analysis, extending the length of the procedure and cost further. Therefore, there is a clear need to develop advanced methodologies to address the above challenges. In addition, current techniques require large quantities of blood for separation; by introducing a microfluidic device it would implement a downscaling of materials required to perform the isolation and therefore less blood would be required.

Application of a microfluidic platform for the isolation of basophils from whole blood has not been studied, although there have been attempts to separate other rare cells such as circulating tumour cells from larger cell populations (Holmes *et al.*, 2009a). Thus, the aim of this part of the project was to explore the potential of microfluidic technology for reducing both the complexity of the protocol and the time required for basophil isolation. In seeking to identify the most appropriate means to carry out basophil isolation with a microfluidic platform for assessing basophil activation *in vitro*, it is necessary to:

- Perform and compare current basophil isolation methods to act as a point of reference
- To explore microfluidic platforms that may be appropriate for basophil isolation
- Evaluate currently available and novel procedures to isolate basophils

2.2 Sample collection and preparation

2.2.1 Patient population

The subjects recruited for this study were healthy volunteers such as informal contacts and laboratory personnel who identified themselves as grass pollen or dust mite allergic. Details of the subjects from whom blood was collected for these studies are shown in Table 3. As per the manufacturer's instructions in regards to CD63 expression, a positive subject i.e. a subject that was allergic to the allergen tested was determine as someone whose CD63 expression was ≥ 15% (Buhlmann, Flow Cast Basophil activation test, Schönenbuch, Switzerland). Subjects were recruited using ethics application (Study No. 05/Q1702/9, Southampton Ethics Committee).

2.2.2 Blood samples

Up to 60 ml blood was drawn from the cubital vein of healthy donors with informed consent. The volume depended on the experiment, with 60 ml blood used with density gradient/microfluidic isolation methods and 9 ml for microdevice studies. Blood was collected into 9 ml ethylenediaminetetraacetic acid (EDTA)-coated vacutainers using a winged infusion set. Each vacutainer was inverted eight times before being stored in a carrier for transport of biological samples (Bio-bottle^{TM}). EDTA-coated tubes were used to prevent coagulation of the blood sample. Samples were placed on a roller (Spiramix 5, Denley) at room temperature to ensure mixing.

2.2.3 Staining and cell counting

For cell counting Kimura stain was used containing: 0.05% toluidine blue solution, 0.03% light green solution, saponin white saturated in 50% ethylalcohol, 6% phosphate buffer at pH 6.4 (Kimura *et al.*, 1973). A 20 µl cell sample was withdrawn and mixed with 20 µl stain in a 500 µl aliquot to create a 1/2 dilution. From the aliquot, 10 µl of the suspension was pipetted into a haemocytometer to count the number of basophils. The cells were imaged by mixing 20 µl of the cell sample with 20 µl Kimura stain, and then adding 10 µl was added to a Neubauer haemocytometer to count the number of stained cells on the light microscope (Leitz Wetzlar, Germany) using a 10X objective. This way can be confirmed if necessary by using 45X objective to visualise the multi-lobed nucleus of the basophils. Cell viability was confirmed by NucGreen 488 (Thermofisher, Waltham, Massachusetts, United States); 2 drops were added to 1 ml of cell suspension and an incubated for 15 minutes to highlight any dead cells within the sample.

Table 3: Details of healthy volunteers tested for FACS analysis

Subject No.	Atopic or non-atopic based on medical history	Age	Sex	Known history of allergy	Symptoms
1	Atopic	25	Female	None	N/A
2	Non-atopic	35	Female	Grass pollen	Sneezing, itching
3	Non-atopic	19	Female	None	N/A
4	Non-atopic	32	Female	None	N/A
5	Atopic	20	Female	Peanut, House dust mite	Swollen lips, bronchial constriction
6	Non-atopic	25	Male	None	N/A
7	Atopic	26	Female	Mustard-seed House dust mite	Itching, urticarial
8	Non-Atopic	29	Female	None	N/A
9	Non-atopic	24	Male	None	N/A
10	Non-atopic	26	Male	None	N/A
11	Non-atopic	24	Male	None	N/A
12	Atopic	24	Female	Grass pollen	Flu-like symptoms
13	Non-atopic	26	Female	None	N/A
14	Non-atopic	24	Male	None	N/A
15	Atopic	22	Female	Nut, House dust mite	Urticaria
16	Non-atopic	29	Male	None	N/A

17	Non-atopic	21	Male	None	N/A
18	Atopic	20	Female	Grass pollen	Itchy eyes
19	Atopic	27	Male	Grass pollen	Sneezing
20	Atopic	22	Female	Grass pollen	Sneezing, itching
21	Atopic	31	Male	Grass pollen	Flu like symptoms
22	Atopic	27	Female	Grass pollen	Flu like symptoms
23	Atopic	26	Male	Grass pollen	Sneezing
24	Atopic	26	Female	Grass pollen	Flu like symptoms
25	Atopic	29	Female	House dust mite	Wheezing, flu like symptoms
26	Atopic	28	Female	House dust mite	Sneezing, itchy eyes
27	Atopic	32	Male	House dust mite	Bronchial constriction
28	Atopic	24	Female	House dust mite	Sneezing, itchy eyes
29	Atopic	24	Female	House dust mite	Sneezing, itchy eyes

2.3 Isolation of basophils using density gradient centrifugation and/or negative immunomagnetic separation using both MACS & EasySep

2.3.1 Peripheral blood mononuclear cell (PBMC) isolation using cell density gradient centrifugation

Blood samples were diluted 1/2 with buffer 1X from stock of 10X phosphate buffered saline (PBS, pH 7.4, Gibco, Life Technologies, Waltham, MA, USA), 0.05% bovine serum albumin (BSA, albumin fraction V from bovine serum, ProLabo VWR Chemicals, Radnor, PA, USA). To a centrifuge tube, 9 ml Lymphoprep (density 1.077 g/ml; Fresnius Kabi Norge AS, Østfold, Norway) was added and 9 ml diluted blood was carefully layered on top. Samples were centrifuged at 18°C at 350 *g* for 45 minutes. The layers created as demonstrated in Figure 7 .The plasma layer was removed and expelled in Virkon (Thermo Fisher Scientific, Waltham, PA, USA) using a pipette. The buffy coat layer was obtained using a syringe and placed into a new centrifuge tube with a 1/3 dilution to 1X PBS. The buffy coat was centrifuged at 18°C at 400 g for 10 minutes, and the pellet re-suspended in 9 ml 1X PBS and centrifuged again. Prior to centrifugation, 20 µl sample was withdrawn for cell counting as described in section 2.2.3. The suspension was washed by centrifugation and the pellet was re-suspended. To remove remaining erythrocytes within 9 ml deionised water (dH_2O), vortexed for 6 seconds, and 1 ml 10X PBS was added, removing erythrocytes. The sample was then centrifuged for 10 minutes at 350 *g* at room temperature.

2.3.2 PBMC isolation using dextran density gradient centrifugation

Once fresh blood was acquired, the sample was diluted 1/6 with HetaSep™ (StemCell Technologies); containing hetastarch (6% w/v), sodium chloride, anhydrous sodium lactate, dextrose, calcium chloride dehydrate, potassium chloride, magnesium chloride hexahydrate, in a 15 ml high-clarity polypropylene conical tube (Falcon, Corning, Amsterdam, Netherlands). The conical tube was inverted to ensure mixing and then centrifuged 120 *g* for 6 minutes at room temperature with the brake off. The sample was then incubated at room temperature for 10 minutes to allow further sedimentation until the plasma/erythrocyte interface represented approximately 50% of the total volume as per the manufacturer's instructions (StemCell Technologies). The leukocyte rich plasma layer was harvested into a 50 ml polypropylene conical tube (Falcon) and mixed with a 4-fold volume of 1X RoboSep™ buffer 2 (Stemcell Technologies). The sample was then centrifuged for 10 minutes at 120 *g*, at 37°C with the brake off to remove platelets. If excess platelets were present post centrifugation, this step was repeated. The suspension was decanted into Virkon and re-suspended in 1 ml 1X RoboSep™ buffer 2.

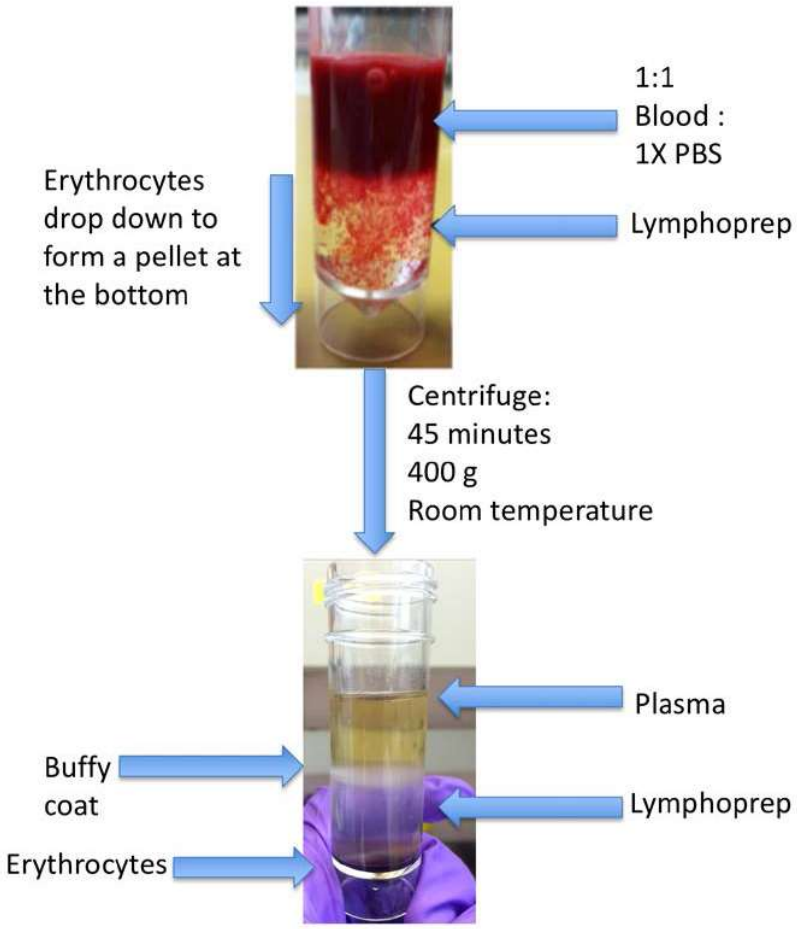

Figure 7**:** Blood separation flow chart demonstrating separation of blood using Lymphoprep

Whole blood was mixed in a suspension at a 1:1 ratio with PBS and then layered on top of an equal volume of Lymphoprep to create a density gradient. This was centrifuged for 45 minutes at 400 *g* at room temperature.

2.3.3 Negative immunomagnetic separation

2.3.3.1 MACS negative selection

MACS is a method for separation of various cell populations depending on their surface antigens as described by Haisch (1999) for separating basophils from whole whole blood to near homogeneity (Haisch *et al.*, 1999). The protocol was continued from that described for the cell density gradient centrifugation. Post centrifugation, and the pellet was aspirated and supernatant re-suspended with 30 µl of buffer (PBS 0.05% BSA), 10 µl of FcR antibody cocktail (containing antibodies against: CD3, CD4, CD7, CD14, CD15, CD16, CD36, CD45RA, HLA-DR and CD235a (glycophorin A), and anti-biotin) and 10 µl FcR blocking reagent using a MACS negative selection (basophil isolation kit II, MACS, Miltenyi Biotec, Germany) as illustrated in Figure 8. The sample was mixed and incubated for 10 minutes in a fridge at 2-8^{o}C. Cells were washed in 2 ml buffer and centrifuged at 300 *g* for 10 minutes; the pellet was aspirated prior to final re-suspension in 500 µl buffer. The MACS MS column was placed in a magnetic field and prepared by washing through with 500 µl buffer. The cell suspension was allowed to flow through the column, and the flow-through fraction was collected. The column was washed with buffer three times with 500 µl and unlabelled cells were collected. The enriched fraction collected was then counted using staining procedure described in section 2.2.3. The remaining cells were centrifuged at 200 *g* for 10 minutes to form a pellet. The pellet was re-suspended in 500 µl of buffer. The sample was then either used for FACS analysis (described in Section 3.2.4.3) or was fixed onto slides using the cytospin as described in Section 2.3.3.4.

2.3.3.2 Basophil enrichment using EasySep immunomagnetic negative selection

The buffer for immunomagnetic negative selection was made by dissolving 0.372 g EDTA in 1000 ml 1X PBS (without Ca++ or Mg++) to create a 1 mM EDTA solution. The EDTA solution was decanted into a flask (490 ml) and 10 ml foetal bovine serum (FBS) was added (2%). Alternatively, the EasySep commercial buffer (Robosep buffer 2, StemCell Technologies) was used alongside the HetaSep blood preparation protocol in Section 2.3.2. The pellet was re-suspended in 1 ml EasySep buffer in a 14 ml polystyrene round-bottomed tube. The protocol for separation is illustrated in Figure 9 with the volumes based on 5x10^{7} cells/ ml. A 50 µl aliquot of EasySep isolation cocktail (EasySep Human Basophil Enrichment Kit, StemCell Technologies) was added that contained monoclonal antibodies was added to the cell-surface antigens: CD2, CD3, CD14, CD15, CD16, CD19, CD24, CD34, CD36, CD45RA, CD56 and glycophorin A. This was added and incubated at room temperature for 10 minutes. EasySep® rapid spheres (magnetic nanoparticles 100 µl) were added to the antibody-cell suspension and incubated for 10 minutes at room temperature. The tube was then placed into the

Big Easy EasySep magnet and incubated for 10 minutes at room temperature. The unbound cell fraction was decanted into a new tube; and this was repeated twice to ensure the enriched fraction remained.

Following the application of the EasySep protocol the purified fraction was centrifuged at 450 *g* for 10 minutes at 4°C. The pellet was re-suspended in 500 µl of EasySep buffer. The cells were imaged by extracting 20 µl of the purified fraction, and mixing with 20 µl Kimura stain as described in section2.2.3. The number of purified numbers were recorded and the purified sample, 50 µl was pipetted per 0.5 ml microcentrifuge tube and stored in the freezer -20°C. These were stored for future use as a standard for basogranulin assays.

2.3.3.3 Flow cytometry analysis using CCR3 for both whole blood and enriched fractions

Briefly, 150 µl aliquot of stimulation buffer (BAT Flow Cytometry kit, Buhlmann, Schönenbuch, Switzerland) was added to 5 ml polystyrene round-bottomed tubes. In addition, 50 µl whole blood, density gradient samples or immunomagnetic negative selection samples were added along with 20 µl stain containing both CCR3-PE (phycoerythrin) and CD63-FITC (fluorescein isothiocyanate) (Basophil Activation Test Flow Cytometry kit, Buhlmann). The two round-bottomed tubes were then incubated in the water bath at 37°C for 15 minutes, avoiding direct sunlight. Following incubation, 2 ml lysing reagent was added to each tube and vortexed lightly for six seconds to remove erythrocytes. This step was not applied to enriched cell fractions, as illustrated in Figure 10. Samples incubated for 10 minutes at room temperature prior to centrifugation (6 minutes at 500 *g* at room temperature). Supernatant was then decanted onto blotting paper. Wash buffer (300 µl, Buhlmann basophil activation test flow cytometry kit) was then added to each tube. Stained cells after re suspension were then processed in the FACS calibur for analysis.

FACS Calibur, flow cytometry equipment capable of detecting four colours (BD Biosciences) was pre-set with beads for compensation and values of FITC and PE were entered into the software as too few basophils in samples to carry compensation on the machine. The negative sample was used to acquire the initial gating. Positive controls, such as FMLP and Fc RI, were used to determine that the sample was valid, thus determining that the basophils were functional. Following this, the experimental samples containing allergen could be tested. All steps are illustrated in Figure 11. Further analysis of FACS data was performed with FlowJo software (BD Biosciences, New Jersey, USA) in order to obtain the percentage of CD63 positive and CD63 negative cells within the basophil gate.

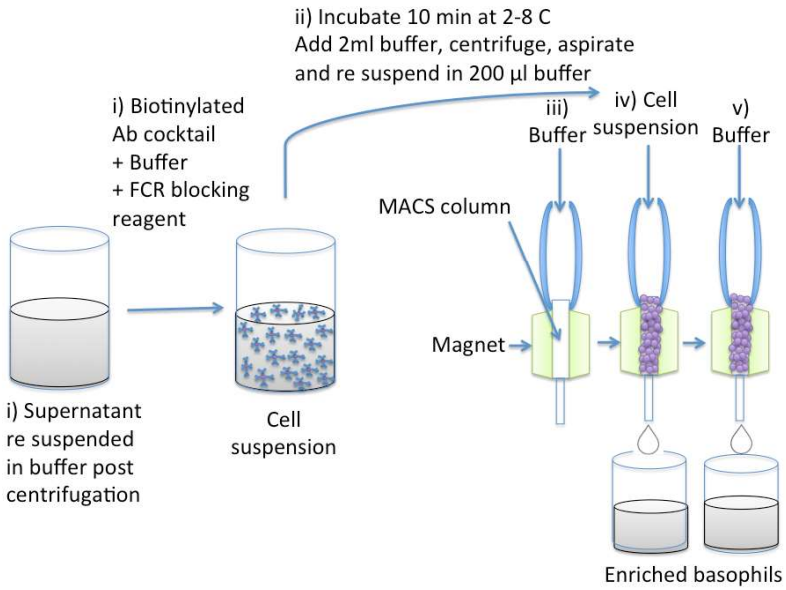

Figure 8: Isolation of basophils from buffy coat using negative selection MACS

i) FcR Blocking reagent and 10 µl of basophil biotin-antibody cocktail were added to cell supernatant. ii) Sample was mixed and incubated for 10 minutes. Cells were washed in 2 ml buffer and centrifuged for 10 minutes; the pellet was aspirated and re-suspended in buffer. iii) MACS MS column was placed in a magnetic field and washed with buffer. iv) The cell suspension was allowed to flow through the column, and the flow-through fraction was collected. v) The column was washed with buffer three times with buffer and unlabelled cells were collected.

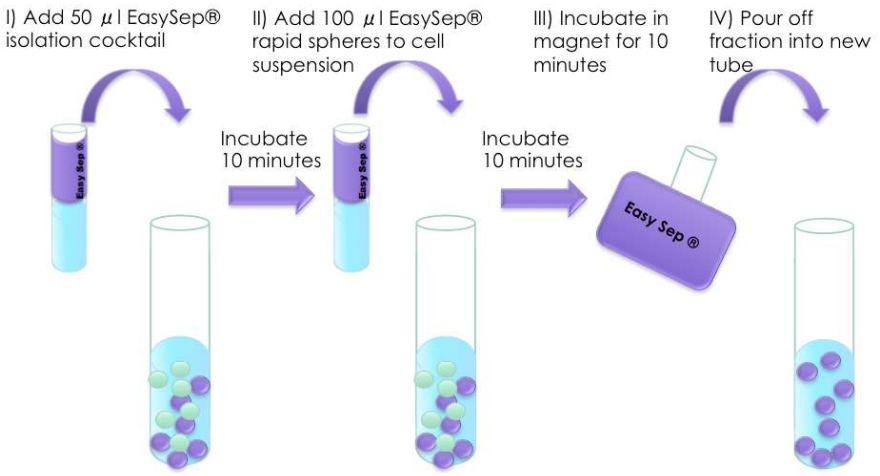

Figure 9: EasySep enrichment protocol (Adapted from Gibbs *et al* 2008)

i) A 50 µl aliquot of EasySep isolation cocktail was added that contained monoclonal antibodies and incubated at room temperature for 10 minutes. ii) EasySep® rapid spheres were added to the antibody-cell suspension and incubated for 10 minutes at room temperature. iii) The tube was then placed into the Big Easy EasySep magnet and incubated for 10 minutes at room temperature. iv) The unbound cell fraction was decanted into a new tube; and steps iii) and IV) were repeated.

A)

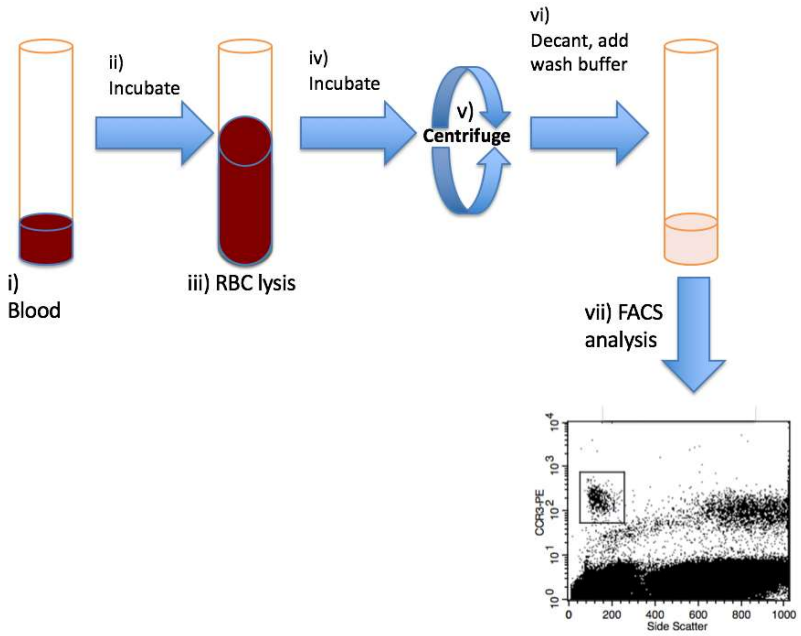

B)

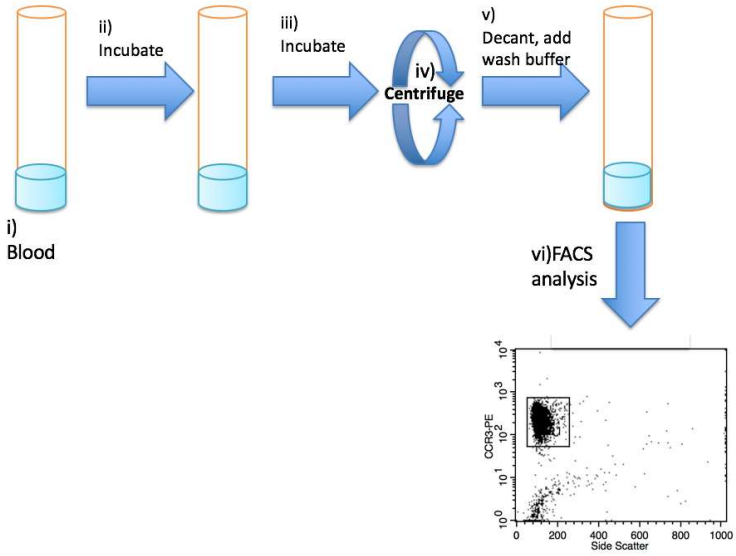

Figure 10: FACS protocol for (A) whole blood, (B) enriched fraction (Adapted from (Gibbs *et al.*, 2008))
A) (i) Once 20 µl staining reagent was added, tubes were covered with foil. (ii) Samples were incubated in the water bath for 15 minutes. (iii) lysing reagent was added to each tube (iv) Samples incubated for 10 minutes. (v) Samples were centrifuged (vi) Supernatant was then decanted onto blotting paper. Wash buffer was then added to each tube (vii) FACS analysis
B) The above steps were repeated without the erythrocyte lysis step

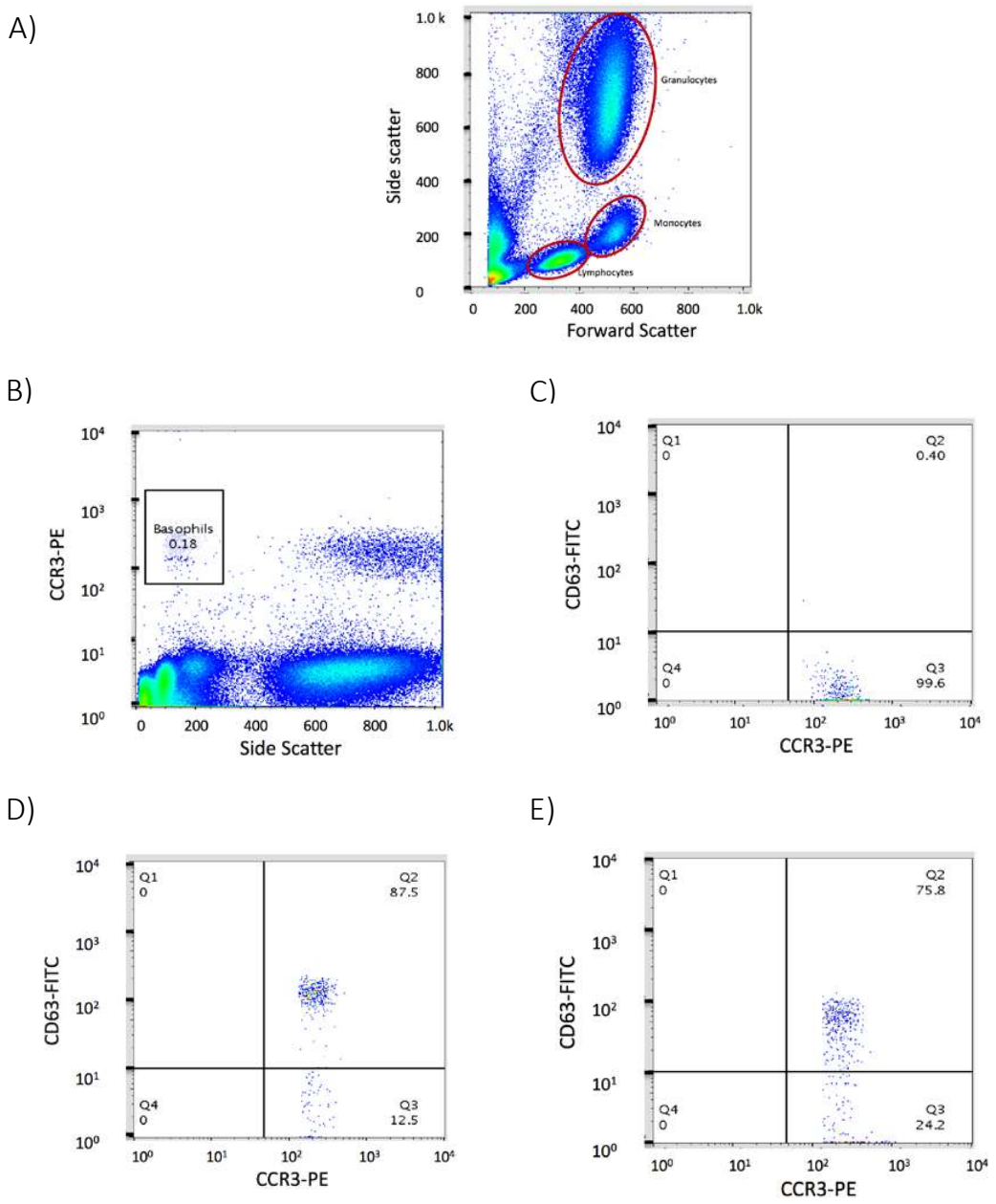

Figure 11: Flow cytometric data acquisition using negative control (stimulation buffer) to acquire correct parameters using whole blood

A) Forward scatter (FSC) and side scatter (SSC) were plotted to ensure the leukocyte population was separated into three discrete populations. B) A second histogram plotted CCR3-PE against SSC to determine region one (R1) to select 500 events for cells which were $CCR3^{Positive}$ / SSC^{Low} to exclude eosinophils (SSC^{High}). C) CD63-FITC against CCR3-PE was plotted within R1 to determine percentage of $CD63^{Positive}$ cells by drawing quadrants to determine activated (Upper Right (UR) quadrant) and inactivated (Lower Right (LR) quadrant) basophils for C) Negative control (0.4% activated) of cells stimulated with FACS buffer D) positive control anti-FcεRI (87.5% activated) E) Positive control of cells stimulated with FMLP (75.8% activated). Analysis of quadrants enabled the percentage of activated (UR) basophils to be determined.

2.3.3.4 Cytocentrifugation

In order to concentrate the small population of basophils on a slide, cytocentrifugation was employed. Poly-L-lysine coated slides were inserted into a cytospin device chamber and blotter (Cytospin 3, Shandon, Scotland). Firstly, the basophil pellet was re-suspended in 2 ml 2% paraformaldehyde and incubated at room temperature for 10 minutes. The sample was centrifuged at 200 *g* for 10 minutes and the pellet was washed in 500 µl 1X PBS. Next, 100 µl of the fixed basophils containing x 10^6 basophils were added into each slide chamber. Centrifugation was for three minutes at 500 *g* at room temperature. Chambers were then removed from the cytospin, opened and the blotter was carefully removed. Lastly, the slide was removed from the chamber and left to dry overnight. Depending on the experiment, slides were stained with alcian blue stain to quantify basophils.

2.3.3.5 Lysate preparation and storage

In order to determine the stability of basogranulin under various storage conditions, the assay was conducted using samples that had been collected fresh on the day, and then repeated using sample stored in the freezer for one week. To a basophil-enriched fraction, 1.8 ml distilled water was added and stored overnight at -20°C. Samples were freeze-thawed and 200 µl 10X PBS was added to make a 1/10 dilution. Sample was vortexed prior to centrifugation at 450 *g* for 10 minutes. Sample was then re suspended in 1.5 ml 1X PBS and then syphoned into aliquots of 100 µl, containing 1x10^6 cells, to be stored in the freezer -20°C to be tested for basogranulin using BB1 as primary antibody in a dot blot procedure as described later in Section 2.6.2.

2.3.4 The effect of erythrocyte depletion agents on basophil function

Various agents and procedures that deplete erythrocytes have been widely used for enriching leukocyte populations from whole blood. Among these is saponin that has been employed when using an impedance cytometer for cell separation (Holmes *et al.*, 2009b). In order to test whether basophils remain viable and functional after exposure to erythrocyte depleting agents; saponin, ammonium chloride and hypotonic shock treatments were investigated on whole blood samples. A mixed leukocyte population of cells were then tested for histamine release in response to various stimuli.

2.3.4.1 Saponin erythrocyte depletion

Blood (2 ml) was added to a 50 ml tube containing 10.6 ml of saponin (0.05%) depletion solution and a final concentration of 0.12% w/v formic acid as employed by Hans *et al* (2012) in a study involving microfluidic erythrocyte depletion of human blood for leukocyte analysis (Han *et al.*, 2012). The solution was vigorously vortexed and the reaction was stopped after 6 seconds with 1 ml quench solution 0.06% w/v sodium carbonate (3% w/v sodium chloride). Tubes were centrifuged for 10 minutes at 500 *g* at 20^{o}C. Excess buffer was removed from the centrifuged sample and the pellet was re-suspended in 950 µl of Tyrode's buffer. From the sample 200 µl was aliquotted and 800 µl of distilled water was added, and this was freeze-thawed twice for total histamine release measurements using dry ice. Cells were used for a later experiment.

2.3.4.2 Ammonium chloride erythrocyte depletion

Erythrocyte depletion stock solution (10X) was made using ammonium chloride (NH_4Cl, 8.02 g), sodium hydrogen carbonate ($NaHCO_3$, 0.84 g), EDTA (0.37 g) and made up to 100 ml with distilled water. A working erythrocyte depletion buffer 1X ammonium chloride solution was made with a 1/10 dilution of stock solution (10X) with distilled water and left at room temperature until use. To 20 ml of erythrocyte depletion buffer, 1 ml of whole blood was added and mixed gently. The samples were then wrapped in foil and incubated for 15 minutes on the roller. Samples were then centrifuged at 350 *g* for 10 minutes at room temperature and re suspended in 6 ml of Tyrode's buffer. For total histamine determination, 200 µl of sample was aliquotted and 800 µl distilled water was added to be freeze-thawed twice-using dry ice. The supernatant was aspirated from the centrifuged sample, allowing the pellet to be re-suspended in 5 ml (1/6 dilution) 1X Tyrode's release buffer, creating 6 ml total volume, ready for use.

2.3.4.3 Hypotonic shock erythrocyte depletion

Whole blood (1 ml) was added to 9 ml distilled water and vortexed for 10 seconds. Immediately following this, 1 ml of 10X PBS was added to a 15 ml tube. The sample was centrifuged at 350 *g* for 5 minutes. The 200 µl sample was aliquotted and 800 µl of distilled water was added to be freeze thawed twice using dry ice. Supernatant from original sample was aspirated and re-suspended in 5 ml 1X Tyrode's buffer.

2.4 Isolation of basophils using microfluidic platforms

Two types of microfluidic platforms were explored, namely, spiral sorter and acoustofluidic based microfluidic platforms. The spiral sorter was an inertial force based microfluidic device, which can allow size-based separation of larger sized leukocytes from whole blood. The acoustofluidic based microfluidic platform was designed to take advantage of combining both acoustic force (for placing mixed blood cells on an antibody-coated surface) and antigen-antibody binding force with antibodies specific for basophils to enable basophil capture. These devices were used to compare two different approaches and determine which would be appropriate for this work; a closed (spiral sorter) and an open device (acoustofluidic device) for blood separation. The spiral sorter was chosen as a closed device because previous work by Chatterjee *et al* (2011) has modelled whole blood separation into different leukocyte populations by using beads based on the different leukocyte populations. In addition, there have been numerous studies working with spiral sorters and whole blood suggesting that the isolation of basophils could be achieved (Bhagat *et al.*, 2008; Wu *et al.*, 2012b; Nivedita and Papautsky, 2013). Wu *et al* achieved 80% separation efficiency of polymorphonuclear leukocytes (7 – 10 μm sphere) and mononuclear leukocytes (10 – 12 μm sphere) from whole blood using a trapezoid cross-section spiral sorter providing a label free method of separation. Therefore basophils 12-15 μm sphere from whole blood, (and the remaining leukocyte population), could be separated using this label-free methodology.

The device adapted in these studies was originally used for the separation of bacteria from water. In this study, the concentration of bacteria was increased 60 fold by using a thin reflector device to enable bacteria to exit *via* a different outlet to be reviewed by microbial analysis. Therefore, a thin reflector device could be adapted so that the reflector layer acts as a basophil capture zone, by coating a basophil specific antibody onto the reflector, thus maximising basophil isolation from whole blood without affecting spontaneous histamine release.

2.4.1 Spiral Sorter

2.4.1.1 Design & fabrication

Originally, pre-made spiral sorter chips were obtained in both zeanor and poly (methyl methacrylate) (PMMA) form (dimensions illustrated in Figure 12: Dimensions of spiral sorters supplied by Microfluidic Chipshop (labelled A, B, C, D) Each has a single inlet in the centre and multiple outlets and Table 4; Microfluidic Chipshop, Germany). The aim was to carry out preliminary tests with beads prior to fabricating a spiral sorter with optimal parameters for blood separation. The premade chips were initially selected to determine parameters required for basophil separation from whole blood.

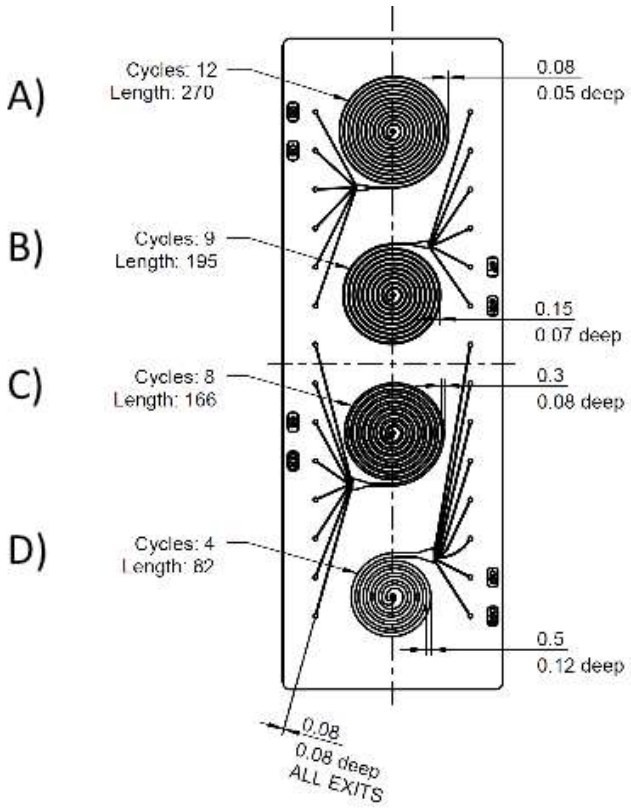

Figure 12: Dimensions of spiral sorters supplied by Microfluidic Chipshop (labelled A, B, C, D) Each has a single inlet in the centre and multiple outlets

Table 4: Parameters of each spiral sorter tested

	No. of Cycles	Length (mm)	No. of outlets	Width (µm)	Depth (µm)
A	12	270	6	80	50
B	9	195	6	150	70
C	8	166	8	300	80
D	4	82	8	500	120

2.4.1.2 Platform set up

In order to efficiently identify the microparticles that were to be used in the device, a camera speed of 150 frames per second were used to captured *via* CCD camera (Thor 2, Thorlabs, New Jersey, USA). The original set-up is depicted in Figure 16. In addition, it was found that the inlet connections could not withstand flow rates higher than 5 ml/h without leaking and thus the surface of the micro tubing were modified. The end of the tubing into the outlet was coated with PTFE tape to provide a tight seal and prevent the tubing blocking the micro channel with any fibres it may contain post washing. Epoxy glue was used to secure the inlet into place and prevent any future leakages and ensure an airtight seal, as shown in Figure 14. With the new surface adaption, the device was able to withstand flow rates up to 25 ml/h without leaking or causing any damage to the device. A gas tight Hamilton syringe (USA) was used to prevent air bubbles/contamination and fixed to the inlet *via* screw connectors at the non-glued end of the tubing. This had previously been an issue causing fibrous strands to block the outlets, causing clogging in the device and preventing beads from exiting the outlets. Additionally, due to the sorter being a closed system, it was harder to unclog and thus vigorous sessions of plunging detergent in and out of the device *via* a syringe were required for unclogging.

2.4.1.3 Initial testing of spiral sorter

A particle suspension was created to contain both $2.5x10^6$ polystyrene 4.5 µm beads and 15 µm beads in water and drawn up into syringe and placed in a syringe pump at varying flow rates from 0.1 ml/h to 25 ml/h. Bead sizes were chosen based on their similarity to erythrocytes (4.5 µm) and leukocytes (15 µm). In later experiments, this suspension was modified to simulate the viscosity of whole blood; microparticles were suspended in 25 parts detergent (liquid soap), 75 part distilled water. These were microparticles with diameters of 2, 4.5, 6, 10, 12 & 15 µm (latex beads, carboxylate modified polystyrene, Sigma Aldrich, USA). Different sizes of microparticles were used either singularly or combined in mixed sizes within each of the four spiral channels at flow rates varying from 0.5-25 ml/h. Work on the optimisation of the spiral sorters was undertaken in collaboration with visiting researcher Dr Yuchao Zhao.

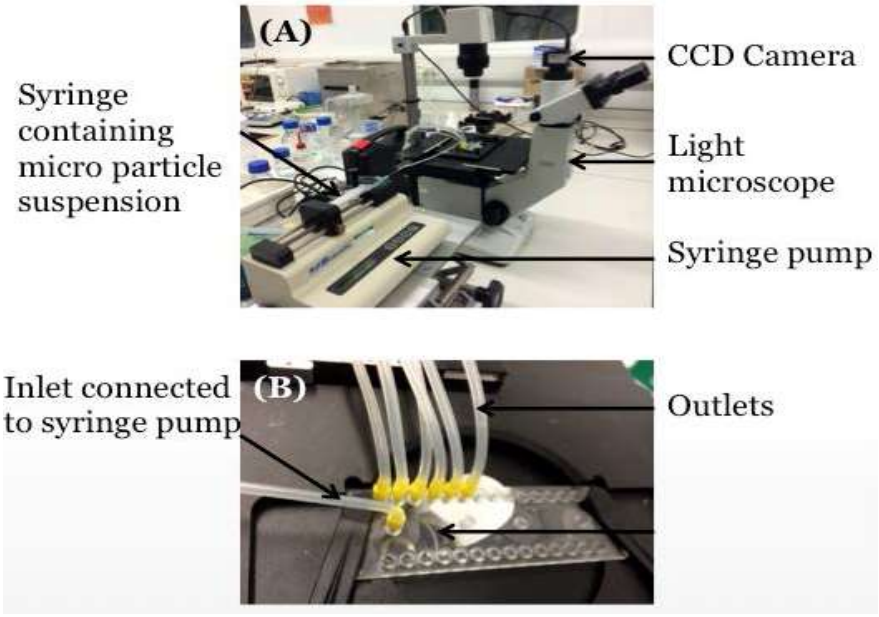

Figure 13: Experimental set up of spiral chip

(A) Experimental set-up of microscope; images were captured using a Thor 2 CCD camera.

(B) Capillary tubing (inner diameter 500 μm, 1/16" Up-church Scientific, Worcestershire, England) was connected from the syringe to the inlet of the device and more tubing was linked from the outlets of the device into tubes.

The syringe pump (Harvard apparatus pump 11 Elite, USA) that controlled flow rate into the inlet at the centre of the devices was connected to the inlet *via* polytetrafluoroethylene (PTFE) tubing. The syringe pump controlled flow rate into the inlet at the centre of the devices, it was connected to the inlet *via* PTFE tubing. The microscope (Leitz Wetzlar, Germany) and CCD camera (Thor 2 1280 x 1024 pixels) were positioned over the chip outlets to record particle preference at the outlets at 500 frames per second.

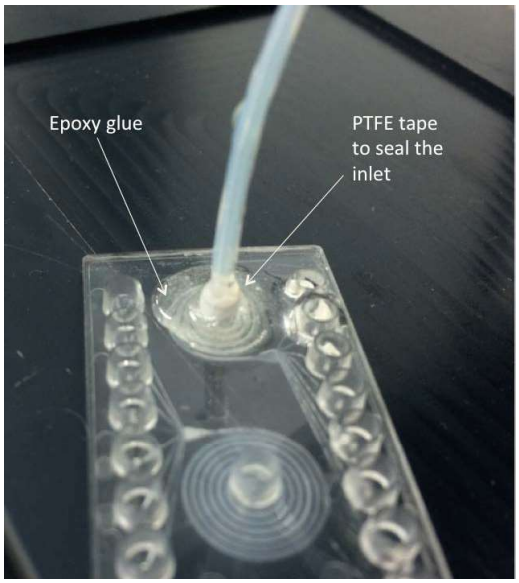

Figure 14: Modifications to the spiral sorter to optimise flow rate and prevent leakage on Spiral D

PTFE tape was wrapped around the bottom of the PTFE tubing to create a tight seal. Epoxy glue was additionally used to create an airtight seal and keep the tubing in place to ensure minimal chance of leakage at the inlet when the bead suspension was pumped into the device.

2.4.1.4 Experimental techniques using blood

After optimisation of the device using both beads and surface adaptions of the structure, the device was ready to use with blood in Spiral 'B' and Spiral 'C' (both were found to be best for particle sorting as described in the results Section 3.1.2. As indicated previously, 4 ml blood samples were acquired *via* venepuncture into heparin-coated vacutainers. Samples were diluted with 1X PBS into 1/10, 1/100, 1/200, and 1/500 prior to entering the device. Millipore filtered water was initially pumped through the device; followed by EDTA. Dilutions were tested in the device at 2.5-20 ml/h at 2.5 ml intervals. 500 images/second were acquired at each flow rate at different dilution factors. It was calculated that there were approximately 500 erythrocytes/ leukocyte in a 1/10 dilution.

2.4.2 Acoustofluidic device

2.4.2.1 Design and fabrication

The design and fabrication of the acoustofluidic device for basophil isolation was based on a previously used device for bacteria manipulation, which was developed by Filip Plazonic (Mechatronic Research Group, Faculty of Engineering and the Environment). The main structure of the device (as depicted in Figure 6) comprised four layers with air boundaries on either side, a stainless steel carrier layer and a glass reflector layer, where a lead zirconate titanate (PZT) transducer was attached to the bottom of the carrier layer and the fluid flew between the carrier and reflector layers demonstrated in Figure 15.

The first section within the channel was the half wave section (Figure 15 C), where the transducer emits a half-wave resonance frequency to focus cells to the centre plane of the channel. The second part of the channel is a thin-reflector section (Figure 15 C) that forces cells up onto the anti-CD203c coated reflector layer (1 mm glass slide) to enable binding. Planarity of cells, based on the thin-reflector standing wave, vastly improves the percentage of cells reaching the reflector by ensuring all cells take the same time to be pushed up before exiting the channel. Due to the size of basophils, in comparison to bacteria, only the thin reflector part of this device was used for basophil isolation on the slide, as this was effective enough.

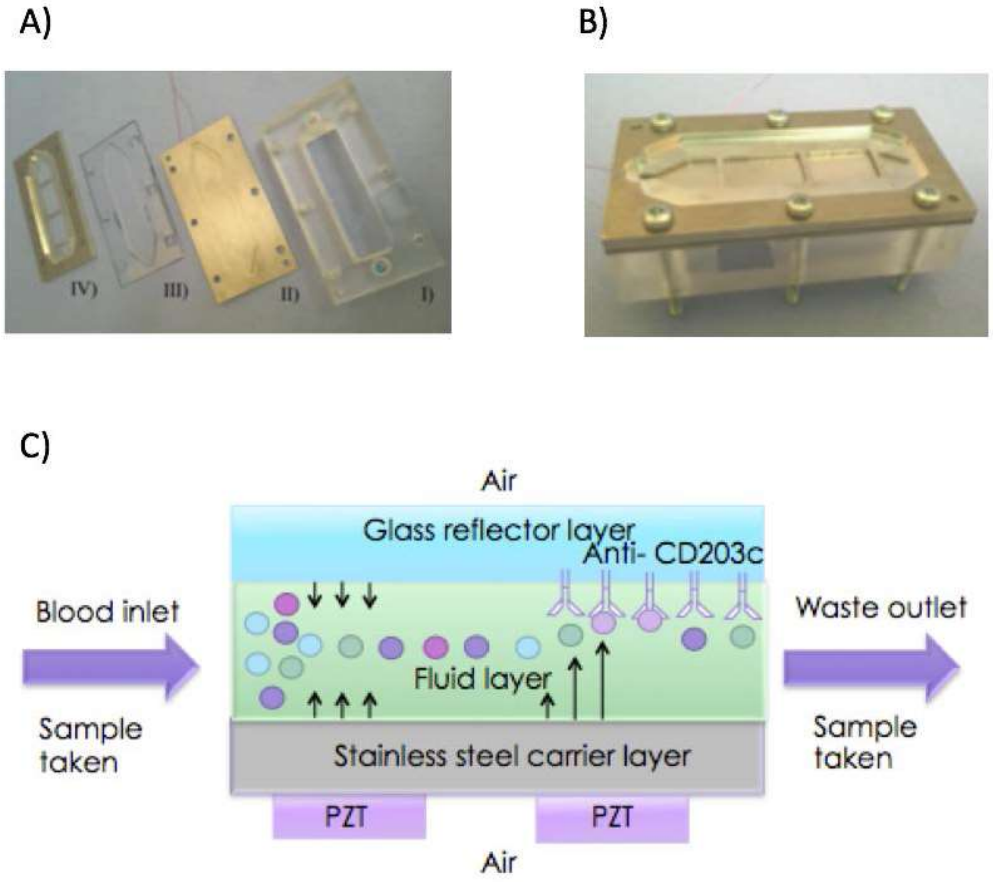

Figure 15: Depiction of the steel carrier layer device (SCL); dimensions depicted in Table 5

A I) Acrylic manifold II) SCL with transducers on the back side and the groove that creates the fluid channel to which the gasket fits into III) Cellulose acetate spacer IV) Metal frame. Glass cover slip slots between III) and IV).

B) Assembled device

Schematic of the half wave/ thin resonator device

Table 5: Parameters of SCL 1000 device

Component	Length (µm)	Width (mm)	Height (mm)
PZT Transducer	1000	12	21
Carrier Layer	900	75	40
Fluid Layer	130	12	63
Reflector layer	170	75	22

The device manifold was manufactured by the Engineering Design and Manufacturing Centre (EDMC) within the Faculty of Engineering and the Environment. The channel created was approximately 100 µm thick (with approximately 120 pN radiation by using the stainless steel carrier layer demonstrated in Figure 16; which means the highest resonance to push the cells up to the reflector layer can be achieved). The two transducers oscillate at different voltages and based on compressibility and density of material entering the device it is possible to predict suitable amplitude to allow particles to be concentrated in the centre plane of the device.

Theoretical analysis was carried out to identify the optimal thickness for a stainless steel carrier layer. In addition, the force experienced by a particle in the fluid layer for a variety of carrier layer thicknesses and materials prior to fabrication, examining the following materials:

- Glass (*rho* = 2500 kg/m^3, *c* = 5872 m/s),
- Macor (*rho* = 2540 kg/m^3, *c* = 5510 m/s),
- Stainless steel (*rho* = 7890 kg/m^3, *c* = 5790 m/s),
- Aluminium (*rho* = 2730 kg/m^3, *c* = 6380).

Where *rho* is density of the material, and *c* is conductance

The carrier thickness was explored in 100 µm steps from 100 µm to 1400 µm. The top was chosen as such because at that point the force started to severely drop and the optimal thickness had already been reached.

The keystroke-level model (KLM) was a 1D mathematical impedance-based model implemented in MATLAB used to estimate the force inside the fluid layer and an additional script was implemented to capture the force data from the bottom (at the carrier layer), middle, and the top (at the reflector layer) of the fluid layer. This was then plotted for all four materials. Thus calculating how much energy is transferred between layers depending on the impedance mismatch.

The thicknesses of each of the other layers were chosen as Transducer = 1000 µm, Silver = 1 µm, Glue = 1 µm, Carrier – Variable, Fluid = 100 µm, Reflector = 170 µm. The *Q* factor was 100 for all layers (viscous boundary correction factor). When the fluid layer was changed by 10 µm in either way, the results were not significantly impacted.

Based on findings with the simulation experiments, designs were made for two acoustofluidic device designs and the device main manifolds were fabricated in EDMC, creating two sets of two carrier layers in stainless steel that had the same design as the initial carrier layer.

The two carrier layers implemented into devices were:

- Stainless steel carrier layer 1000 µm thick - SCL1000
- Stainless steel carrier layer 600 µm thick - SCL600

A)

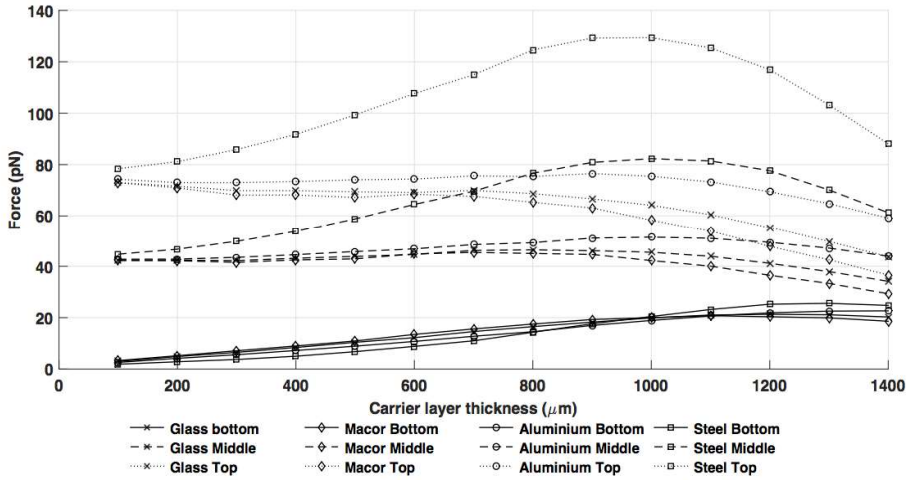

B)

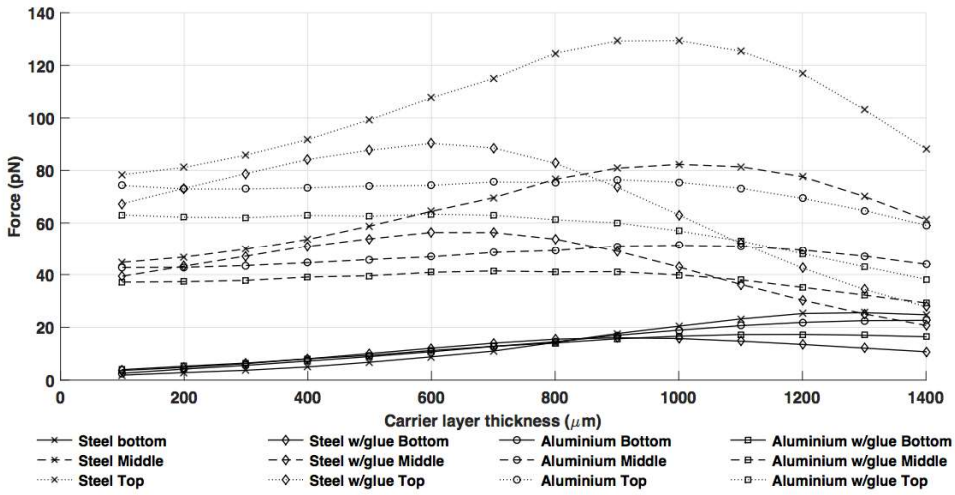

Figure 16: Depiction of the variability of radiation force on a 10 µm bead when using A) carrier layer thickness variation throughout the fluid layer, B) when the glue layer is either 1 µm or 10 µm thick A) The force changes are shown with varying carrier layer thicknesses for the three points in the fluid layer. Stainless steel, with its high speed of sound and density that matched that of the transducer (*rho* = 7700 kg/m^3, *c* = 4529.8 m/s) was taken as the best choice as it provided the highest force. The best thickness (through compromise) was at 1000 µm. The performance of the device was insensitive to small changes in the carrier layer thickness. B) Demonstrates how aluminum and stainless steel would perform with a glue layer that is 10 µm thick, and with a *Q* factor of 30. The best thickness is reduced from 1000 to 600 µm for stainless steel, which is still the best option.

2.4.2.2 Initial testing of the acoustofluidic device

The glass cover slide was washed with 70% ethanol; the device was assembled and kept planar to maintain the standing wave.

The impedance and admittance were measured over a wide range of frequency with a Cyphergraph oscillope (San Mateo, USA) which were plotted using Cyphergraph and its corresponding software (Cypher instruments C-60 impedance analyser) to determine the desired frequency. Firstly, air was pumped through the device and plots were run, secondly distilled water was run through the device with a syringe with no beads and no flow rate (peak expected at 1 MHz). The impedance comparison between air and blood determined the resonant frequency of the fluid channel by determining the peak that appears on the blood graph but not the air graph. A sample plot is illustrated in Figure 17.

Once the potential resonance frequency was determined, the direct digital synthesiser (DDS) function generator was switched on to detect the drop and rise in amplitude. Pumping a bead suspension of an unknown concentration into the device tested the model predictions. This was pumped using either a BD Plastipak 3 ml or 12 ml syringe (Becton Dickinson, USA) attached to (Harvard apparatus pump 11 Elite, USA) syringe pump. The syringe was connected *via* PTFE tubing (inner diameter 500 µm, 1/16" Up-church Scientific, USA), secured to the inlet by screw fitting (Upchurch). Halogen light source was switched on the microscope and a sweep was performed between 7.7 Vpp – 21 Vpp. Images were taken at 10X and 4X magnification in the carrier layer. Waste exits *via* the same tubing as the inlet, however is connected to a 50 ml conical tube. The acoustofluidic device set-up is depicted in Figure 18 and Figure 19.

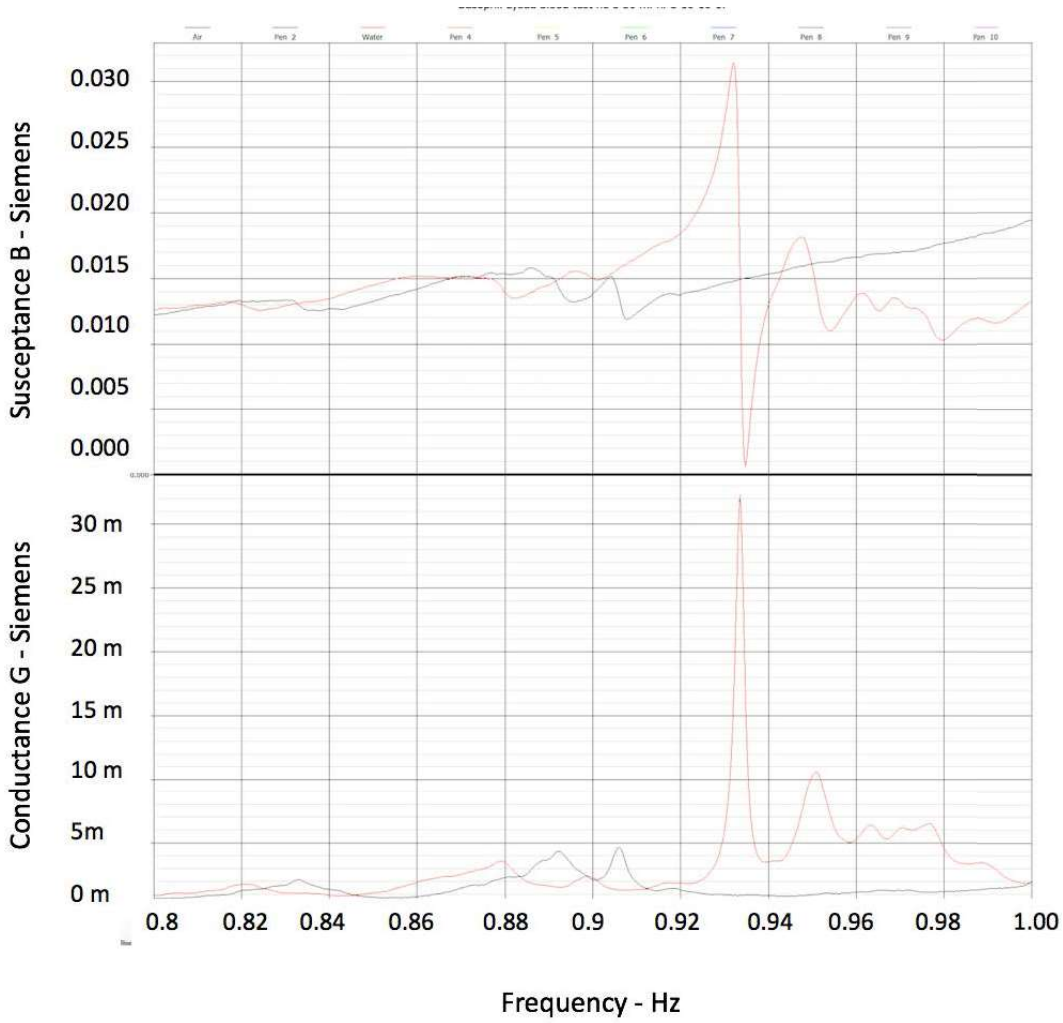

Figure 17: Impedance plots of air (black) and blood (red) preparation within the HW/TR device

Both air and water's conductance were plotted in Hz against each other using different colours to distinguish between the two. The peak present in blood and not air (32 mS) at approximately 880 MHz was investigated to determine the resonance. For this example, the resonance was found to be from 885 MHz and thus a continuous sweep (20 mHz) was performed throughout the experiment once the syringe pump had started.

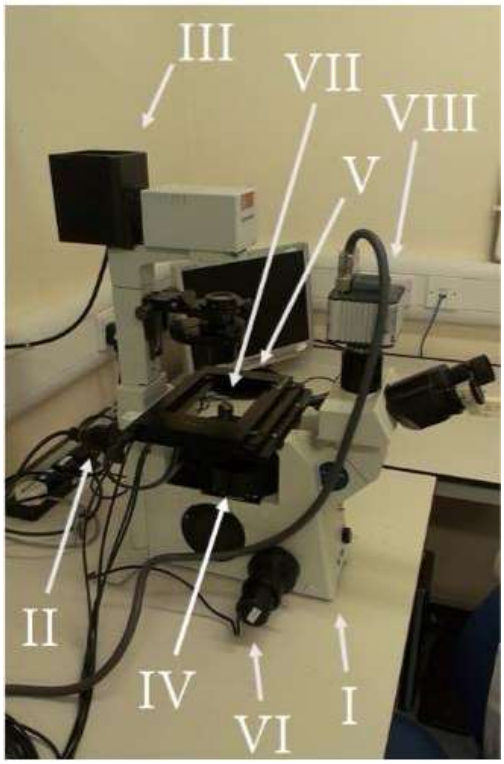

Figure 18: Microscope set up

I) Inverted microscope,
II) Halogen light source,
III) Visible light source,
IV) FITC cube,
V) Automated XY stage,
VI) Automated Z-stage,
VII) Objective turret,
VIII) Charged Coupled Device (CCD) camera

The device was mounted on an automated XY stage (Thorlabs MLS203). In order to take full images of the whole slide once the basophils were fixed, a Z stage (Prior ES10ZE) was added.

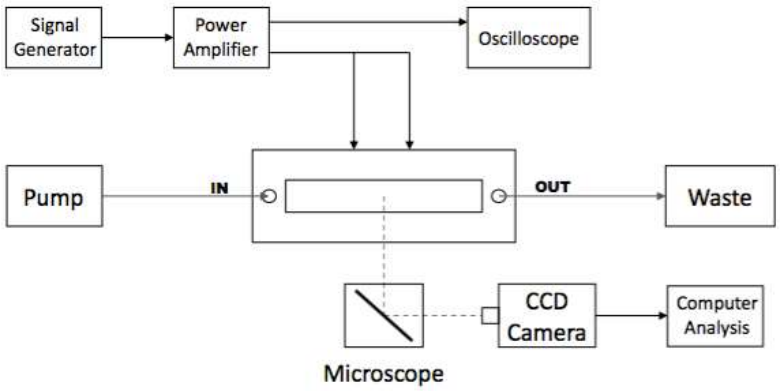

Figure 19: Schematic diagram of the experimental setup for the thin resonator (TR) resonator device, flow controls, sine-wave generation, and imaging

The custom-made power amplifier was driven by a programmable signal generator (TTi TG2000 20 MHz direct digital synthesizer (DDS) Function Generator) enabling signal modification. The signal output was connected to the transducer by two wires. The oscillope (Agilent Technologies DSO1102B Digital Storage Oscillope) was connected to the circuit (as shown) to measure amplitude and frequency going to the transducer. Images on the inverted microscope (shown in Figure 18) were taken *via* CCD camera (Thor Technologies) to enable identification of basophils. Preliminary identification of basophils on the set-up was completed using purified basophils fixed on PLL slides in paraformaldehyde.

2.4.2.3 Acoustic platform setup

In order to visualise basophils using the Kimura stain, a colour camera was employed (Retiga 2000 RGB camera, Q-Imaging, Canada). However, this camera is not commonly used with micromanager and thus additional software and white balance calibrations were required. The following parameters were found to be suitable and used: 2.5849 blue, 1.011 green, and 1.000 red using the G-B-R-G setting for the adaptor smooth hue 8-bit. To identify basophils a scale bar was used within Image J software (National Institute of Health, Maryland, USA). This was created by measuring one side of a square within a haemocytometer (0.05 mm) in pixels to determine how many pixels there were per μm. Based on this, it was possible to estimate the size of a basophil in pixels.

2.4.2.4 In-house antibody printing

To enable specific binding of basophils to the top surface of the flow channel, i.e., the inside surface of the reflector layer which was a glass slide. The inside surface of the slide was coated/printed with antibodies. Originally, anti-IgE was used as the capture antibody, but because of its potential to activate basophils through cross-linking of IgE on high affinity IgE receptors, anti-CD203c was chosen as an alternative. Basophils express CD203c on their surface, and these are up regulated on basophil activation. Basophils should not become activated when bound by this antibody.

Pure human CD203c antibodies, 30 μl (dilution 1:11, clone FR3 16A11, Miltenyi Biotec, Bergish Gladbach, Germany) were printed at 50% relative humidity onto a glass slide coated with N-hydroxysuccinimide (Nexterion Slide H, Schott, Germany). The slides were incubated in slide holders designed by Filip Plazonic depicted in Figure 20, these were made to ensure maximum surface area coverage and additionally prevent the use of a microscope slide to cover in-house (IH) slide whilst incubating. The principles of slide coating and printing are depicted in Figure 21. Slides were placed in a slide humidity chamber at 75% humidity overnight to ensure maximum coupling efficiency to the surface. The slides were submerged in blocking solution (25 mM ethanolamine (C_2H_7NO) in 100 mM sodium borate ($Na_2B_4O_7.10H_2O$) buffer at pH 8.5) for 1 hour to deactivate remaining functional groups in a clean conical tube. The slides were then washed three times with washing buffer I (137 mM sodium chloride (NaCl), 2.7 mM potassium chloride (KCl), 4.3 mM disodium phosphate (Na_2HPO_4) at pH 7.5 with 0.05% Tween 20) and then washed with distilled water. The slides were then dried in air, ready for insertion into the device.

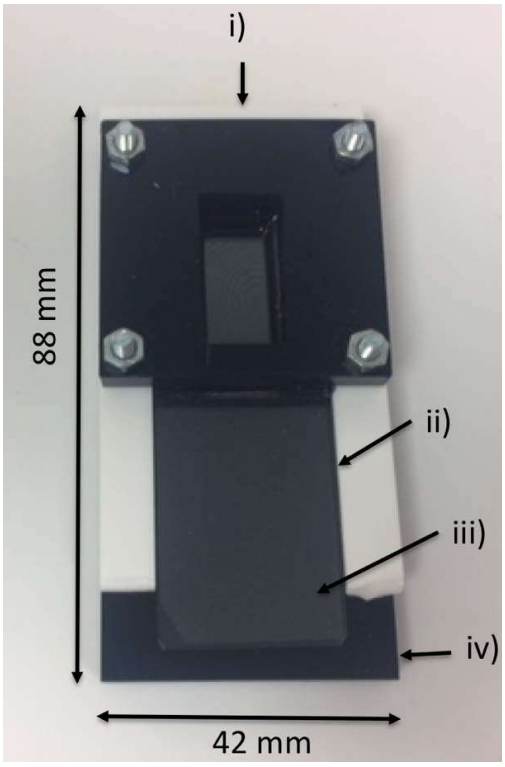

Figure 20: Slide holders for antibody printing 42 x 88 mm

i) Window for the antibody to be pipetted onto the slide, creating the active area for basophil binding

ii) Barrier of the slide holder to ensure the slide fits tightly and there are no leakages

iii) Slide holder, where the IH slide would be inserted

iv) Base of the slide holder

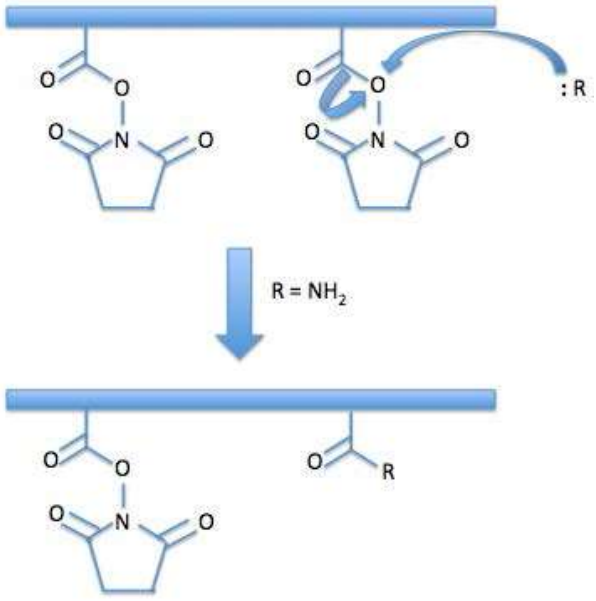

Figure 21: Antibody coated slide covalent binding to exposed antibody amine groups (R)

The antibody coated Nexterion slides have a multi-component polymer layer, which contains N-hydroxysuccinimide (NHS) esters which can react with the amine groups (R) of anti-CD203c antibody. This occurs *via* the activated carboxylic acid groups within the NHS allowing covalent immobilisation of antibodies to the surface of the glass slide. The resistant polymer based layer of the slides inhibits non-specific binding

2.4.2.5 Outsourced slide printing

Polymer dip pen nanolithography is a hybrid between lipid dip pen nanolithography (whereby the phospholipid head group is modified as ink to create a pattern) and micro contact printing (μCP). It creates arrays by 'drawing' on the surface of the slide by manipulating the tip of an atomic force microscope to create a pen (Sekula-Neuner *et al.*, 2012; Kumar *et al.*, 2016). Polymer dip pen nanolithography works by repeated stamping to create a pattern, this method enables printing of large areas (cm^2), flexibility of design and offers an inexpensive fast way to coat slides by using less material 5 μl antibody per slide (Kumar *et al.*, 2016). Microscope coverslips (75 x 25 mm, Logitech) were coated with 3-(glycidoxypropyl)-trimethoxysilane (GPTMS) prior to polymer dip pen nanolithography with anti-human CD203c. The writing procedure was conducted by spin coating 2 μl biotinylated pure anti-human CD203c (Miltentyi Biotech) onto a 5 x 5 mm stamp with a pitch of 100 μm at 3000 rpm for 10 seconds. This was then printed onto GPTMS coated glass at 60 – 80 % relative humidity and left to incubate over night. The slide was first washed with distilled water before being blocked with 10X BSA for 20 minutes. Slides were then washed three times with distilled water and then incubated with streptavidin (STV_cy3) for 30 minutes. Lastly, the slides were washed three times with distilled water and left to dry. In order to image the slides to observe the binding, slides were blocked with 10X BSA for 40 minutes at room temperature and then washed with 1X PBS. Slides were incubated with secondary antibody goat anti-mouse FITC (Millipore) at 5μg/ml for 40 minutes at room temperature. These were then washed with 1X PBS and images whilst wet using NikonTE2000.

2.4.2.6 Blood preparation for the acoustofluidic device

Blood was diluted 1/10, 1/20 and 1/50 with 1X PBS. The dilution of blood entering the device was one of the variables investigated during optimisation.

2.4.2.7 Shear stress

In the study of Kang *et al* (2016), the viscosity of blood at flow rates over 7 ml/h was found to be 3.3 ± 0.05 cP and 1X PBS 0.7 cP. In order for these values to enter the shear stress calculation (Equation 3.1) (Jacobs *et al.*, 1998; Schneider *et al.*, 2001; Ainslie *et al.*, 2005), centipoise was converted to poise (P) and ml/h was converted to $cm^3\ s^{-1}$.

$$\tau = \frac{6\mu Q}{wd^2} \quad \text{(Equation 5)}$$

Table 6: Experimental conditions corresponding to shear stress

	Symbol	Units	Value
Channel depth	*D*	Cm	0.063
Channel width	*W*	Cm	1.2
Fluid Viscosity	μ	P	0.033

The normal physiological fluid shear stress of leukocytes in blood is 1.5 dyn/cm^2 (Fukuda *et al.*, 2000); therefore at the current flow rates

Table 7: Shear stress of cells based on flow rates within the device

Flow rate (*Q*) (ml/h)	Shear stress τ (dyn/cm^2)		
	1 blood : 10 PBS	1 blood : 5 PBS	1 blood: 1: PBS
20	0.035	0.045	0.073
30	0.053	0.067	0.110
40	0.071	0.090	0.147
50	0.088	0.112	0.184
60	0.106	0.134	0.220

2.4.2.8 Optimisation of operational conditions for the acoustofluidic device

The key parameters for operating the acoustofluidic device included amplitude, flow rate and dilution factor of the blood sample. For optimisation studies the voltage was set to 25 V, and a syringe pump set variations in flow rate (10 to 50 ml/h in 10 ml/h increments) in order to determine the optimum conditions for antibody capture of basophils using an anti-CD203c coated slide. As with flowing particles, admittance and impedance plots were run. For each individual test due to screw tightness variability a 2-scan analysis was performed at fixed frequencies in Hz. Optimum frequency ranges for each slide enabled the frequency sweep conducted per test. Once the possible frequencies were determined, the DDS function generator was switched on to detect the drop and rise in amplitude. The device was pre-wetted with the blood suspension. The halogen light source was switched on the microscope. The syringe pump was set to run for 10 minutes at each of the predefined flow rates and samples were collected for each 2-minute interval i.e. 0 – 2, 2 – 4, 4 – 6, 6 – 8 and 8 – 10 as demonstrated in Figure 22. Two additional samples were taken prior to entry into the device (time 0) and 500 µl was taken when 1X PBS was flown through the device after the ultrasound was switched off post ten minutes (flush). Two controls were run to determine the efficiency of the device 1) coated slide with no ultrasound, 2) ultrasound on, non-coated glass slide.

To determine optimal conditions for basophil binding, a range of flow rates were tested: 10 ml/h, 20 ml/h, 30 ml/h, 40 ml/h and 50 ml/h. Three slides were used per subject and samples of blood suspension both before and after (waste outlet) were tested in using both FACS to determine the percentage of basophils gated, and cell associated histamine determined to compare percentage of basophils bound to the glass slide. FACS analysis was conducted using the protocol described in Section 2.3.3.3. The approximate total number of basophils bound to the device were calculated by using the following equation:

$$\left(\frac{Number\ of\ basophil\ events\ pre\ entry - number\ of\ events\ post\ entry}{\%\ gated}\right) \times 100 = Total\ number\ of\ basophils\ bound \quad \text{(Equation 6)}$$

The acquisition for region one of the FACS analysis had be to altered to 150 events in order to compensate for the 1/10 dilution of the blood sample in 1X PBS. There were 500 basophils in whole blood for each sample; therefore, at a 1/10 dilution theoretically there would be 50 basophils. However, in the initial samples, up to 150 basophils were tested, whereby each

sample was run for 5-minutes total. The pre inlet and outlet samples were compared to determine how many basophils were within the sample. Thus, the before and after values were plotted, alternatively the difference between entry and exit could be compared. As an alternative means for assessing relative numbers of basophils before entering and on leaving the device, cell suspensions were collected for the measurement of cell associated histamine (according to the method described in Section 2.6.1). These were subjected to three rounds of freeze-thawing and stored at – 80°C. All samples were assayed together and the following equation was used to determine the percentage difference:

$$\left(\frac{Total\ histamine\ pre\ entry - total\ histamine\ post\ entry}{Total\ histamine\ pre\ entry}\right) \times\ 100\ = \%\ difference \quad \textbf{(Equation 7)}$$

Total numbers of basophils for these experiments ranged between 2.7 x 10^5 – 3.5 x 10^5. For each sample, the maximum number of basophils per time point was calculated using the following equation:

$$Mean\ no.of\ basophils\ bound = basophils\ per\ time\ point\ \times \frac{mean\ adherance}{100} \quad \textbf{(Equation 8)}$$

Equation 8 enabled an accurate approximation of the number of basophils in the sample at each time point and a cumulative addition was performed to determine the total number of basophils that had bound. A sample calculation is provided in Table 8.

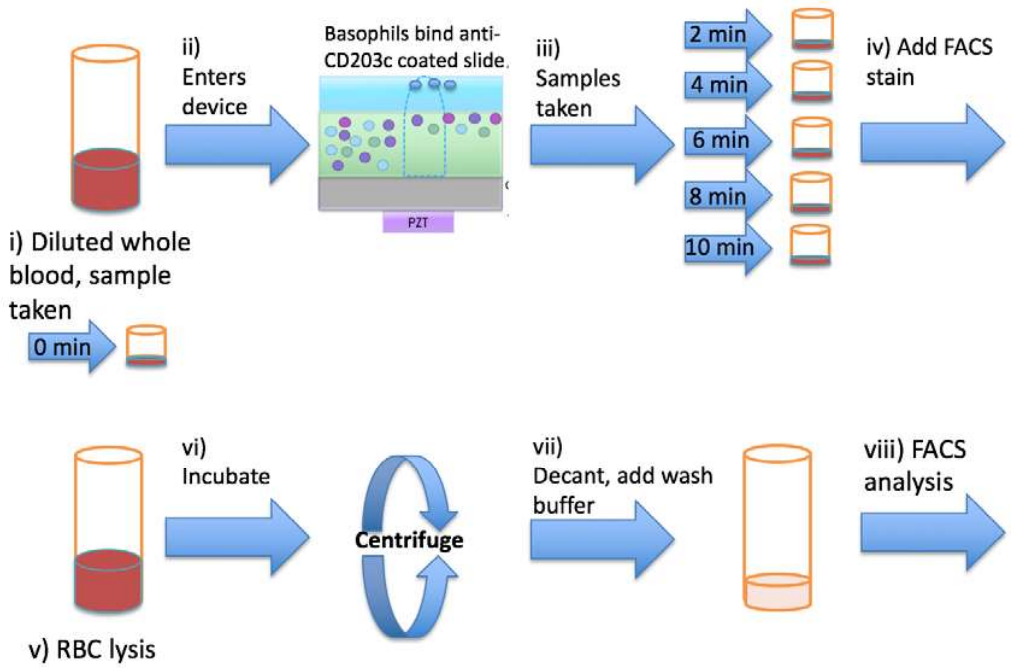

Figure 22: Indirect measure of basophil numbers captured within the device

i) Whole blood was diluted 1 in 5 with 1 x PBS, and a 500 μl sample was taken (time 0 sample) ii) Blood enters the device via syringe pump and the speed was set in ml/h, all cells are pushed up through the carrier layer into the reflector layer (anti-CD203c coated slide) where basophils bind. iii) Samples were taken at either 2 minute intervals (as shown in the diagram) or at the end of the experiment and approximately 6 samples were taken from the final sample (10 minutes). iv) Staining reagent (20 μl) and 150 μl stimulation buffer was added to each 50 μl sample and incubated for 15 minutes in a water bath. v) Following incubation 2 ml lysing reagent was added to each tube. vi) samples were incubated for 10 minutes and then centrifuged vii) supernatant was decanted onto blotting paper and was buffer was added to each tube. vii) FACS analysis was run for each sample for 5 minutes, total number of basophils was counted and percentage of basophils within sample recorded. Results were entered into Equation 6.

Table 8: Total number of basophils bound to the antibody-coated slide, as calculated according to on Equation 8

Flow rate (ml/h)	Total no. of basophils x 10^5	Total volume in 10 min (ml)	Approximate no. of basophils per time point x 10^4	Mean basophils bound (CD63 expression) x 10^4	Mean basophils bound (Net histamine) x 10^4
10	3.27	1.66	0.524	0.775	0.62
20	3.27	3.33	1.09	1.7	0.78
30	2.53	5.00	1.27	3.22	3.25
40	3.38	6.66	1.00	0.305	1.04
50	3.38	8.33	1.25	0.61	0.60

An example of the calculation is shown below for 10 ml/h:

Flow rate = A; total number of basophils x 10^5 = B,

Total volume in 10 min (C)= ((A/60) *3.27) *100

Approximate number of basophils per time point (D) = C/5

2.4.2.9 Histamine assay using the samples from the acoustofluidic device

Samples were taken before and after the blood was run through the device (50 µl). The sample taken after flow through was considered the waste. These samples were added to 150 µl of distilled water, labelled and stored in the -80°C freezer to later determine total net histamine (further details are described in Section 0). This assay was used to evaluate relative numbers of basophils bound to the cover slide within the acoustofluidic device.

2.4.2.10 Basophil identification in the acoustofluidic device

After cell capture experiments, the acoustofluidic device was disassembled for washing with Virkon and 70% ethanol. The reflector glass slide was then fixed using 16% formaldehyde ampules for 10 minutes, and washed three times with 1X PBS. The capture slide was imaged on the confocal microscope by adding 10 µl of Kimura stain to the binding area, which was covered with a microscopy slide prior to imaging. Kimura stain was used to identify cells within the device and stains basophilic granules pink. Images were taken using 10X and 40X objectives and the Q-Imaging Retiga 2000 colour camera by micromanager. Images were later analysed by Wekka, an analysis plug-in within Image J to determine the total numbers of basophils bound.

2.5 Investigating basophil activation

The flow cytometric based basophil activation test has been reported to be a reliable way of measuring the basophil response on between 150 – 2000 basophils when allergen cross links with IgE (Hoffmann *et al.*, 2015). Basophil activation tests are increasingly being considered as reliable tools in the diagnosis of allergy to a broad range of allergens. At present, there are several commercially available kits, though differences in the protocols employed make direct comparison between methods difficult.

The key aim in this project is to develop a new technology for efficient and rapid basophil activation testing as a means for diagnosis. Thus, current experimental techniques must first be assessed in order to compare with what is already available, as no direct comparison of methods has yet been published.

2.6 Basophil activation and measurement

Basophil activation was assessed following experimental activation by determining membrane expression of the activation marker CD63 by FACS, and also by measuring the release from secretory granules of the markers histamine and basogranulin. There are a range of methods used for *in vitro* basophil activation testing. Methods explored in this thesis are flow cytometric measurement of CD63, net basogranulin measurement and net histamine measurement in basophils. Positive controls for such experiments were an antibody specific for FcεRI and the bacterial peptide FMLP. The allergens used for the purpose of these studies were: *Dermatophagoides pteronyssinus* (ALK 503 house dust mite Aquagen^{R} for specific immunotherapy measured in SQ-U/ml) and Grass pollen Phleum pretense extract (measured in SBU).

2.6.1 Measurement of net histamine

Peripheral blood leukocytes were challenged with various concentrations of FMLP, antibody specific for IgE, an extract of dust mite and grass pollen Phleum thalis extract. Tests were performed in duplicate and the mean value calculated for each individual concentration of challenge agent/control. Diluted 1/6 whole blood (180 µl) was stimulated with 20 µl of stimulus (diluted in Tyrode's buffer) per well of a 96-well plate and incubated for 30 minutes at 37°C. The plate was then centrifuged at 800 *g* for 10 minutes at 4°C. Following this, the supernatant was transferred onto ice. For measuring levels of total cell-associated histamine or basogranulin, separate aliquots with the same numbers of cells were subjected to two freeze-thaw cycles. Samples were stored at - 20°C for measurement of histamine or basogranulin. The protocol is depicted schematically in Figure 23. Net histamine release from basophils was calculated by using the following equation:

$$Net\ Histamine\ Release\ (\%) = \left(\frac{Release\ on\ challenge - spontaneous}{Total\ Histamine\ \ Content}\right) \times\ 100$$

(Equation 9)

Relative histamine release was measured using the following equation:

$$Relative\ Histamine\ Release\ (\%) = \left(\frac{Release\ on\ challenge}{Total\ Histamine\ \ Content}\right) \times\ 100$$

(Equation 10)

In order to quantify data obtained from the histamine assay, cell lysate collected from the assay was frozen until required.

Net basogranulin release was determined by using the mean value in arbitrary units for total basogranulin, where the spontaneous release and background noise (mean of the PBS wells) were deducted from all the values using the following equation:

$$Net\ Basogranulin\ Release\ (\%) = \left(\frac{Release\ on\ challenge - spontaneous}{Total\ Basogranulin\ \ Content}\right) \times\ 100$$

Equation 11

Relative basogranulin release was measured using the following equation:

$$Relative\ Basograunlin\ Release\ (\%) = \left(\frac{Release\ on\ challenge}{Total\ Basogranulin\ Content}\right) \times\ 100$$

Equation 12

In order to determine concentrations of histamine in leukocytes and leukocyte supernatants, cells from healthy donor samples were tested. Briefly, supernatants (50 μl) were pipetted into 96-well plates pre-coated with monoclonal antibody to histamine according to the manufacturer's instructions (Neogen Life Sciences, Lexington, USA) EIA Kit for measurements in ng/ml). The method is illustrated in Figure 23. Enzyme conjugate (50 μl) was added to the well and left on the shaker at room temperature for 45 minutes. Incubation enabled competition for binding sites between the enzyme–labelled histamine conjugate (horse radish peroxidase) and unbound histamine within the sample. Post incubation the sample was washed three times with 300 μl 1X PBS allowing unbound material to be removed from each well, so that only the bound remains. Colour was generated by bound enzyme conjugate *via* the horseradish peroxidase, 150 μl enzyme conjugate was added per well, the plate was sealed and placed on the rocker at room temperature. Optimal colour was generated after 30 minutes; meaning the most accurate colour change could be measured and the reaction was stopped with 1 N HCl stop solution. The samples were read on a microplate reader (450 nm).

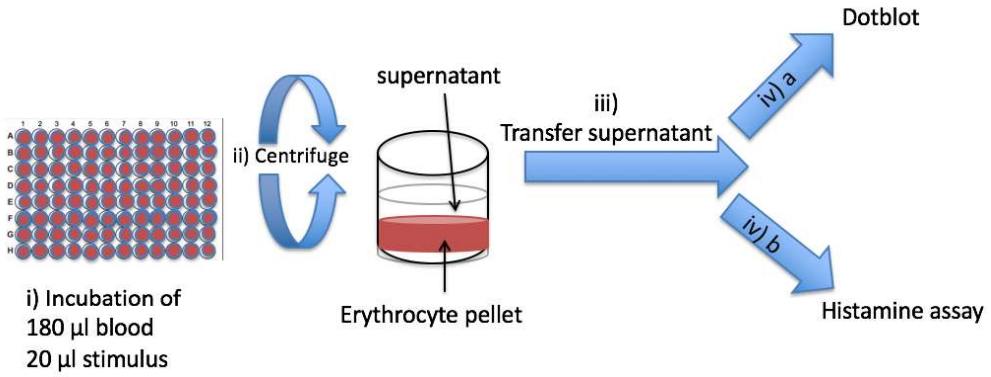

Figure 23: Whole blood challenge for measurement of net basogranulin and net histamine i) 20 µl of stimulus diluted in Tyrode's buffer) and 180 µl of whole blood sample were pipetted into each well of 96-well plate and incubated for 30 minutes at 37°C . ii) The plate was then centrifuged at 800 *g* for 10 minutes. iii) The supernatant was transferred onto ice. iv) For measuring levels of total cell associated histamine or basogranulin, separate aliquots with the same numbers of cells were subjected to two freeze-thaw cycles. Samples were stored at -20°C for measurement of histamine or basogranulin.

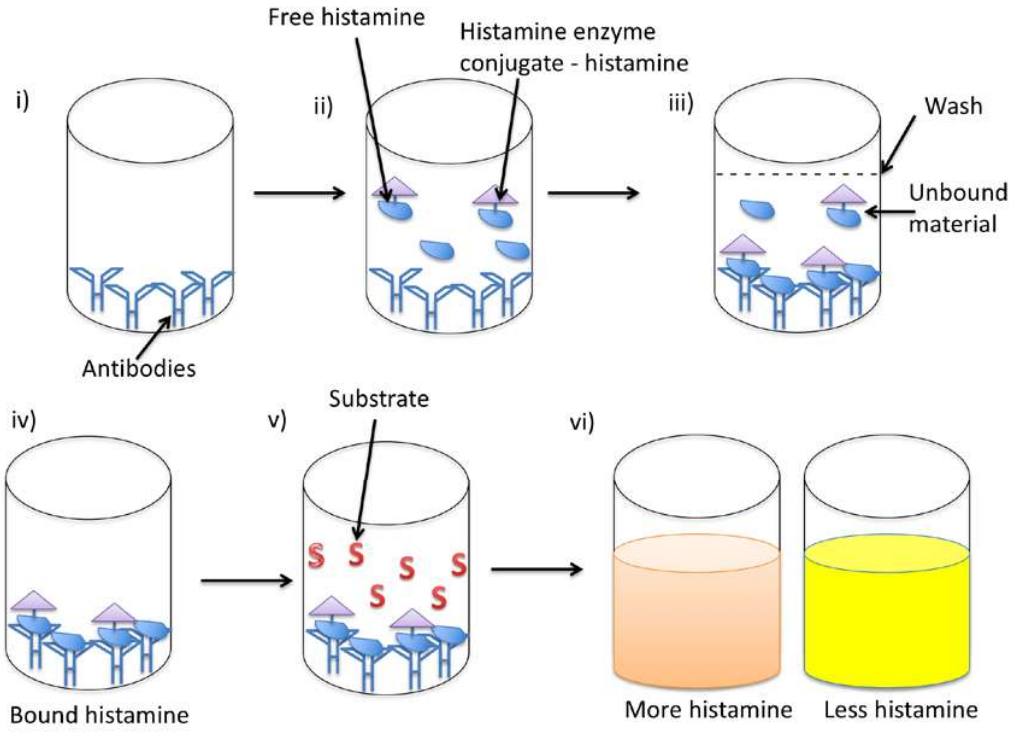

Figure 24: Enzyme immunoassay for histamine

i) Histamine and blood samples were added to a 96 well plate ii) Enzyme conjugate was added to the well creating competition for binding sites between the enzyme–labelled histamine conjugate (horse radish peroxidase) and unbound histamine within the sample. iii) Post incubation the sample was washed, thus removing unbound material. iv) Only bound material remains. v) Substrate was added to each well and colour was generated vi) The less analyte present, the brighter the colour; in the presence of histamine (less analyte) pale/no colouring of the well.

2.6.2 Measurement of basogranulin release

Frozen samples of cell supernatants following experimental activation, or cell lysates, or BAL fluid samples (obtained from study LREC no.05/Q1702/165) were thawed and serially diluted in blocking buffer (1% BSA, 20 ml PBS-T, 30% H_2O_2, 0.1% NaOH); neat, 1/2, 1/4, 1/8, 1/16, 1/32 to be used as standards. Whole blood (1 ml) was diluted with Tyrode's buffer (1/6 dilution) to be challenged; erythrocyte depleted blood (as described in 2.1.2.4) was also tested in a 1:6 dilutions. Following this, 180 µl of cell suspension (whole or erythrocyte depleted) was pipetted into a 96-well plate and 20 µl of stimulus (FMLP or grass pollen) at varying dilutions were added. Tests were performed in duplicate and a mean calculated for each individual concentration of challenge agent/ control. These were incubated for 20 minutes, centrifuged at 800 *g* for 10 minutes at 4°C before the lysate was transferred onto a new plate over ice. Samples were transferred into the dot blot apparatus using a multichannel pipette when required.

PVDF membrane (Biorad) was soaked in methanol for 30 seconds then placed in 1X PBS. The gasket was pre-wetted with PBS 1X, and the membrane was laid onto the inner template without causing bubbles. The upper part of the apparatus was assembled and the valve was drained. PBS was pipetted (100 µl) into each of the 96 wells and removed using the vacuum and repeated 3 times. Samples were then applied to the 96-well dot blot apparatus and allowed to flow through with gravity for one hour. Remaining sample was removed gently using the vacuum. Dot blot membrane was disassembled from the dot blot apparatus and was washed twice with PBS-T (0.1% Tween) for 5-minute intervals each time. Membrane was then incubated for one hour with blocking buffer at room temperature on rocking shaker at 10 rpm. The membrane was then washed twice with PBS-T at 5-minute intervals. The membrane was incubated with primary antibody (2 µl of 5 mg/ml BB1 supernatant diluted in 20 ml blocking buffer) overnight in the fridge and covered with foil. The membrane was then washed three times with PBS-T at set intervals (5 minutes, 15 minutes, 5 minutes). The membrane was incubated with secondary antibody – polyclonal rabbit anti-mouse immunoglobulin/HRP (Dako Cytomation, Denmark) (1/5000 dilution in blocking buffer 4 µl/20 ml) for two hours at room temperature. This was washed with PBS-T six times at 5-minute intervals. The membrane was taken to the analyser and laid on top of a clear sheet of acrylic within the reader. Chemiluminescent substrate (Luminata™ Forte Western HRP Substrate) was added to cover the membrane and another acrylic sheet was laid on top. Upon the application of the chemiluminescent substrate catalysis of luminol into 3-aminophthalate resulted in light emission that was then read in the Syngene Image Analysis. Images were taken at 2-minute intervals for 20 minutes (Figure 24).

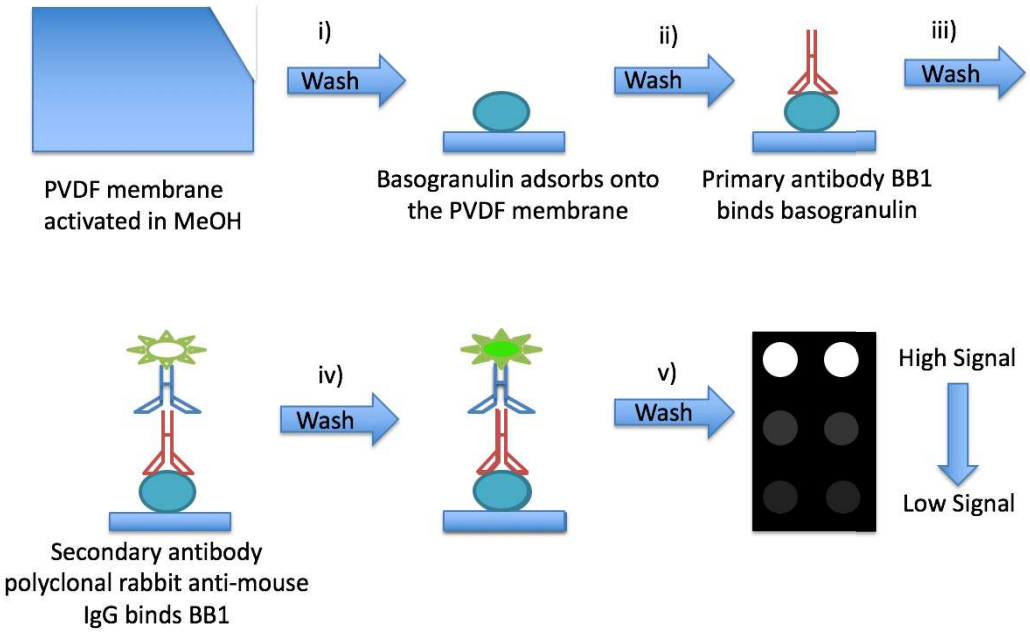

Figure 25: Schematic diagram for the dot blot procedure for basogranulin assay

i) Membrane was activated in MeOH and washed. ii) Samples are added to the membrane allowing basogranulin to adsorb onto the membrane. This is then washed 3 X for 5 minutes. The membrane is placed in blocking buffer for 1 hour; this is then placed in primary antibody overnight. iii) After several gentle washes, the membrane was incubated with rabbit anti-mouse immunoglobulin as tagged with horseradish peroxidase as the secondary antibody. iv) Chemiluminescent substrate, is added and produced a light emission that was then read in the Syngene Image Analysis System. v) The more basogranulin in the sample/ well, the more light emitted and thus a visible dot can be formed.

To calculate the concentration of basogranulin present in the sample, the dots were analysed by Syngene analysis software. This enabled the read out of the raw volume of each dot. Samples were entered into the dot blot in duplicate and thus a mean was taken of the raw volume of these wells. Based on the assumption that the whole blood sample mean was 100%; the following calculation was performed:

$$\frac{(Basogranulin\ in\ sample - spontaneous\ release)}{Total\ basogranulin}\ x\ 100 = Net\ Basogranulin\ release$$

2.6.3 Detection of basophil activation

Based on the comparison of basophil activation markers, CD63 was selected for the marker for basophil activation in the device. Basophils were isolated from whole blood using density gradient centrifugation (HetaSep, StemCell Technologies), followed by immunomagnetic negative selection (EasySep, StemCell Technologies). Following centrifugation at 800 *g*, for 5 minutes, at room temperature, the suspension was decanted into 3% disinfectant and the pellet was re suspended up to 0.5 ml with RoboSep buffer (StemCell Technologies). The remainder of the protocol is illustrated below in Figure 26. Basophils (50 μl) were aliquotted into 5 ml round bottom tubes and buffer (negative control), anti-FcεRI or FMLP (positive controls) was added. Basophils were incubated for 15 minutes in the water bath. Following this; an equal volume of 2% paraformaldehyde (PFA) was added to each tube and incubated for 15 minutes. The cells were then centrifuged 300 *g* brake 4, acceleration 4 for 5 minutes. The suspension was decanted and cells were re-suspended up to 150 μl, ready to enter the cytospin (further description in section 3.2.4.4) 500 *g* for 3 minutes. Anti-CD63 Alexa Fluor 647 (Biolegend) was pipetted (20 μl) onto each slide. Slides were incubated for 10 minutes, and then washed with 1X PBS. DAPI (4',6-diamidino-2-phenylindole, BioLegend) was diluted 1/500 with RoboSep buffer and then 20 μl was added to each slide. Slides were incubated for a further 10 minutes, and then washed with 1X PBS. Slides were left to dry and then mounted buffer was added and sealed with glass microscopy (20 x 50 mm # 1,5; Menzel-Glaser) and imaged on the confocal Leica SP5 (Leica Microsystems).

2.6.4 Basophil activation protocol conducted outside of the acoustofluidic platform

Basophils were separated from whole blood using the density gradient centrifugation protocol described in section 2.3.2 and immunomagnetic negative separation protocol; prior to their transfer into the device. The optimal flow rate for basophil capture was determined to be 30 ml/h. Samples were taken at 2 minute intervals for a total of 10 minutes for both FACS and histamine analysis. Slides were removed from the device and either incubated in 100 μl for 15 minutes with either buffer,

FMLP or anti-FcεRI to create controls for measuring fluorescence. Slides were then washed three times with 1X PBS and then transferred into 2% paraformaldehyde for 10 minutes. The slide washing step was repeated and slides were stained first for ten minutes with Alexa Fluor 647 tagged CD63 (Miltenyi Biotech), washed and then stained with DAPI for a further 10 minutes. Slides were washed and left to dry, following this 20 µl of mounting medium (Mowiol® 4-88, Leica) was added to the active area of each slide and a coverslip (75 x 25 mm, Logitech) was added on top to seal the slides for later imaging with an SP5 confocal microscope (Leica) using an 63 x inverted glycerol objective.

2.6.5 Statistical Analysis

Statistical analysis was performed using statistic software graphpad Prism 7 (GraphPad Software Inc. San Diego, USA). When choosing the statistical method to analyse the data, it was first decided whether the data assumes normal statistical distribution i.e. demonstrates a bell shaped curve or does not. Non-parametric tests are used for continuous data that does not meet the normal distribution requirements. To decide whether the data had normal distribution a histogram was plotted. If the data is roughly symmetrical it can be assumed that the data has normal distribution and a parametric test can be used such as t-test, ANOVA, regression analysis and correlation coefficient. If the data does not have normal distribution, then one of the non-parametric tests can be used such as 1-sample Wilcoxon signed rank test, Friedman test, Kruksal-Wallis Signed Rank test, Mann-Whitney test, Dunn's test and Spearman's rank correlation coefficient. For example, to compare measurements of two different samples either a t-test on the two independent samples could be run (parametric) or Wilcoxon matched paired signed-rank test (non-parametric data). T-tests were used to calculate P values. P values were considered statistically significant if less than 0.05.; significance was rated using a star (*) system; whereby the more stars; the more significant the result. The Data are reported as mean ± SEM. To test the association between two quantitative variables on the same sample, if normal distribution was determined, the Pearson's correlation test was performed, if found that the data's distribution was not normal, the non-parametric test Spearman's rank correlation coefficient test was performed. Statistical analysis of the results of measurement of histamine in whole blood and plasma was made using non-parametric tests, as there was no evidence that the variables measured were normally distributed. To compare two quantitive measurements from the same individual, the Wilcoxon signed-rank test was used. In order to compare means between three or more individual means, the Kruksal-Wallis test was used.

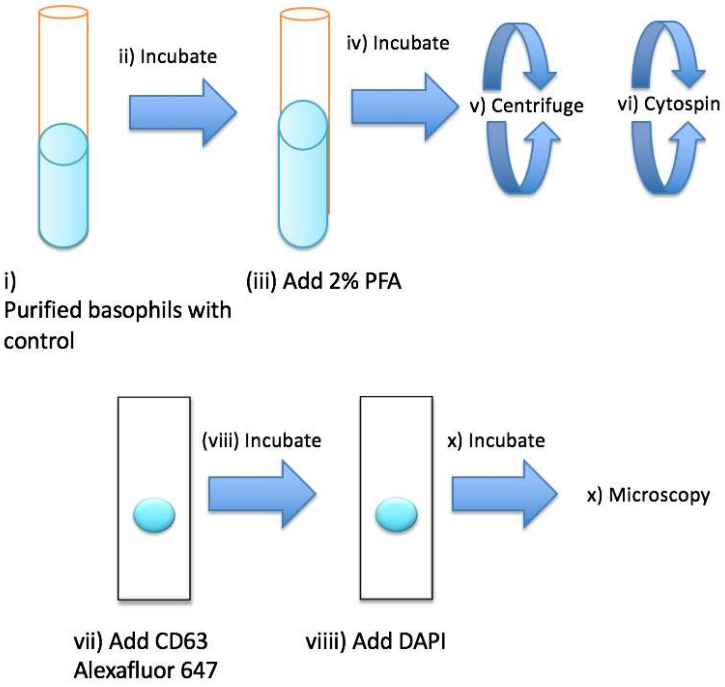

Figure 26: Basophil staining protocol

i) Basophils (50 μl) were aliquotted into 5 ml round bottom tubes and controls were added. ii) Basophils are incubated for 15 minutes in the water bath. iii) PFA (2%) was added to each tube. iv) Incubate for 15 minutes. v) Centrifuge for 5 minutes. vi) Decant suspension and re suspend, ready to enter the cytospin for 3 minutes. vii) Anti-CD63 Alexa Fluor 647 was pipetted onto each slide. viii) Incubate 10 minutes, then wash with 1X PBS. viiii) Diluted DAPI was added to each slide. x) Incubate 10 minutes, then wash with 1X PBS. Slides were left to dry and then mounted buffer was added and sealed with glass microscopy and imaged.

Chapter 3: Results

3.1 Basophil separation

3.1.1 Negative Immunomagnetic separation

Flow cytometry was successfully employed to study the basophil population following various methods of isolation from whole blood. Conclusions as to which negative immunomagnetic separation method was most effective was based on the technique that produced the highest mean basophil percentage population, measured by CCR3-PE expression (demonstrated in Figure 27). The immunomagnetic procedure allowed cell enrichment up to 100,000 basophils/ml in comparison to whole blood (10,000 basophils/ml). Density gradient centrifugation was used prior to that of the negative immunomagnetic separation. When density gradient centrifugation was compared to whole blood, there was an increase of up to 9-fold in the percentage of basophils (Figure 28). The effect of erythrocyte depletion methods on basophil function were explored by comparing the measurement of histamine release from cells following depletion of red cells to that with whole blood. When saponin was incubated with whole blood, it was found that the spontaneous net histamine measurement increased from a mean of 4.6% in whole blood to 73% (Figure 29). Conversely, little net histamine was measured in samples incubated with saponin. Controls α-IgE and FMLP were performed to demonstrate the test was working effectively. As a result of allergen exposure, subjects elicited a bell shaped curve response when samples were measured in the absence of saponin. Results demonstrate that saponin had a significantly reduced net histamine release response in comparison to whole blood. This suggests that the saponin concentration used impaired basophil functionality. The data does not fit the bell shaped normal distribution curve and thus is non-parametric. As this data is comparing samples from the same individual, the Wilcoxon paired signed-rank test on each of the data sets to test the hypothesis that the use of saponin affected the basophil's ability to release histamine. P values for this test were small varying from 0.063 – 0.438; and thus we can conclude that the median difference between whole blood and saponin is not due to chance and that saponin does have a detrimental effect on basophil ability to release histamine. Following these tests, Spearman's rank correlation coefficient test was run for each of the samples, p values were non-significant, thus despite coming from the same donor, the results did not correlate. In addition, A) – 0.5 and D) – 0.360 had inverse r^2 values, thus suggesting that the regression model predictions cannot approximate the real data points, as these do not fit the model well. Therefore, despite coming from the same donor, within the same test, the saponin has produced independent results from whole blood for each donor and thus should not be used in

future experiments. This is because the results will differ from that of whole blood as demonstrated by the statistical analysis.

Alternative erythrocyte depletion agents were sought and evaluated (ammonium chloride and distilled hypotonic shock treatment) demonstrated in Figure 30. Histamine release was measured when hypotonic shock solution was exercised - up to 100%; whereas the maximal net histamine response for samples incubated with ammonium chloride was 75%. Ammonium chloride elicited a higher spontaneous histamine measurement (30%) in comparison to distilled water (13%). The net histamine release measured suggests that the basophils maintained functionality. Results indicate that distilled water is the better agent when performing net histamine measurement for means of basophil activation testing. The distribution of data was non-parametric and thus to compare two quantitative measurements of blood from the same individual (treated with either distilled water or ammonium chloride) the Wilcoxon signed-rank test was used. Donors 1 – 3 had large p values (0.625 – 0.875) and thus the data does not provide reason to conclude that the overall means differ between groups. The pairing was effective for both Donor 2 and Donor 3, who both had significant p value (0.042 *) and an r^2 value of 1, thus showing that both donors were not sensitive to these concentrations of FMLP. More importantly, these results indicate that the samples when lysed with either technique, demonstrate the same pattern of distribution and thus either could be used for future tests. Donors 1 & 4 did not show significant correlation based on the Spearman's rank correlation coefficient test p value. Furthermore, r^2 values did not explain the variability of response data around its mean, and thus does not fit the regression line. Donor 4 demonstrated inverse correlation between its results between ammonium chloride and hypotonic shock treatment.

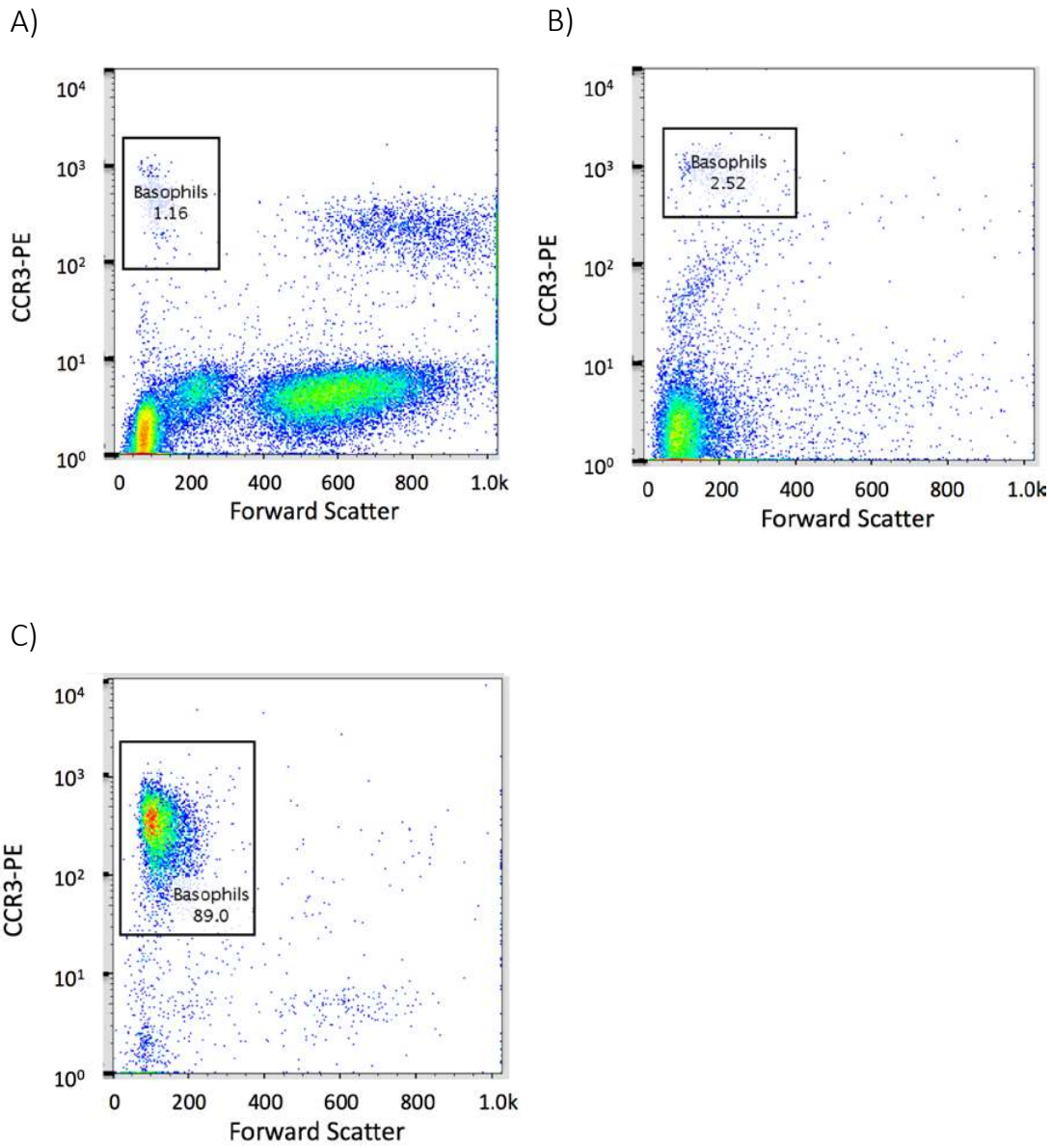

Figure 27: FACS analysis of A) whole blood, and basophils enriched by B) Density gradient centrifugation, or C) density gradient centrifugation followed by negative immunomagnetic separation. Data depicted is for one subject, and is representative of experiments performed in duplicate with five separate donors, representative of 12 separate experiments

The percentage basophil population for each sample condition is indicated in region one

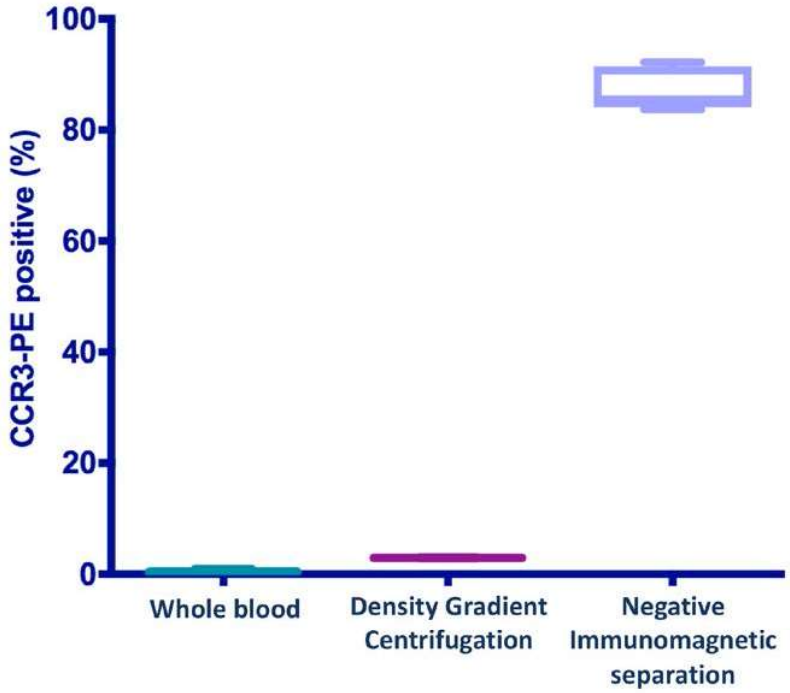

Figure 28: Mean percentage of CCR3-PE positive basophils in whole blood, and following density gradient centrifugation and negative immunomagnetic separation (n = 12)

Density gradient centrifugation percentage CCR3-PE positive cells within region one ranged from 6 – 9%. Negative immunomagnetic procedure increased the baseline basophil population measured in whole blood from 0.1 – 0.3% to 82 – 96%

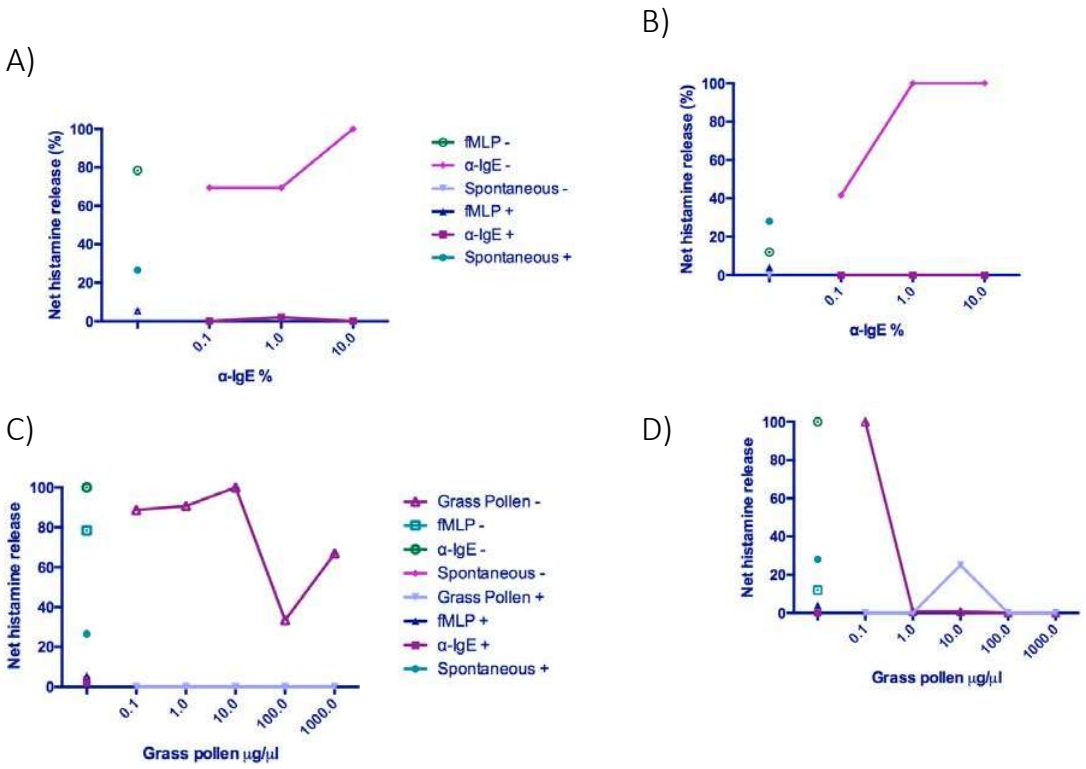

Figure 29: Net histamine release from saponin red blood cell depleted preparations from two grass pollen-sensitive subjects (Subject 1, left and Subject 2, right) in response to increasing concentrations of (A, B) α-IgE and (C, D) grass pollen

The data here does not fit normal distribution and thus non-parametric Wilcoxon paired signed-rank tests were performed to determine if the use of saponin would significantly affect the basophil's ability to release histamine. Correlation between results with and without saponin were measured using Spearman's rank correlation coefficient test (SC). A) $p = 0.250$, $p = 0.667$ (SC), $r^2 = -0.5$; B) $p = 0.250$; C) $p = 0.063$, $p = 0.3$ (SC), $r^2 = 0.342$; D) $p = 0.438$, $p = 0.239$ (SC), $r^2 = -0.360$

Cells had been treated with saponin (teal) or without (pink) to deplete red blood cells. Incubating cells with saponin in most cases abolished the ability of cells to release histamine. Saponin at the concentration employed to deplete red cells appears to be toxic to the cells. This was indicated also by high spontaneous histamine release in the absence of stimulus (73% and 28% with saponin compared with 4.6% and 0% release without saponin for Subjects 1 and 2, respectively). In this instance, subject refers to healthy volunteers who were chosen to donate blood at random for the experiment.

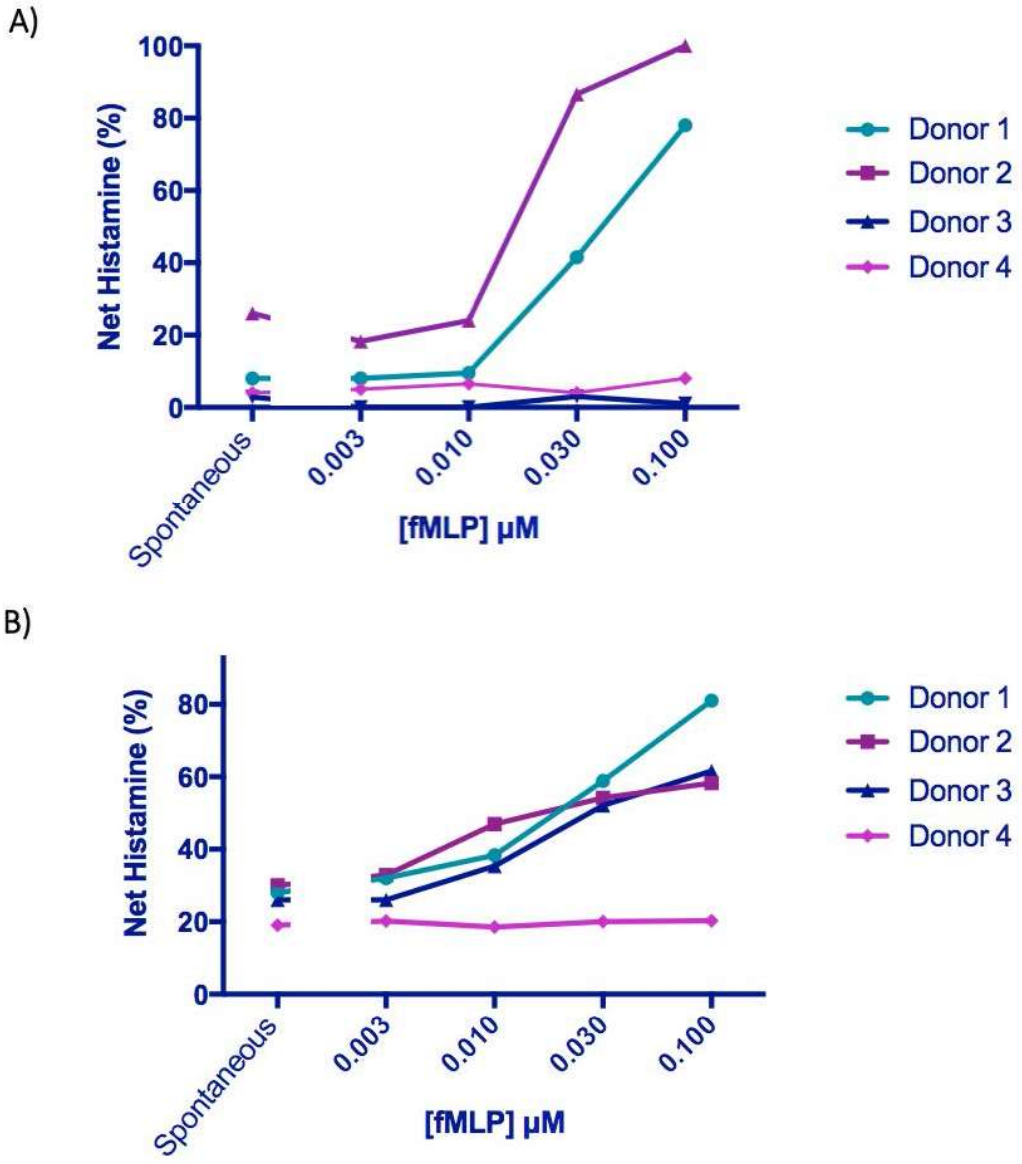

Figure 30: Net histamine release in response to increasing concentrations of FMLP from cells pre-treated with (A) distilled water, or (B) ammonium chloride erythrocyte depletion buffer. Cells were from four subjects (donors 1 – 4). Data shown is the mean of duplicate determinations (n = 4):
Data is non-parametric, in order to compare the donor's mean values between treatments A) distilled water and B) ammonium chloride, Wilcoxon signed-rank tests were performed. In addition, Spearman's rank correlation coefficient (SC) was performed.

- Donor 1: p = 0.625, p = 0.375 (SC), $r^2 = 0.400$
- Donor 2: p = 0.625, p = 0.042 * (SC), $r^2 = 1$
- Donor 3: p = 0.875, p = 0.042 * (SC), $r^2 = 1$
- Donor 4: p = 0.375, p = 0.250 (SC), $r^2 = - 0.633$

3.1.2 Application of microfluidic spiral sorter to achieve basophil separation from both whole blood and erythrocyte depleted blood

Characterisation of the device was achieved using a microbead model, where the microbead size (6 µm diameter and 15 µm diameter) simulated that of erythrocytes and leukocytes (Figure 31). When the four spiral channels differing in width, height, length were tested, it was found that successful separation could be achieved when using Spiral C at a flow rate of 15 ml/h. Microfluidic characterisation was achieved when the 15 µm beads were focused at one outlet (2) whereas smaller particles (10 µm), were focused towards a separate outlet (6).

The employment of whole blood within the spiral sorter visually implies that leukocyte separation was achieved; however the CCD camera at 500 frames per second was not sufficient enough to capture all of the leukocytes exiting the outlet (Figure 32). Leukocytes were manually identified based on size (10-22 µm) and with the application of the rationale that erythrocytes are smaller (4-6 µm) in comparison. Therefore, to enable basophil separation, results indicated that an alternative method for basophil separation must be employed. Image J analysis was attempted on the images captured by the camera, however due to the frame rate and the quality of the camera, the software was unable to determine the difference in cell size. In addition, due to the known variance in leucocyte circumference, without staining pre-entry, it was not plausible to completely determine which cells were in fact basophils. Due to the large number of issues encountered, including the clogging of the closed device, an open device new alternative was sought.

A)

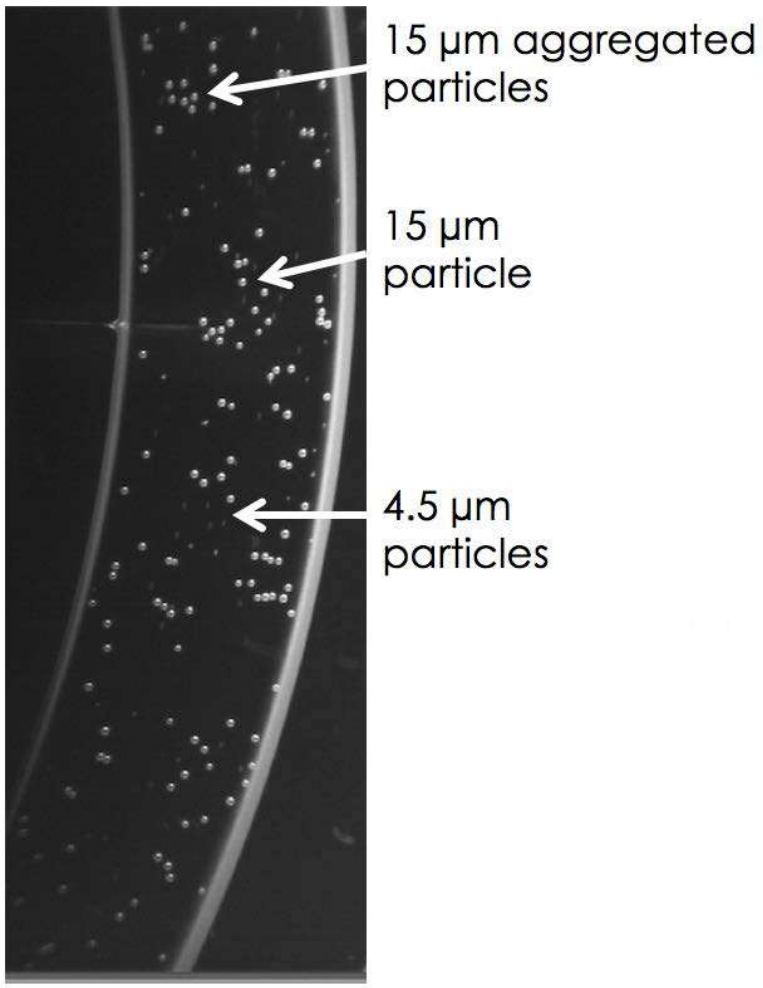

B)

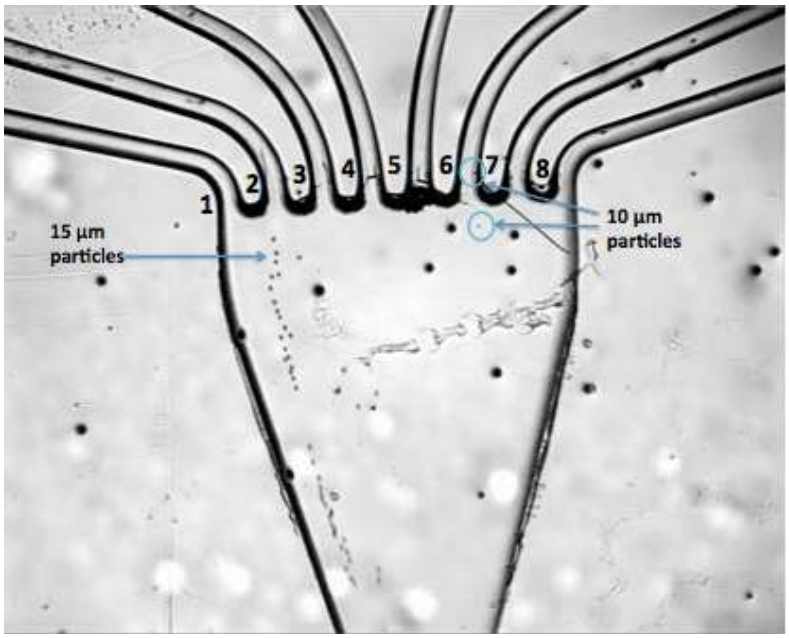

Figure 31: Example of A) 15 µm and 4 µm micro particle focus; B) 15 µm and 10 µm micro particle focus in spiral sorter C using a 4X objective and a flow rate of 15 ml/h

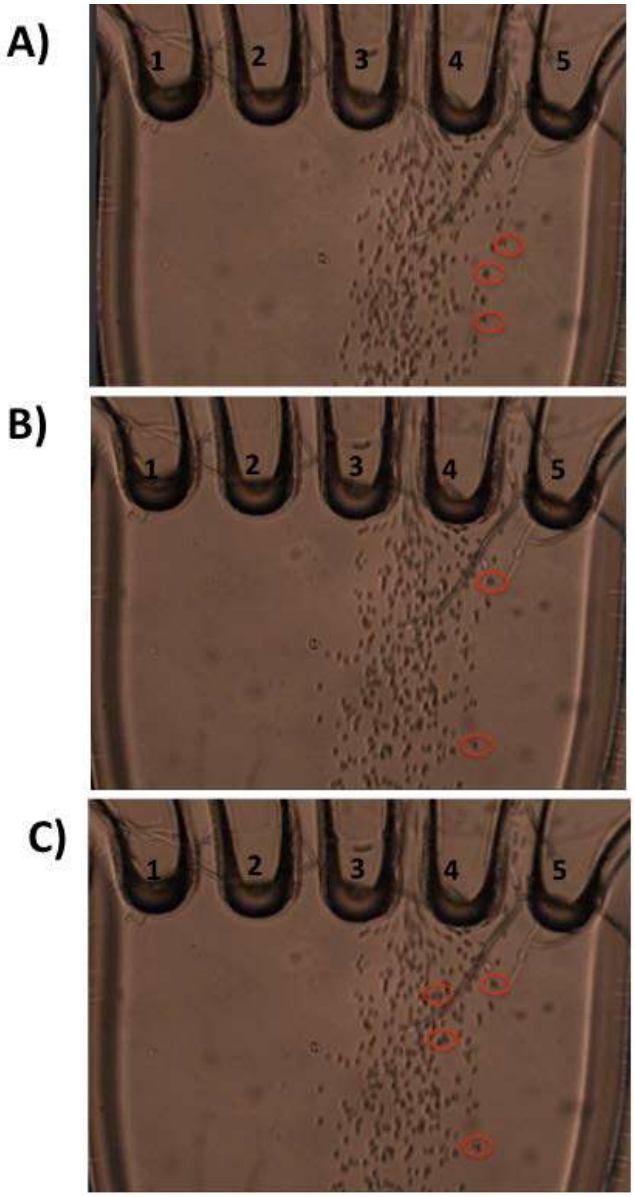

Figure 32: Identification of leukocytes in spiral sorter B from 1/100 dilution of whole blood at 20 ml/h flow rate, 10X resolution (with leukocytes highlighted in red). (A), (B) and (C) depict three consecutive frames during a recording at 500 frames/second

The blood cells are focused on two main channels, but as highlighted by the red circles there was no evident independent focus of leukocytes at this time point

3.1.3 Application of an acoustofluidic device to achieve basophil separation from both whole blood and erythrocyte depleted blood

3.1.3.1 Initial testing (no gasket)

When the initial testing of the device was performed with the gasket present, no beads were observed within the carrier layer. This suggested that the gasket had increased the thickness of the fluid layer and thus diminished all forces that would normally act on the beads in the channel. Therefore, the gasket was removed. During the acoustofluidic characterization, considerable trapping was demonstrated in part (A) but only at the midpoint of the channel (B) (Figure 33). It was demonstrated that the beads were still spread out evenly, as noted prior to the ultrasound force being applied (C). The objective banding (4X) suggests strong lateral forces, though due to leaks there were a lot of bubbles present and thus a new gasket was required.

3.1.3.2 Determination of the percentage of basophils bound to the acoustofluidic device reflector layer

The resonance peak was identified by first running air through the device to create an initial peak, followed by water or diluted blood that should form a second peak. The new peak was used to identify the frequency of the wave required to push the cells or beads to the roof of the device into the reflector layer. Figure 34 demonstrates the differing peaks observed for air and how the screw tightness affects the second peak created within the device. Numerous runs were required to obtain the correct peak, if the screws of the device were too loose, leaking would occur and no peak would be observed, equally if the screws were too tight, the slid could break and no peak would be observed. Figure 35 demonstrates both the individual (subjects A - E) and mean percentage basophil adherence (F) calculated through the indirect measure of basophils present within the sample. Flow rates 10 – 50 ml/h were tested for enriched basophil samples to determine the optimal flow rate within the device. The flow rate that resulted in the highest measurement of basophil adherence was found to be the most effective. When an enriched basophil sample was added to the device at a flow rate of 30 ml/h, the maximum percentage of basophils bound to the slide approached 80%. To validate this, the Kruksal-Wallis test was performed to compare the means of basophil adhesion at each flow rate, which was found to be significant $p = <0.0001$. This indicates the populations have different distributions at each flow rate. Patterns obtained may indicate that increasing the flow rate from 10 – 30 ml/h, provides more basophil binding opportunities, as more cells will have run through the device. However, at flow rates of 40 – 50 ml/h little basophil adherence was obtained (less than 5%), suggesting that the flow rate was too fast for the basophils to adhere. The flow rate of 30 ml/h was decided to be the best flow rate to obtain optimal basophil adherence.

A)

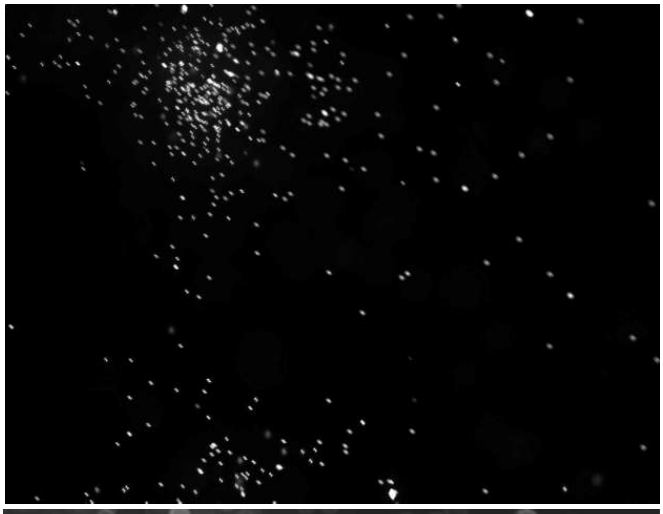

B)

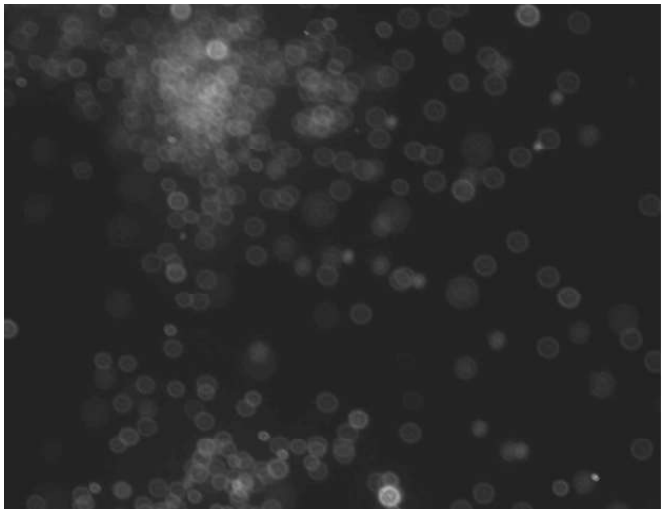

C)

Figure 33: Initial testing of the acoustofluidic device using a micro particle suspension illustrating (A) Trapping; (B) Trapping at the midpoint of the carrier; (C) Beads at the carrier layer before the ultrasound force was applied

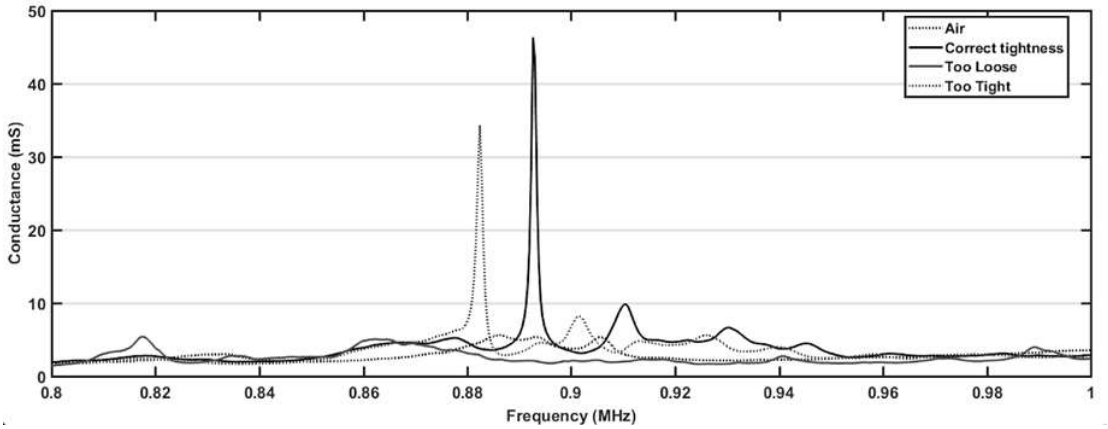

Figure 34: Variance in resonance peaks observed when the gasket is i) the correct tightness, ii) too loose, and iii) too tight.

This demonstrates the importance of the correct screw tightness that controls the space between the gasket and the liquid. Too loose and a very small peak is observed at 0.9 MHz, too tight and a slightly larger peak is observed at 0.91 MHz. If correctly assembled a large peak of 47 mS is observed at 0.89 MHz, strong enough to push the cells or beads to the reflector layer.

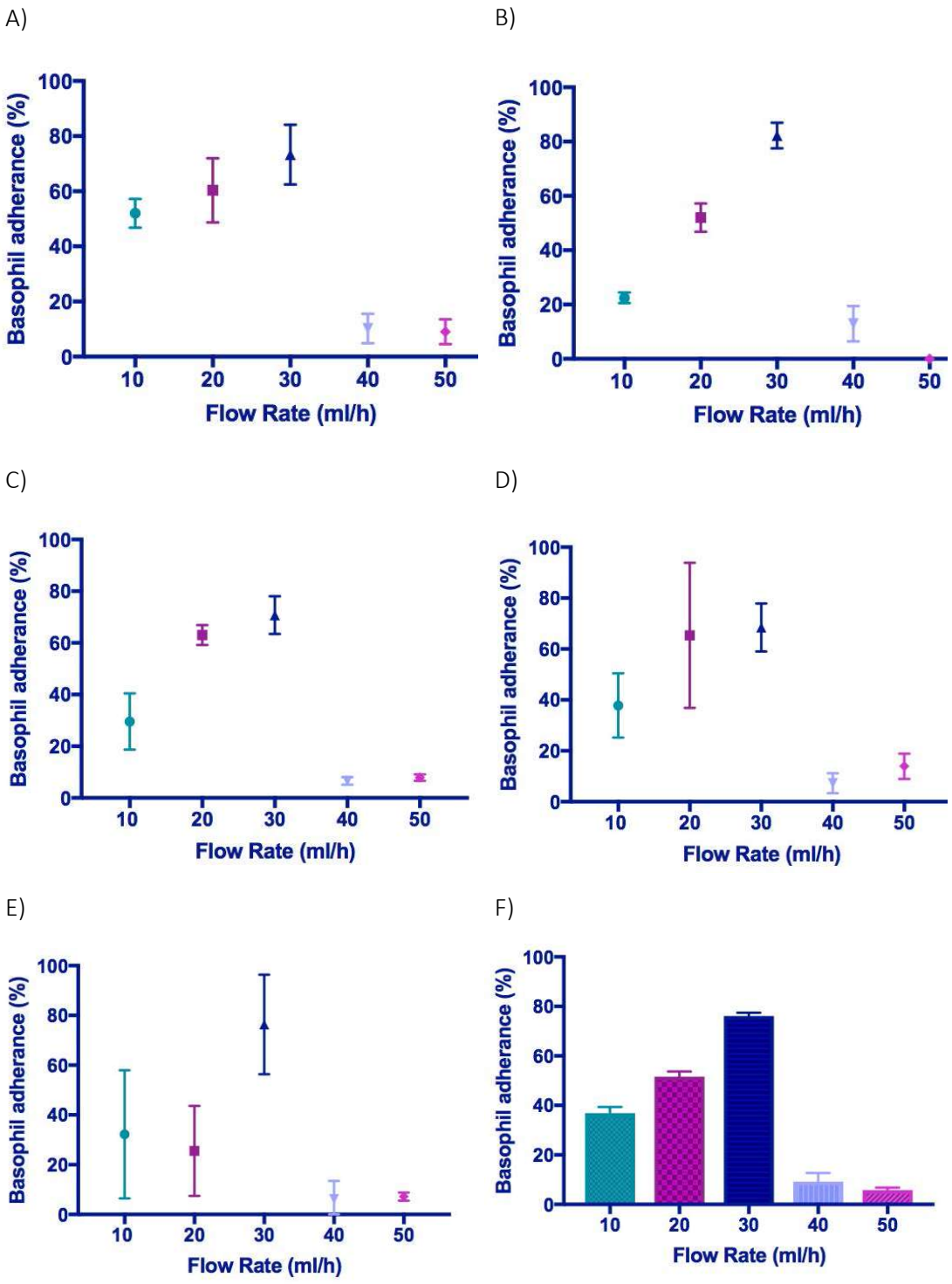

Figure 35: Individual subjects' percentage basophil adherence (A-E) in relation to flow rate experiments conducted at 10 ml/h intervals (10 ml/h – 50 ml/h) based on CCR3 expression analysis. Data is representative of one subject's data repeated 3 times at each time point. F) Mean percentage basophil adherence based on the data of five individual subjects with vertical bars indicating the SEM (standard error of the mean), Kruksal Wallis test was performed to compare flow rate, p = <0.0001 ****.

Further flow rate experiments were performed to ensure that 30 ml/h was the optimal flow rate. Samples were taken from the outlet at two-minute intervals for ten minutes. Figure 36 illustrates an individual's basophil adherence at each flow rate over the ten minutes, repeated in triplicate. The highest mean basophil adherence was observed at 30 ml/h C), however a minimum of 10% error was observed at each time point. It has been noted that the largest error is observed at the 8-minute time point for each flow-rate; which could be due to the syringe pump leading to the last 2 minutes of sample. The lowest standard error was observed at 40 ml/h and 50 ml/h; however minimal basophil adherence was measured for both flow rates during the ten-minute period (<20 %).

Based on the maximal basophil adherence being observed at 30 ml/h across all subjects; additional experiments were performed in new subjects at two-minute intervals for the ten-minute time period. Figure 37 to measure a more accurate mean basophil adherence for each subject and demonstrates the both the inter, and intra variation of subjects tested. Generally, the basophil adherence is consistent over time and due to the consistent use of the device, the standard error decreased by >5% for each time point. When approximate basophil adherence was calculated over time, it was found that at 30 ml/h, basophils the numbers of basophils bound within the device approached 30,000 basophils. The Kruksal Wallis test was used to compare the means of each individual at the two-minute intervals at 30 ml/h. The means did not vary significantly by <0.05, P = 0.251, and thus it can be concluded that the populations have different distributions and this is why the variance is observed in each donor. These experiments reinforced the idea that 30 ml/h was the optimal flow rate based in both FACS analysis and measurement of total concentrations of cell-associated histamine (Figure 38).

Figure 38 demonstrated that at flow rates greater than 30 ml/h; there were less than 5000 basophils bound over the ten-minute time period based on approximate cumulative calculations. This suggests that the basophils may be moving too quickly and thus are unable to create a strong bond to the CD203c on the reflector layer. The histamine data used to estimate relative numbers of basophils according to levels of cell associated histamine, this was correlated with CD63 expression with the exception of at 20 ml/h (which differed by 11,000 basophils). Both the Wilcoxon paired signed-rank test and Spearman's rank correlation coefficient were performed to compare the approximate number of basophils bound when the samples were analysed by A) FACS or B) net histamine release. This was performed to demonstrate the correlation between these two tests in terms of analysing basophils within the device. Spearman's rank correlation coefficient was significant for all five flow rates ($p = 0.001$ ** - 0.030 *). In addition, the r^2 values of the data indicate that the regression predictions approximate the real data points almost exactly for each of the flow rates 10 ml/h – 30 ml/h $r^2 = 1$. Flow rates of 40 ml/h (0.829) and 50 ml/h (0.943) did have high r^2 values, however these

were not exact and thus it can be concluded that the majority of the variance within the data was accounted for. Wilcoxon paired signed-rank coefficient values were equal P = 0.063; this is a small P value and thus it can be concluded that value variance is due to the populations having different medians. Thus despite the results correlating almost perfectly between the two tests, the approximate number of basophils bound differed.

When five subjects' samples were tested at 30 ml/h, it was found that up to 80% basophil adherence could be achieved (Figure 39). Controls had minimal non-specific binding to the anti-CD203c coated slide; with fewer than 5% bound to the non-coated slide. Results indicated the larger the starting basophil population, the higher the likelihood of basophils making contact with the reflector layer. It was hypothesised that, the larger the number of starting basophils, the higher the chance of basophil contact to the coated reflector layer and thus there being an increased chance of adherence to the slide. However, those with a low starting number of basophils still achieved 40% binding and could achieve a basophil numbers within the region of 30,000. The Kruksal-Wallis test was run to compare mean basophil adherence between the donors (A – E), P = 0.256, thus the difference is due to random sampling.

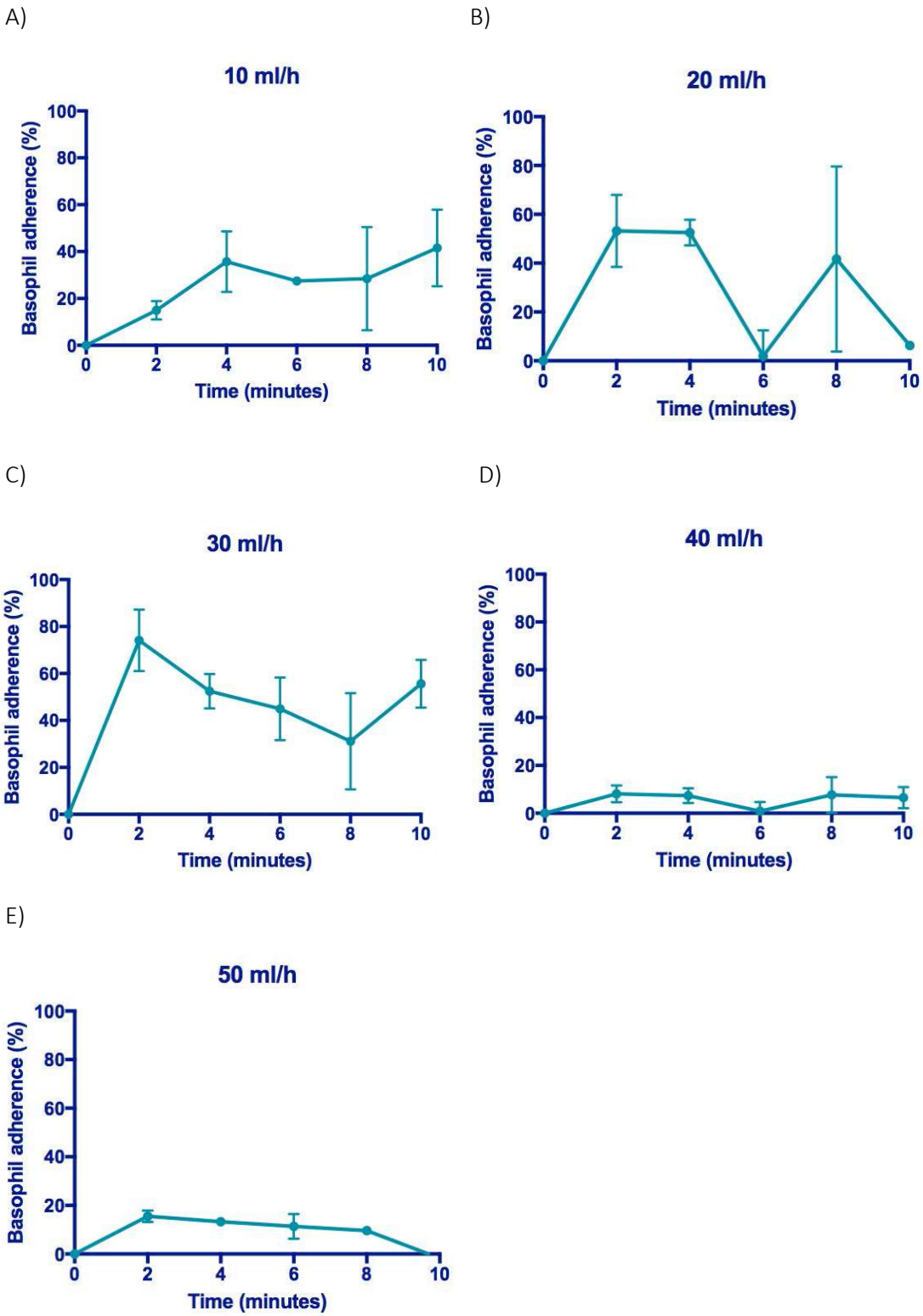

Figure 36: Individual subjects' basophil adherence in relation to flow rate experiments conducted at 30 ml/h with vertical bars indicating the SEM (standard error of the mean). Samples were taken at 2 minute intervals to determine basophil adherence and calculated based on CCR3 expression analysis. Experiments were run at flow rates A) 10 ml/h, B) 20 ml/h, C) 30 ml/h, D) 40 ml/h and E) 50 ml/h. Data is representative of one subject's data repeated 3 times at each time point

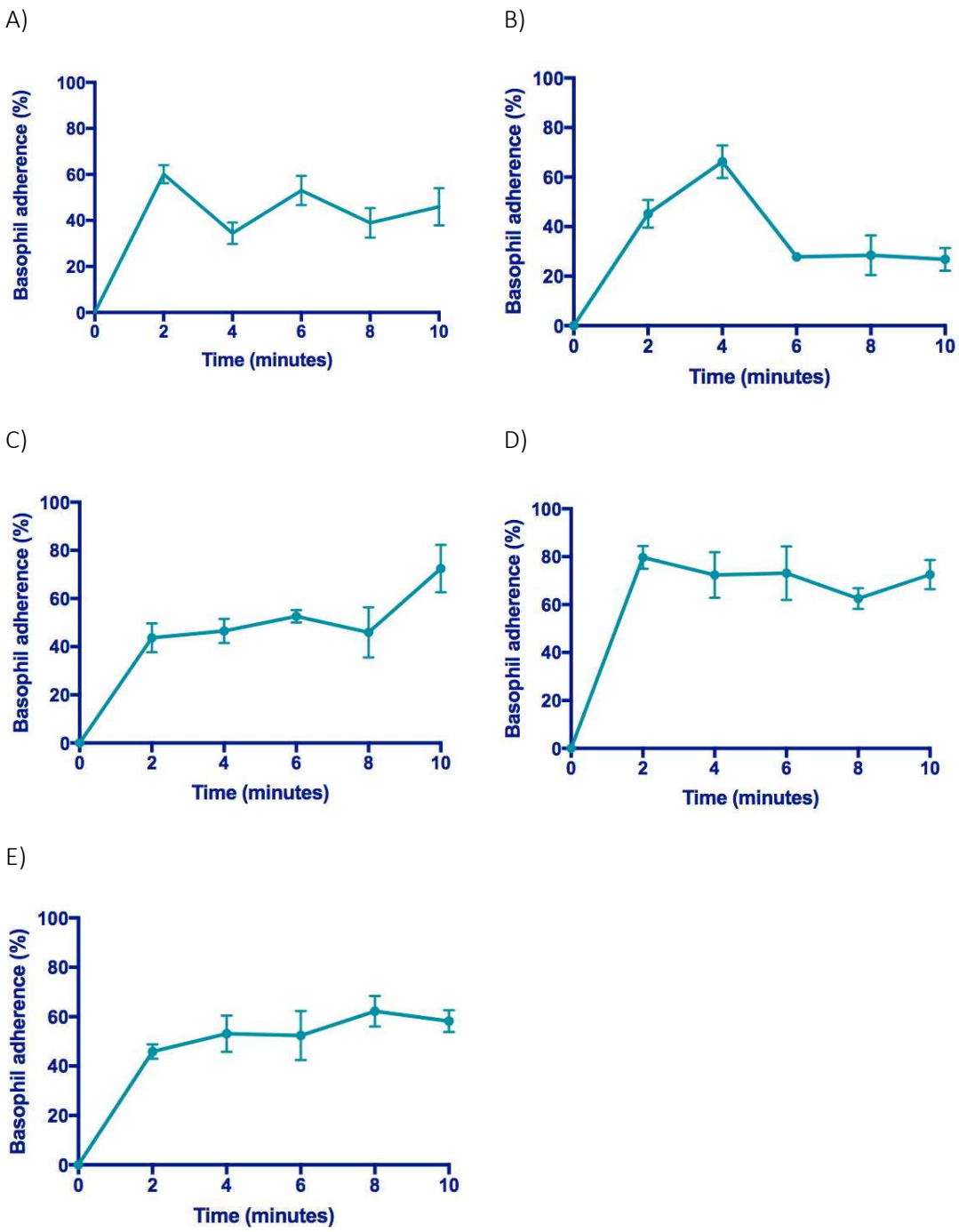

Figure 37: An example of individual's basophil adherence over time at optimal flow rate 30 ml/h based on CCR3 expression analysis. Samples were taken at two-minute intervals to determine basophil adherence and vertical bars indicate mean with SEM. Data is representative of five subject's data repeated 3 times at each time-point. The Kruksal Wallis test was used to compare the means of each individual at the two minute intervals at 30 ml/h. Means did not vary significantly by <0.05
P = 0.251, Kruksal Wallis statistic 5.37

A)

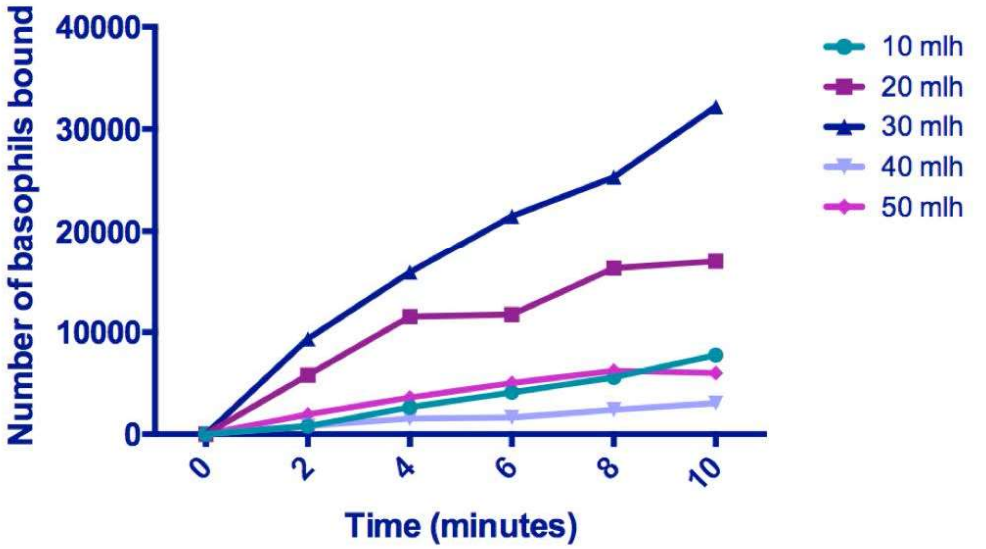

B)

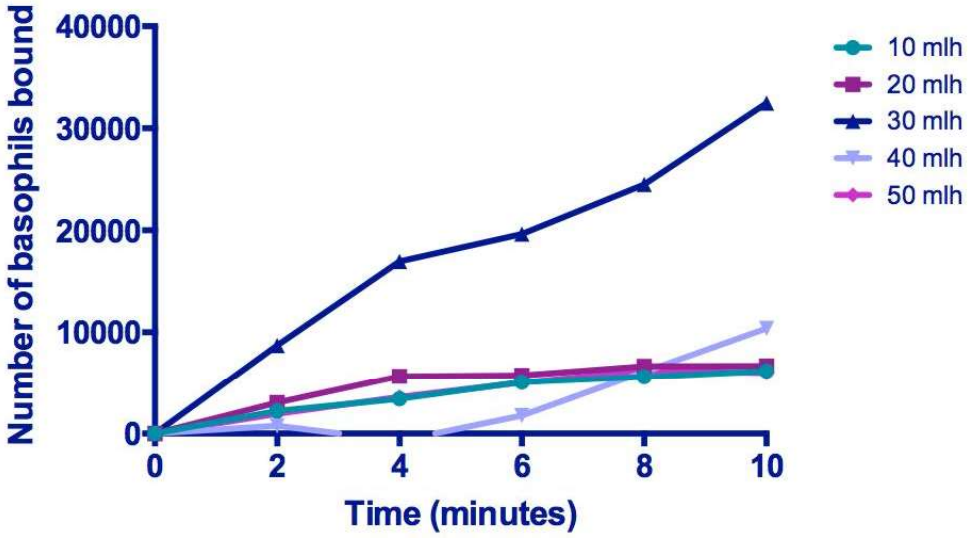

Figure 38: Approximate number of basophils bound over time based on A) CCR3 expression by FACS analysis. B) Net histamine for five subjects (measured in triplicate) when run through the device at 30 ml/h. The data presented are based on definitive numbers i.e. the unbound basophil percentage removed

The Wilcoxon paired signed-rank test was performed to compare the approximate number of basophils bound when the samples were analysed by A) FACS or B) net histamine release.

10 ml/h: P = 0.063, p = 0.001 **(SC), r^2 = 1; 20 ml/h: P = 0.313, p = 0.001 **(SC), r^2 = 1; 30 ml/h: P = 0.063, p = 0.001 (SC), r^2 = 1; 40 ml/h: P = 0.063, p = 0.030 *(SC), r^2 = 0.829; 50 ml/h: P = 0.063, p = 0.008 ** (SC), r^2 = 0.943

A)

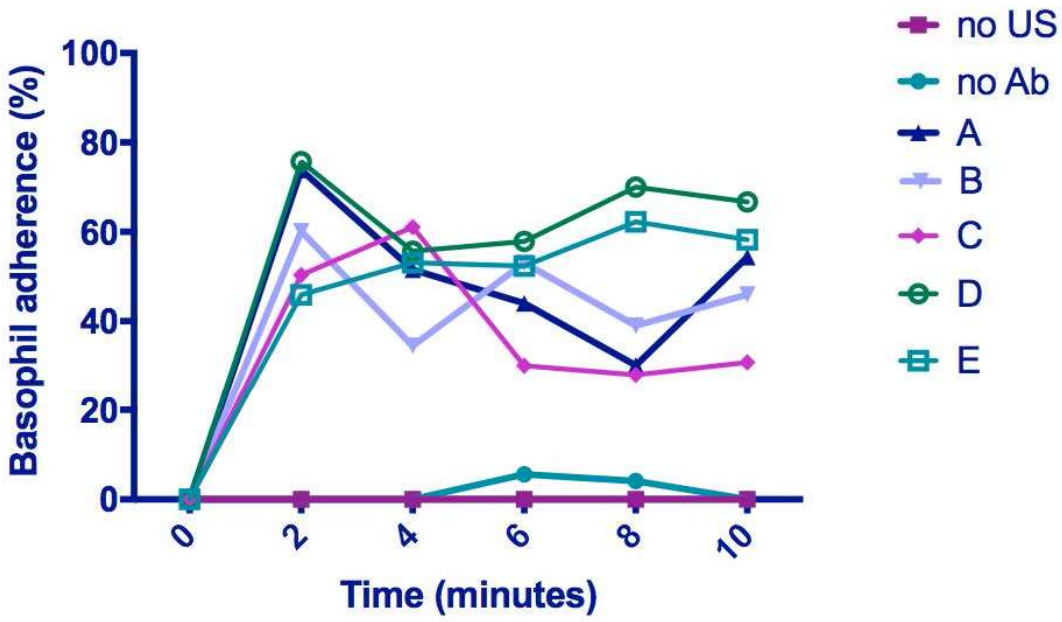

Figure 39: Flow rate experiments conducted at 30 ml/h to determine mean percentage of basophil adherence over time

The data presented are based on definitive numbers i.e. the unbound basophil percentage removed. The Kruksal-Wallis test was run to compare mean basophil adherence between the donors (A – E), at each time point, P = 0.256.

3.1.3.3 Effect of erythrocyte depletion on acoustofluidic sorting

It was observed that basophil enriched samples increased the likelihood of basophil adherence due to the increase in basophils for the slide to capture (Figure 40). When comparing enriched basophil samples to erythrocyte depleted samples over a 30-minute period within the device, a ten-fold difference in basophil adherence to the slide was observed. Maximum binding experiments run for 30 minutes found that in enriched samples, the acoustofluidic device captured approximately 60,000 basophils in comparison to erythrocyte-depleted samples, which reached 6,000 basophils bound. Variation in basophil number is evident, suggesting that adherence is subject dependent. Maximum binding experiments found that purified basophil samples could achieve an average of 72.5% basophil adherence. When maximum binding experiments were performed using erythrocyte-depleted samples, 39% basophil adherence was achieved (Figure 41). This indicates a good basophil binding capacity can be achieved when exposing samples to erythrocyte depletion agents prior to device entry. The largest variation is demonstrated for both A) and B) at 16-minute time point 60 – 80% representative of the introduced large variation created when the syringes were changed. Each time point was compared for enriched basophils and erythrocyte depleted blood using Wilcoxon paired signed-rank test, P = <0.0001 ****. Both erythrocyte depleted and basophil enriched samples showed significant correlation (p = 0.043 *) and thus determined that both methods would produce essentially the same pattern of basophil adhesion.

Polymer dip pen nanolithography (DPN) was explored through a collaboration with Dr Sylwia Sekula-Neuner at the Karlsruhe Institute of Technology (KIT) to create an even distribution of antibody across the slide surface (thereby increasing the binding opportunities for anti-CD203c) (Figure 42). A uniform pattern is observed when the anti-CD203c is printed onto the slides, all dots are visible. When erythrocyte depleted blood was run through the device, it was found that the percentage of basophils bound was dependent on the slide coating technique used. FACS analysis confirmed that approximately 90% bound when using DPN slide; whereas IH slides only achieved 45% adherence (data not shown). Basophil adherence was confirmed by imaging the carrier layer by confocal microscopy, where statistical analysis determined that a mean of 23,450 basophils were bound when using DPN slide; in comparison to 11,380 IH slide. The application of control slides observed that there was minimal non-specific basophil adherence, with a mean of 445 basophils bound in the absence of antibody and mean of 56 basophils bound to DPN slide when no ultrasound was present. When the DPN slide was employed within the acoustofluidic device at optimal conditions, it was found that a mean capture rate of 92% basophil adherence could be achieved. In comparison, IH slides had a lower mean capture rate of 62% (Figure 43). A larger range of basophil adherence 42 – 92% was observed in samples when using IH slides. Wilcoxon paired signed-rank test was used to

compared data between IH and DPN slides for each subject at the different time points. Spearman's rank correlation coefficient determined that there was good correlation between IH and DPN slides, r^2 = 0.771, though not significant (p = 0.051). Results indicate that the uniform distribution of antibody on DPN slide may attribute to the small range observed across samples (8%). In addition, DPN slide indicates the possibility that imaging may be plausible in the device, as the basophil binding area is known.

A)

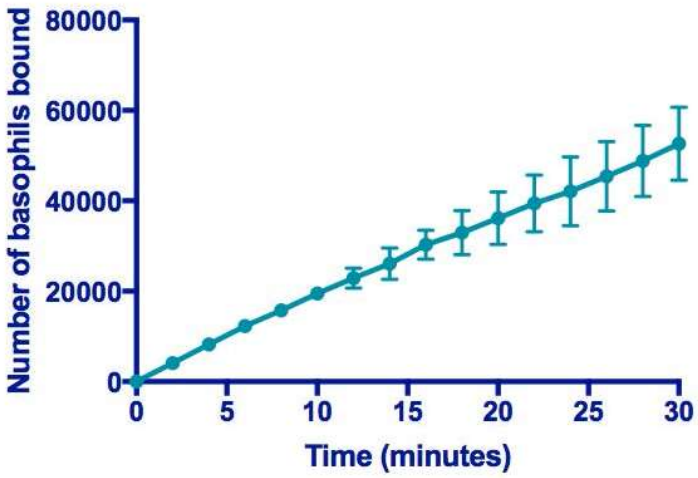

B)

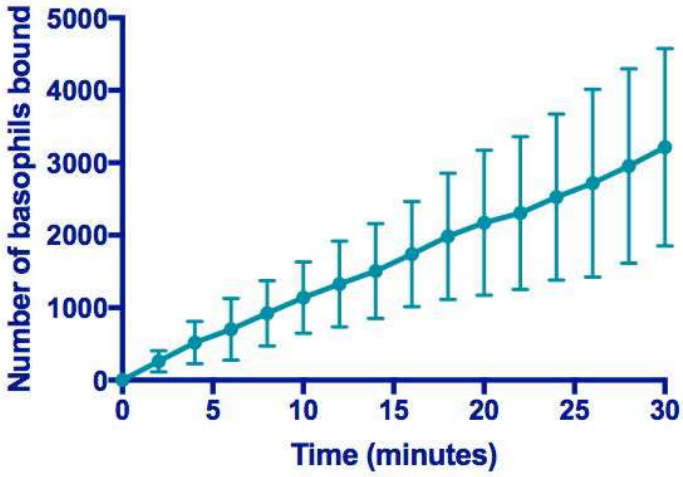

Figure 40: Number of basophils adhering to the slide over a 30-minute time period determined by FACS analysis of A) enriched basophils, B) erythrocyte cell depleted blood when run through the device at 30 ml/h. Samples were taken at 2 minute intervals and vertical bars indicate mean with SEM based on three different subject samples repeated three times.

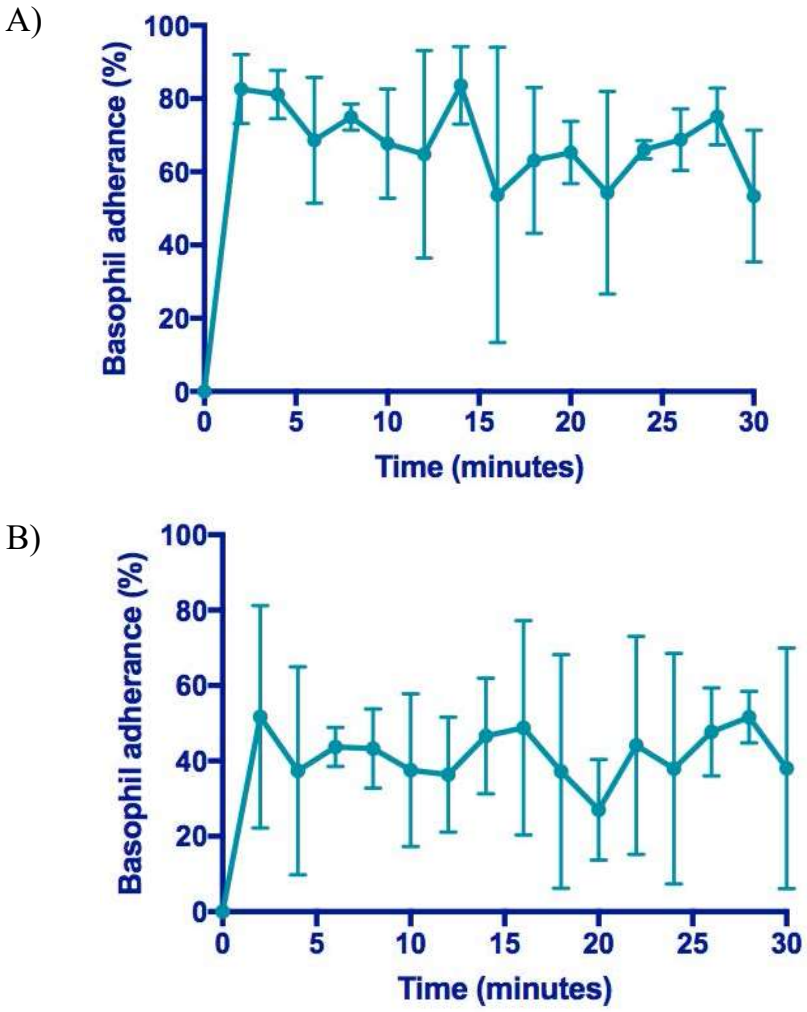

Figure 41: Mean percentage basophils adhering to the slide over a 30-minute time period with samples taken at two-minute intervals measured by FACS analysis in A) enriched basophils, B) erythrocyte cell depleted blood when run through the device at 30 ml/h. Samples were taken at 2 minute intervals and vertical bars indicate mean with SEM based on three different subject samples repeated three times. Means of each time point for both enriched basophils and erythrocyte depleted blood were compared using Wilcoxon paired signed-rank test, and correlation determined by Spearman's rank correlation coefficient. P = <0.0001 ****, p = 0.043 * (SC) and $r^2 = 0.444$

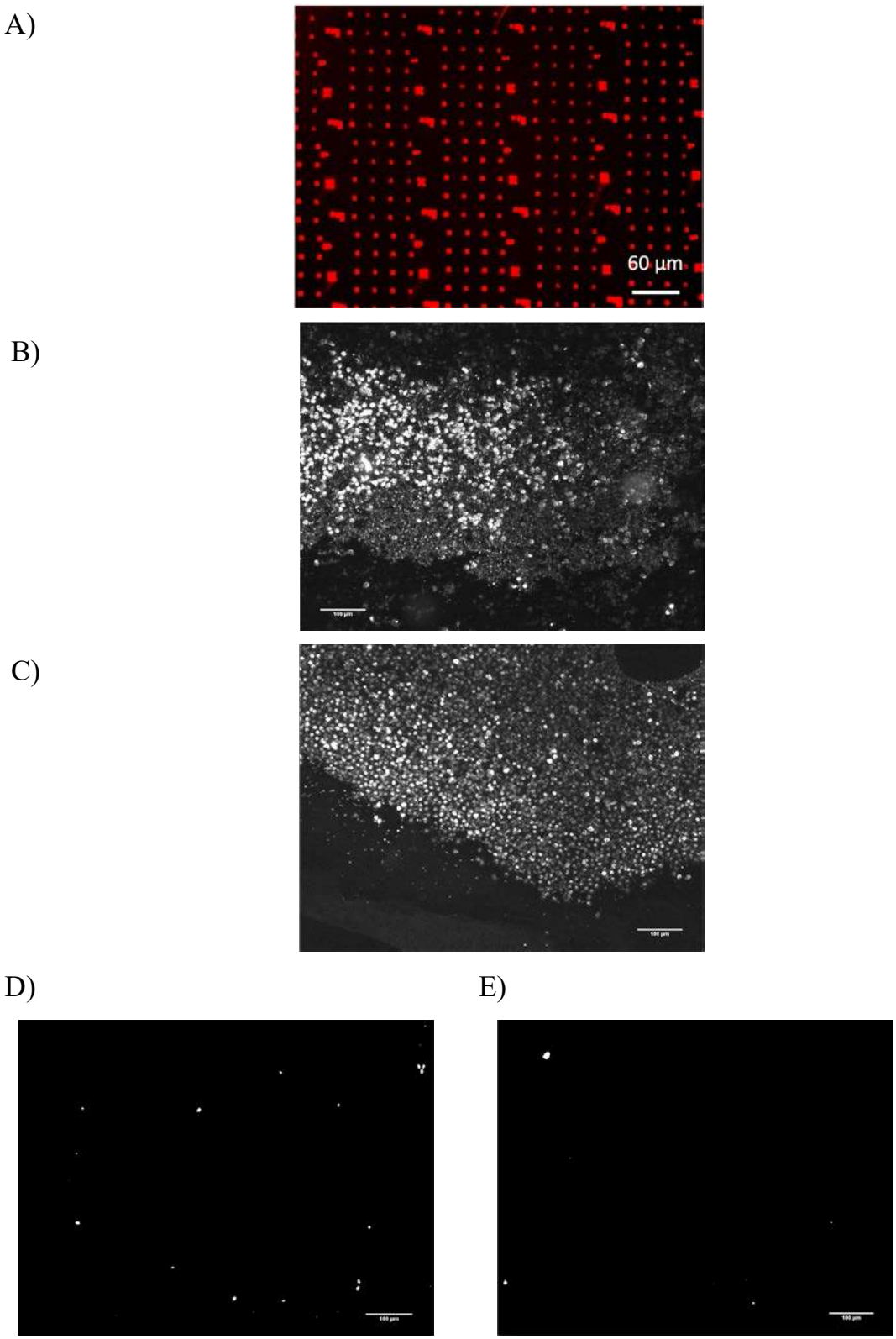

Figure 42: Confocal images using 10X magnification to determine the mean basophils bound in the carrier layer when using erythrocyte-depleted blood A) DPN Slide coated with pure anti-CD203c in the absence of PEG. After spin coating, the stamp is re-inked B) DPN slide, C) IH Slide, D) Control One – no antibody, E) Control Two – no ultrasound

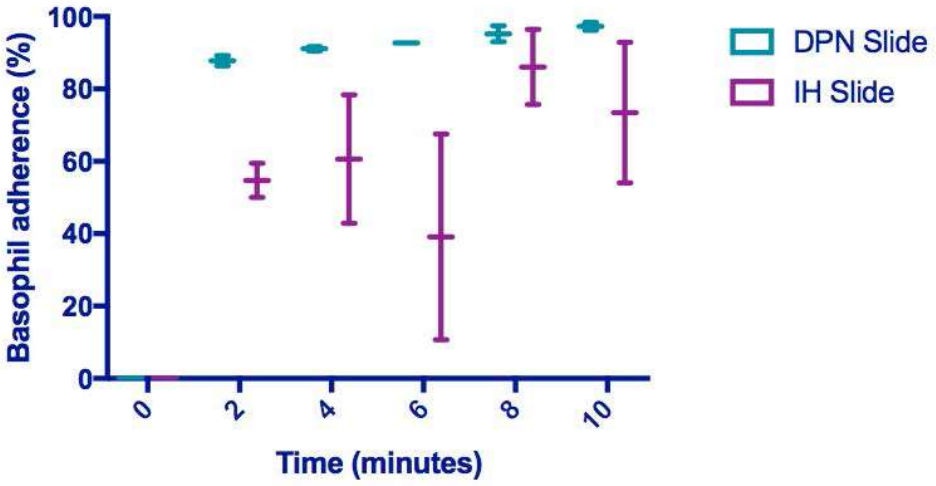

Figure 43: Percentage of basophils adhering to the slide in whole blood when comparing slides DPN (teal) & IH (pink) coated by two different methods with anti-CD203c. Vertical bars indicate mean with SEM based on three different subject samples repeated three times. Wilcoxon paired signed-rank test was used to compare the data between IH and DPN slides for each subject at the different time points. Spearman's rank correlation coefficient (SC) was determined to review the correlation between groups. $p = 0.063$, $p = 0.051$ (SC) and $r^2 = 0.771$

3.2 Basophil activation

3.2.1 Basophil activation determined by fluorescence activated cell sorting (FACS)

Flow cytometric methods were employed to measure basophil activation by means of CD63 expression. When subjects were tested against positive controls anti-FcεRI and FMLP and negative controls, FACS allowed clear visualisation and quantitation of increased CD63 expression (illustrated in Figure 44). A more profound response was observed as a result of anti-FcεRI stimulation (93%) in comparison to other controls. At lower concentrations of dust mite allergen, subject C) indicated that the subject was non-responsive (11.5% activated). However, D) at a much higher concentration 10,000 U/ml P5'S basophils are 87% active. This data highlights the need for numerous log doses testing in basophil activation tests.

When 17 healthy volunteers (Table 3) were tested against increasing concentrations of house dust mite, only eight responded to the allergen (Figure 45). Basophils primed with IL-3, had a 45% increase in CD63 expression in comparison to samples that were not incubated with IL-3 (subjects A & F). Five subjects demonstrated a bell shape curve with the optimal response occurring at 1 U/ml (B, E, F and G) and 10 U/ml (C). Subject H, demonstrated a bell shaped curve with a maximal response of 80% at 10 U/ml. Subject H's data implies there is an anomalous response observed at 0.01 U/ml, this is suggested as high CD63 expression is not achieved until between 1 - 10 U/ml. These experiments highlight the importance of using multiple doses, as many patients did not show any response until much later in testing, when using higher concentrations of dust mite 10 U/ml (subject C). Wilcoxon matched signed-rank tests and Spearman's rank correlation coefficient were performed to determine if there was a significant difference between the measurement of basophil activation in buffer containing IL-3, and samples without. If there were a significant difference, results would not correlate and thus have a large p value and a small r^2 value. Wilcoxon small p values suggested that the difference between the samples incubated with and without IL-3 was due to differing means (P = 0.001 ** - 0.023 *). Generally, those with IL-3 demonstrated higher activation and thus this is a logical analysis. Spearman's correlation coefficient showed significance p = 0.001 ** - p = 0.023 *, with the exception of A) p = 0.273, F) p = 0.0057 and G) p = 0.076. Samples generally correlated well, as expected with r^2 values accounting for the majority of the distribution seen (r^2 = 0.691 - r^2 = 0.922), with the exception of A) r^2 = 0.252; G) r^2 = 0.571.

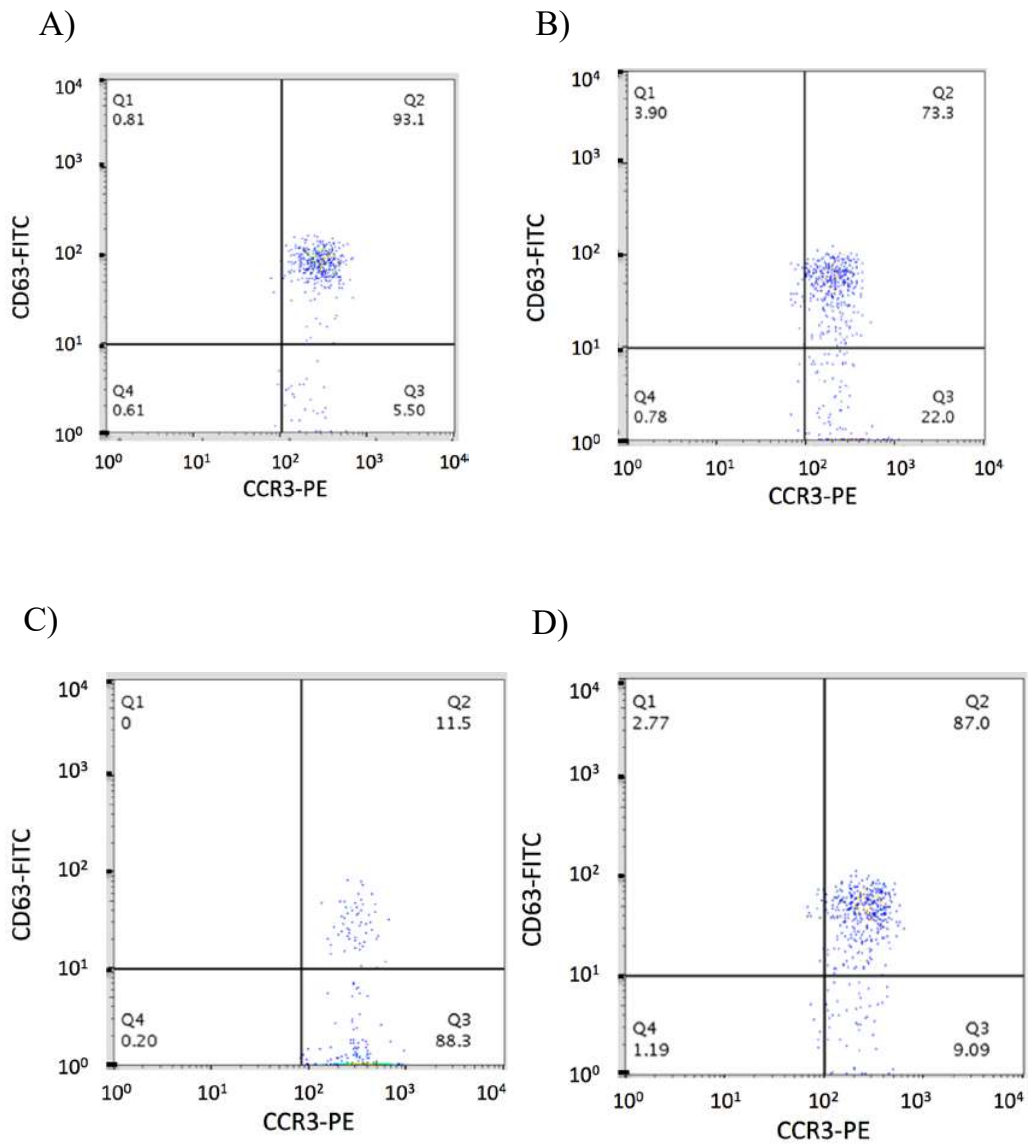

Figure 44: Altered expression of CD63 following experimental activation of basophils, as demonstrated by FACS with cells stimulated with A) Anti-FcεRI antibody B) FMLP C) *D. pteronyssinus* allergen extract at 0.001 U/ml and D) at 10,000 U/ml. Data shown is from one subject (Subject P5), but is representative of that in 18 separate experiments.

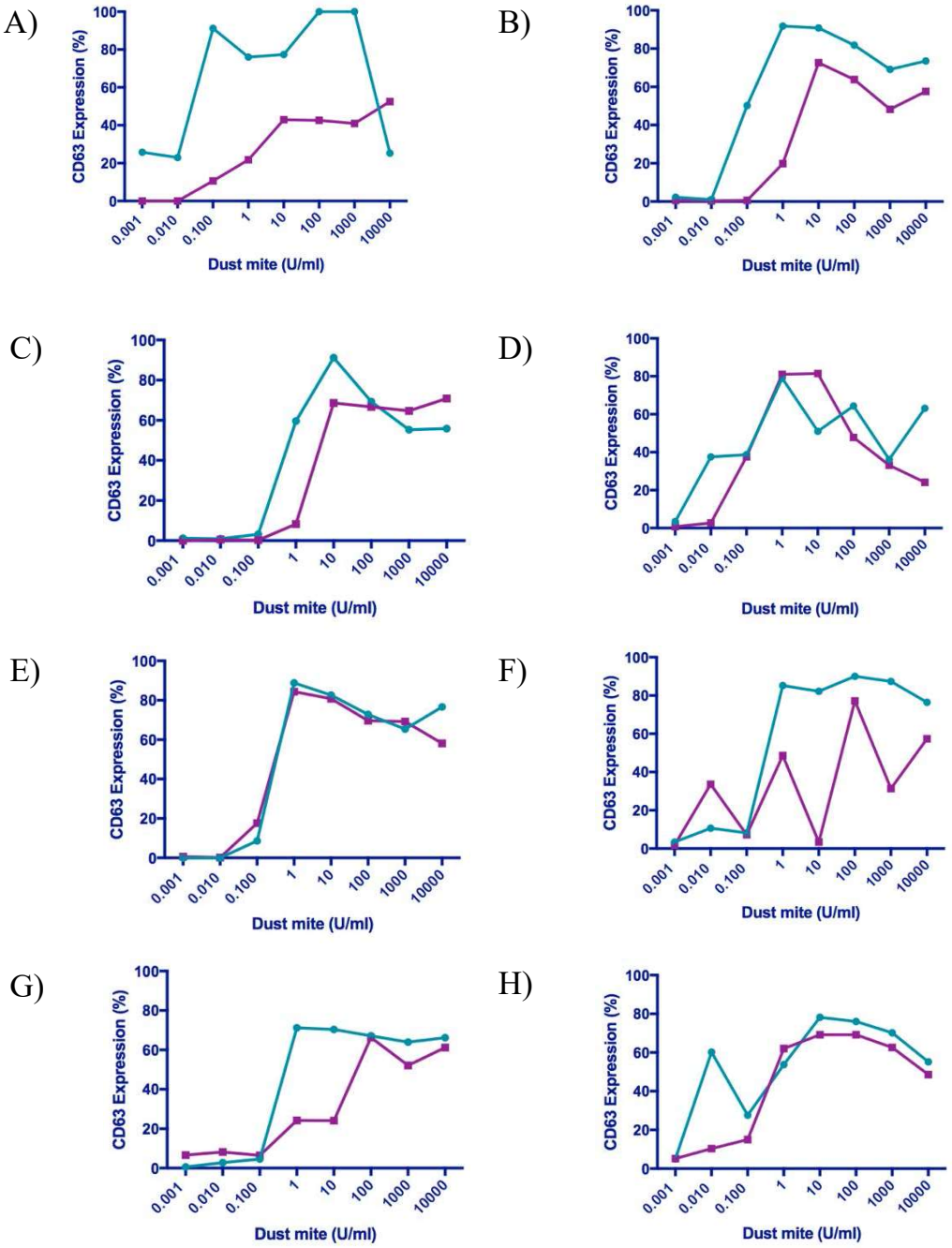

Figure 45: FACS analysis of eight dust mite allergic subjects, with (teal) and without (pink) IL-3 stimulation buffer. 17 subjects were screened in order to obtain eight dust mite atopic subjects.

Data is non-parametric and thus Wilcoxon matched pairs ranked-sign tests were performed to determine if there was a significant difference between results, Spearman's rank correlation coefficient (SC) was also performed. A) p = 0.023 *, p = 0.273 (SC), r^2 = 0.252; B) p = 0.008 **, p = 0.023*(SC), r^2 = 0.738; C) p = 0.383 ns, p = 0.023*(SC), r^2 = 0.738; D) p = 0.195, p = 0.035* (SC), r^2 = 0.691; E) p = 0.742, p = 0.001**(SC), r^2 = 0.922; F) p = 0.078 ; p = 0.057 (SC), r^2 = 0.619; G) p = 0.382, p = 0.076 (SC),r^2 = 0.571; H) p = 0.109, p = 0.009**(SC), r^2 = 0.826

Figure 46 depicts grass pollen allergic subjects' responses to increasing concentrations of grass pollen allergen measured in standard biological units (SBU). When eight grass pollen sensitive subjects were tested against increasing concentrations of grass pollen, all participants, (with the exception of D) produced a bell shape curve. A maximal response in all subjects demonstrating this are achieved at doses of either 1 SBU (participants A, E, G and H) or 10 SBU (Sub B, C, F). Subject elicited a response at the low concentrations, suggesting that the subject is very to grass pollen.

When percentage CD63 expression of anti-FcεRI was compared against FMLP; subjects tested generally had a much larger elicited response with anti-FcεRI (Figure 47). Furthermore, the responder population had a much higher CD63 % than non-responders and a much smaller range (65 – 95 %). Non-responders were found to have a larger range 5 – 80%. Non-responders had a slightly higher mean CD63 % when incubated with positive control FMLP, suggesting that non-responders' basophils may be more strongly activated through the FMLP activation pathway.

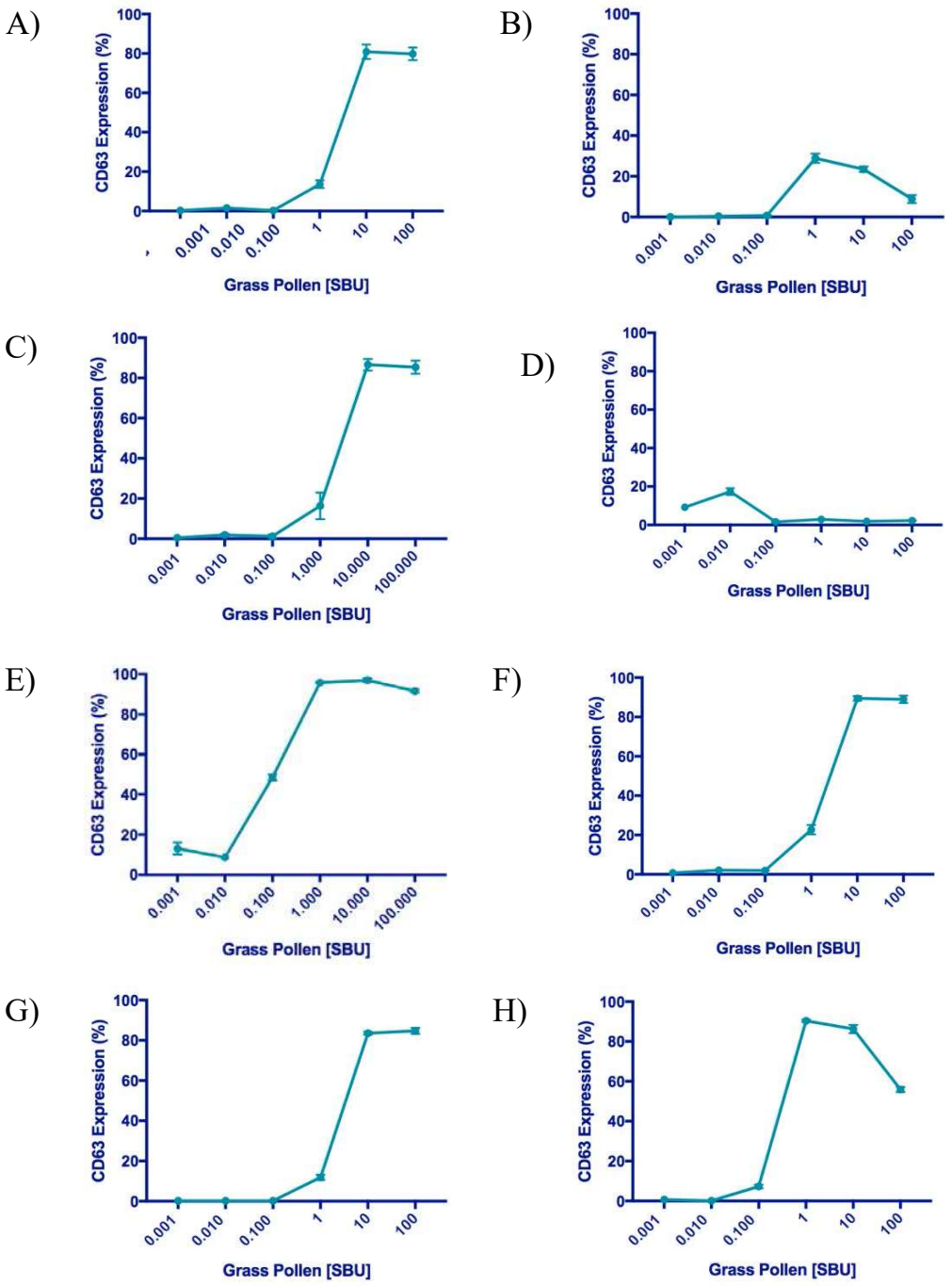

Figure 46: CD63 expression of basophils in grass pollen atopic subjects in response to increasing concentrations of grass pollen. 17 subjects were screened in order to obtain eight grass pollen atopic subjects. Results display the standard error of mean.

Results demonstrate subject's sensitivity to grass pollen allergen at different concentrations. Typically, these subjects display a bell-shaped curve response.

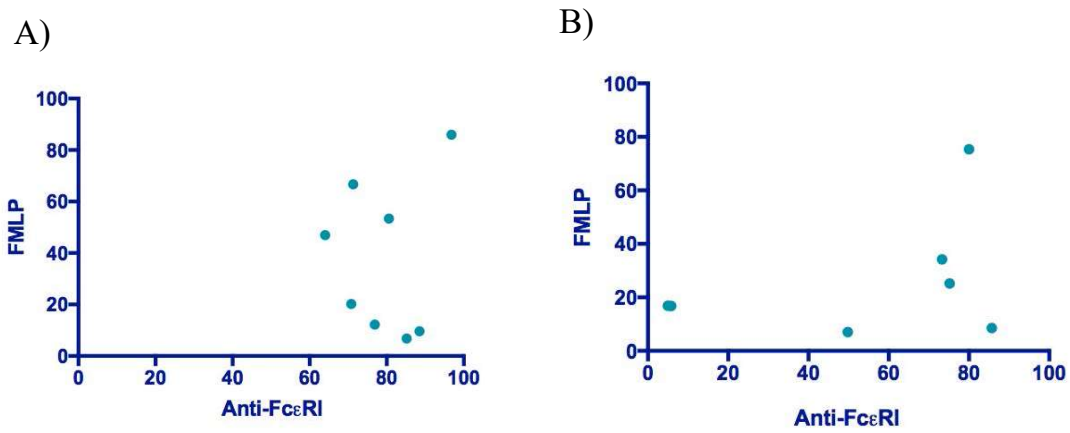

Figure 47: Comparison of the percentage CD63 expression against stimulation Anti-FcεRI and FMLP in A) responders and B) non-responders in the general population. Non-responders were defined as those who did not elicit a response to the allergens tested such as grass pollen and dust mite.

3.2.2 Basophil activation measurement based on secreted mediators

3.2.2.1 Measurement of histamine to determine basophil activation

When subjects with a known history of dust mite allergy were tested against increasing concentrations of dust mite (U/ml) it was found that four subjects elicited a bell shaped curve response (B, D, E, F, H) (Figure 48). The highest responses were elicited between 0.01 – 100 U/ml; with some subjects maintaining 80% activation until 1000 U/ml, suggesting that theses participants are very sensitive to dust mite. This would suggest that when exposed to high concentrations the subject's basophils are desensitised and therefore unable to mount a response. The net relative histamine release was calculated using Equation 9:

$$Net\ Histamine\ Release\ (\%) = \left(\frac{Release\ on\ challenge - spontaneous}{Total\ Histamine\ \ Content}\right) \times\ 100$$

Relative histamine release was measured using Equation 10:

$$Relative\ Histamine\ Release\ (\%) = \left(\frac{Release\ on\ challenge}{Total\ Histamine\ \ Content}\right) \times\ 100$$

Raw data is illustrated in Table 9.

3.2.2.2 Measurement of basogranulin to determine basophil activation

Optimisation of the dot blotting procedure was first achieved by testing bronchoalveolar lavage fluid (BAL), which is rich in basogranulin. When performing the dot blot assay using serial dilutions of BAL, a textbook standard curve was observed (Figure 49). Initially BAL fluid was used as an alternative to lysate samples; that were not immediately available at this experimental stage. Due to a new dot blotting apparatus, the current dot blotting protocol required updating and optimising, before reproducible and reliable results could be observed. BAL samples were used for a standard curve and incubated in different dilutions of primary antibody BB1 to choose the optimum dilution of standard for the basogranulin dot blot as a positive control to determine whether the assay is working. These experiments observed that both 1/3 dilution and 1/5 dilution of antibody BB1 demonstrated the expected standard curve with chemiluminescent output increasing as the dilution factor increased. Despite the anomalous results both for the pure sample of BAL, and for the 1/10 BB1 dilution at 1/16 BAL; the 1/3 dilution of BB1 was considered preferable and thus implemented within the new protocol.

Table 9: Net histamine release and relative histamine release for subjects tested against house dust mite allergen (DM), as illustrated in Figure 48

Raw data is entered in plain text, net histamine release is entered as **bold**, relative histamine release is entered in the table in *italics.* Spontaneous is represented by SP, house dust mite is shortened to DM. Subject letter and total histamine are listed in the first column.

Subject Total (AU)	SP (%)	DM 0.0010	DM 0.0100	DM 0.1000	DM 1	DM 10	DM 100	DM 1000	DM 10,000
A 135.4	27.82	54.006 **39.887** *12.067*	23.838 **17.606** *-10.214*	82.085 **60.624** *32.804*	96.522 **71.287** *43.467*	113.532 **83.850** *56.030*	128.720 **95.067** *67.247*	161.553 **119.315** *91.497*	70.126 **51.792** *23.972*
B 162.88	33.300	109.8 **33.798** *0.184*	104.8 **30.728** *-2.885*	140.8 **52.830** *19.217*	95.04 **24.736** *-8.878*	73.4 **11.450** *-22.163*	84.48 **18.252** *15.361*	69.03 **8.767** *-24.846*	103.5 **29.930** *-3.684*
C 115.8	20.000	39.95 **3.031** *-16.96*	80.73 **38.252** *18.252*	53.54 **14.768** *-5.231*	84.48 **41.489** **21.489**	54.06 **15.217** *-4.783*	108.1 **61.888** *41.888*	60.03 **20.373** *0.373*	71.59 **30.356** *10.356*
D 82.48	20.478	74.83 **90.725** *79.247*	112.6 **136.51** *116.040*	87.43 **106.001** *85.523*	69.81 **684.639** *64.161*	67.67 **82.044** *61.566*	61.85 **74.988** *54.510*	99.06 **120.101** *99.624*	100.3 **121.605** *101.127*
E 76.49	22.081	50.34 **65.812** *43.731*	37.96 **49.627** *27.546*	35.39 **46.267** *24.186*	92.85 **121.388** *99.307*	57.36 **74.990** *52.909*	99.06 **129.507** *107.426*	2.447 **3.199** *18.882*	28.77 **37.612** *15.531*
F	29.6	30.95 **36.018** *6.267*	44.01 **63.770** *34.020*	49.51 **75.457** *45.707*	60.21 **98.194** *68.445*	45.28 **66.468** *36.719*	51.34 **79.346** *49.596*	37.35 **49.618** *19.868*	162.9* **100** ***100***
G 154.1	19.70	0 **0** *0*	154.023 **99.950** *80.250*	129.521 **84.050** *64.350*	131.863 **85.570** *65.870*	146.811 **95.270** *75.570*	154.100 **100** *80.300*	120.845 **78.420** *58.720*	128.951 **83.680** *63.980*
H 149.8	20.34	98.519 **65.767** *45.427*	140.091 **100** *79.66*	149.800 **93.518** *73.179*	149.800 **100** *79.66*	144.134 **96.218** *75.878*	149.800 **100** *79.66*	118.891 **79.367** *59.027*	149.800 **100** *79.66*

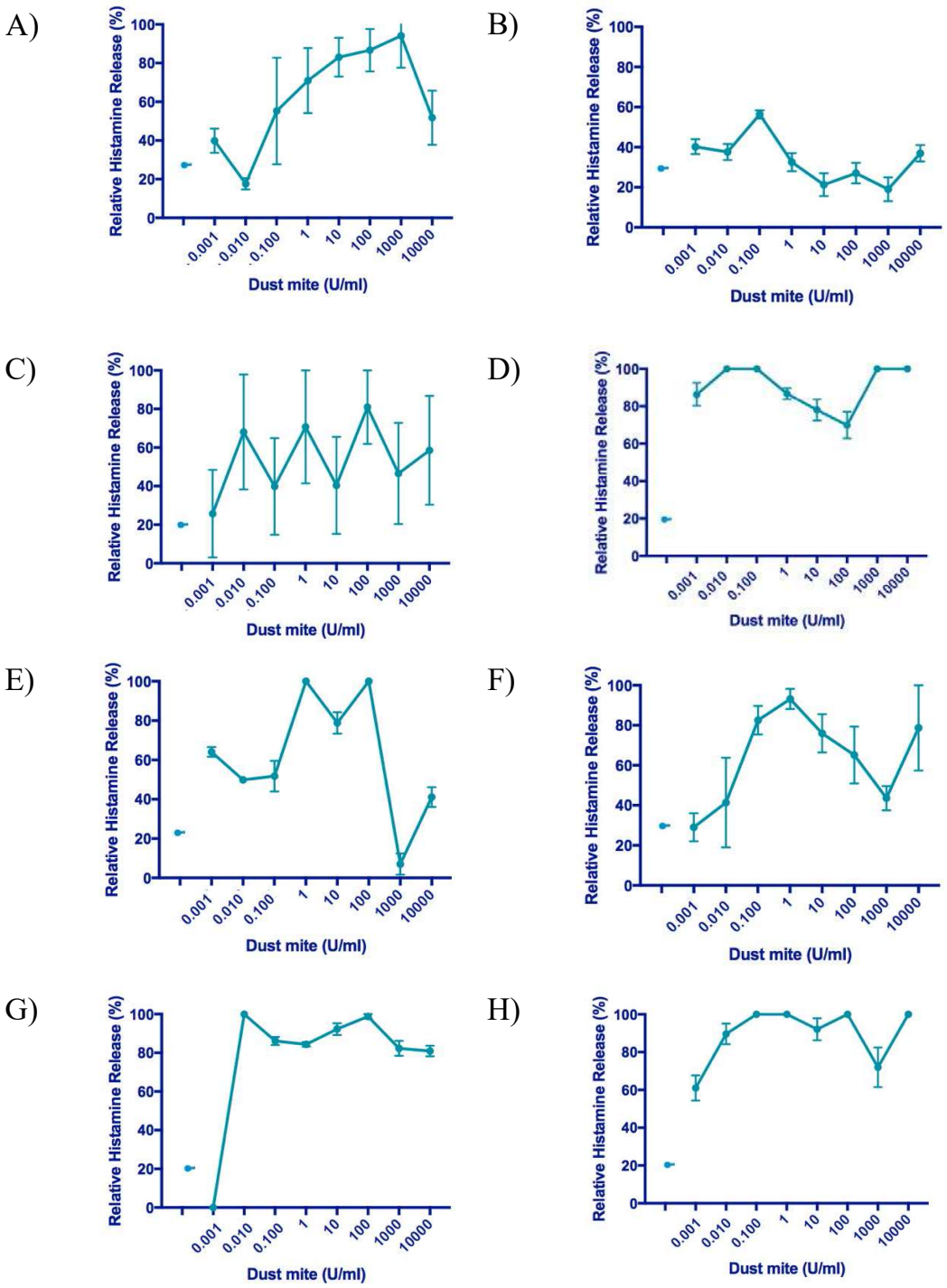

Figure 48: Relative percentage of histamine release from activated basophils in response to increasing concentrations of house dust mite allergic subjects. 17 subjects were screened in order to obtain eight dust mite atopic subjects. Spontaneous values are plotted in blue; standard error of mean is indicated by the bars on the graph at each data point.

A)

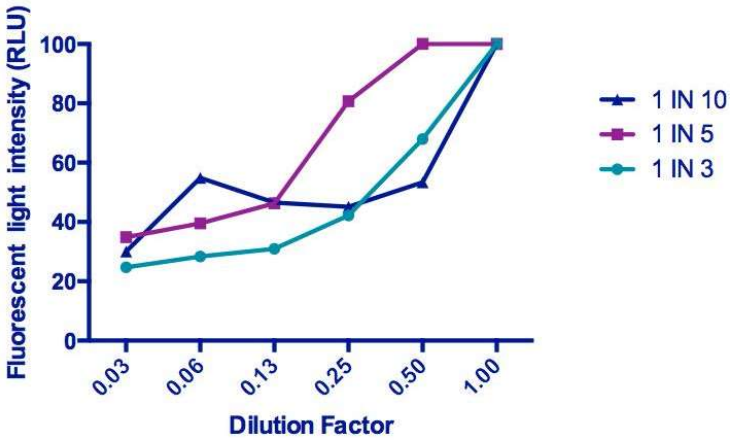

B)

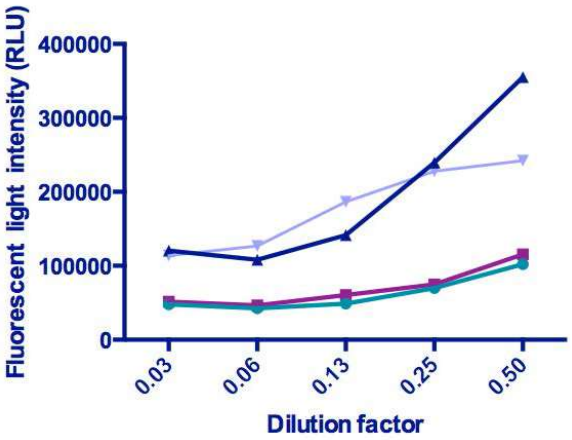

Figure 49: A) BAL standard curve to compare primary antibody dilutions of BB1; B) Signal on dot blots for basogranulin with standard preparations of lysates of purified basophils and a basogranulin-rich preparation of BAL (green). Data represents the mean of triplicate determinations

A) 1 in 3 demonstrated the best standard curve

B) Different lysate samples were used to determine which stock would be the best for replacing the BAL sample (green) that had been initially used. Different batches are highlighted in colours lilac, pink and purple.

3.2.2.3 Basogranulin release in response to aeroallergens dust mite and grass pollen

The effect of storage on basogranulin measurement was tested though the measurement of net basogranulin measurement when samples incubated with either FMLP, anti-FcεRI or allergen (visually in Figure 50 and data in Figure 51). When comparing samples stored at –20°C for one week, against fresh lysate samples, fresh samples generally demonstrated higher relative basogranulin measurement. This conclusion was based on FMLP whole blood ranged from 46 - 61.7% relative basogranulin release; erythrocyte depleted sample ranged from 43 - 46% net relative basogranulin release. Net basogranulin release was calculated using Equation 11:

$$Net\ Basogranulin\ Release\ (\%) = \left(\frac{Release\ on\ challenge - spontaneous}{Total\ basograunlin\ \ Content}\right) \times\ 100$$

Relative basogranulin release was calculated using Equation 12:

$$Relative\ Basogranulin\ Release\ (\%) = \left(\frac{Release\ on\ challenge}{Total\ Basogranulin\ Content}\right) \times\ 100$$

The data for this is displayed in Table 10. Spontaneous values ranged from 25 - 35% for both fresh and freeze thawed repeats. This suggested that the basogranulin output did in fact decrease over time and that the sensitivity of the assay was dependent on the type of sample used i.e. whether that day or freeze thawed samples stored at -20°C. The data is non-parametric and thus to compare the two measurements taken from the same individual, the Wilcoxon matched paired signed-rank test was used alongside Spearman's rank correlation coefficient to measure the relationship between the two sets of data. Despite appearance of the results, all p values from the paired testing were non-significant (p values 0.125 – 0.250). However, the FMLP results showed strong positive correlation rs = 0.8. Inverse correlation was demonstrated for both anti-IgE (rs = -0.5) and dust mite (rs = -1); meaning as one value gets larger, the other gets smaller thus demonstrating that the fresh lysate produced higher levels of basogranulin release than the frozen samples, suggesting reduction of basogranulin output over time under frozen conditions. However, both the fresh and frozen samples showed similar trends.

When eight atopic subjects were incubated with increasing log concentrations of house dust mite (0.001 - 10,000 U/ml); six of the subjects tested were sensitive to doses of dust mite lower than 1 U/ml (Figure 52). In three subjects, maximal net basogranulin release was observed at 0.1 U/ml (A, C, G) suggesting that the participants are sensitive to low doses of dust mite. Net basogranulin

release was calculated using Equation 11, net relative basogranulin release was calculated using Equation 12, the data is displayed in Table 11.

3.2.2.4 Comparison of CD63 expression and the release of histamine and basogranulin

Comparison of measurements of CD63 expression and net release of histamine or basogranulin revealed close similarities suggesting that all methods represent effective means for measurement of basophil activation (Figure 53 and Figure 54). The Wilcoxon matched pairs signed rank test determines if P value is large, that the means of AUC do not differ between tests. For the subjects tested against house dust mite, had large P values for both the AUC for A) net histamine and net basogranulin (P = 0.844) and C) CD63 expression and net basogranulin (0.945). This is not the case for the subjects exposed to grass pollen (Figure 54), whose P values were significantly small, thus indicating that we can reject the idea that the difference is due to chance, and conclude instead that the populations have different medians. When the correlation for area under the curve was tested using Spearman correlation coefficient, no significant results were observed for both dust mite and house dust mite exposed subjects. When the area under the curve for grass pollen allergic subjects using the net histamine release assay and net basogranulin release assay, the lowest p value was observed, though not significant (p = 0.197). For all tests run, r^2 values demonstrated inverse correlation, suggesting as one-mediator increases, the other decreases, this is not typically what was expected based on the literature. CD63 expression was employed in the initial experiments conducted to observe basophil activation in the acoustofluidic device (Figure 55).

Table 10: Net relative basogranulin release and relative basogranulin release for subjects from supernatants of blood cells challenged with A) FMLP, B) anti-FcεRI or C) house dust mite, with fresh samples (A1) and those stored at -80'C for one week (A1R); as illustrated in Figure 51

Raw data is entered in plain text, net histamine release is entered as **bold**, relative histamine release is entered in the table in *italics.* SP represents Spontaneous, house dust mite is shortened to DM, measured in U/ml.

A)

Subject	SP	0.003	0.01	0.03	0.1
A1	34.990	257,614 **16.500** *51.487*	308,333 **26.637** *61.623*	277,267 **20.428** *55.415*	232,349 **11.451** *46.437*
A1R	22.742	279,817 **20.272** *43.013*	303,870 **23.970** *46.711*	290,118 **21.856** *44.597*	285,494 **21.145** *43.886*

B)

Subject	SP	0.01	0.1	1
A1	34.990	268,960 **18.770** *53.754*	234,683 **11.917** *46.904*	243,800 **13.793** *48.730*
A1R	22.74	223,669 **11.641** *34.382*	235,918 **13.524** *36.265*	182,730 **5.348** *28.089*

C)

Subject	SP	0.1	1	10
A1	34.990	225,386 **10.059** *45.046*	227,690 **10.520** *45.506*	184,178 **1.823** *36.810*
A1R	22.74	236,284 **13.580** *36.321*	226,733 **12.112** *34.853*	296, 756 **22.876** *45.617*

Table 11: Net relative basogranulin release and relative basogranulin release for subjects tested against house dust mite allergen (DM), as illustrated in Figure 52

Raw data is entered in plain text, net histamine release is entered as **bold**, relative histamine release is entered in the table in *italics.* Spontaneous - (SP) house dust mite - (DM).

Subject Total (AU)	SP (%)	DM 0.0010	DM 0.0100	DM 0.1000	DM 1	DM 10	DM 100	DM 1000	DM 10,000
A 191,535.342	29.867	370,905 **51.640** *21.773*	341,169 **47.500** *17.6330*	384,128 **47.886** *21.614*	343,942 **47.886** *18.019*	439,801 **61.232** *31.365*	377,961 **52.622** *22.755*	372,644 **51.885** *22.018*	385,933 **53.732** *23.865*
B 107,365.562	30.000	189,511 **56.654** *26.654*	134,032 **40.069** *10.069*	140,283 **41.937** *11.937*	134,270 **40.139** *10.139*	179,298 **53.601** *23.601*	205,416 **61.409** *31.409*	239,544 **71.611** *41.611*	264,427 **79.050** *49.050*
C 27,961.215	44.610	187,483 **14.914** *69.534*	149,525 **0.836** *55.456*	277,560 **48.322** *100*	137,817 **3.506** *51.114*	146,428 **0.323** *54.307*	152,927 **2.098** *56.718*	216,990 **25.858** *80.477*	242,651 **35.375** *89.994*
D 66,529.382	39.500	328,930 **20.226** *59.794*	275,019 **10.426** *49.994*	225,635 **1.450** 41.019	267,013 **8.971** *48.539*	275,547 **10.521** *50.090*	307,627 **16.354** *55.922*	354,780 **24.925** *64.494*	348,107 **23.712** *63.280*
E 219,911.230	26.700	474,059 **46.389** *73.158*	238,510 **10.039** *36.807*	198,101 **3.803** *30.571*	202,210 **4.437** *31.205*	277,452 **16.049** ***42.816***	265,349 **14.181** *40.949*	309,519 **21.000** *47.765*	386,892 **32.938** *59.706*
F 1,251,298.420	33.1	1,929,091 **64.860** *90.006*	1,103,474 **22.915** *56.061*	619,880 **1.653** *31.492*	815,229 **8,271** *41.417*	539,839 **-5.720** *27.426*	347,149 **15.509** *17.637*	491,078 **8.197** ***24.949***	1,012,426 **18.289** *51.435*
G 51,013.941	55.800	672,209 **7.589** ***63.400***	506,048 **8.082** *47.728*	1,216,739 **58.947** ***100***	506,760 **-8.015** *47.800*	479,550 **10.581** *45.229*	425,027 **15.724** ***40.087***	494,611 **9.161** *46.650*	709,951 **11.149** ***66.960***
H 283,993.284	41.000	1,340,732 **21.182** *62.279*	1,193,396 **14.338** *55.435*	996,775 **5.205** *46.301*	511,724 **-17.326** *23.770*	707,709 **8.222** *32.874*	540,686 **15.981** *25.116*	635,841 **11.560** *29.536*	737,635 **6.832** *34.264*

3.2.2.5 Comparison of whole blood and red blood cell depleted blood samples with dot blot

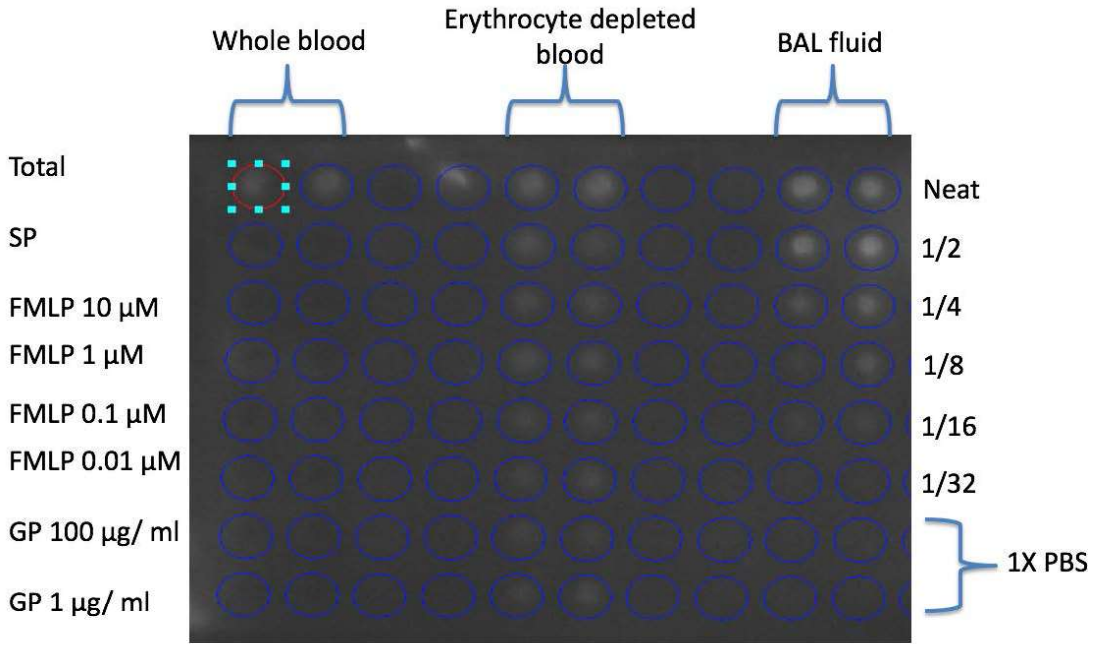

Figure 50: Dot blot image for basogranulin expression in whole blood and erythrocyte depleted blood stimulated with a range of concentrations of positive control FMLP (F) or with allergen (grass pollen (GP)) extract

A basogranulin-containing BAL fluid sample served as an assay standard. As a means of estimating total cell associated basogranulin (Total), cells were erythrocyte depleted (also carried out for all treatments (central traces). Buffer alone was added to cells to determine spontaneous (SP) release. Experiments were carried out in duplicate determinations.

A)

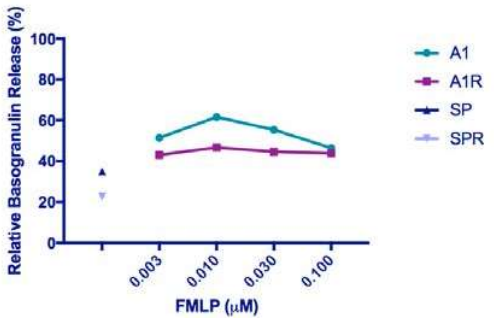

B)

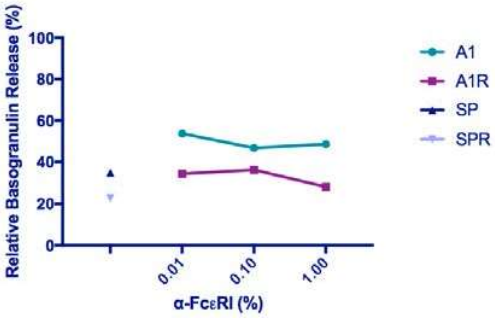

C)

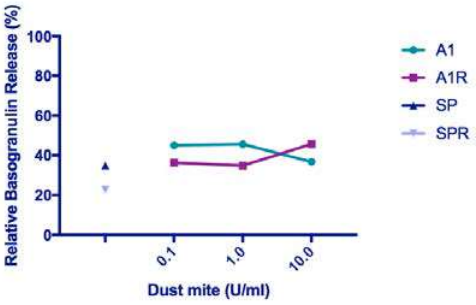

Figure 51: Relative basogranulin release from supernatants of blood cells challenged with A) FMLP, B) anti-FcεRI or C) house dust mite, with fresh samples (A1) and those stored at -80'C for one week (A1R). Spontaneous release is shown with fresh sample (SP) and with frozen samples (SPR). Data is representative of 12 separate experiments

Overall, fresh lysate samples produced higher levels of basogranulin release than the frozen samples, suggesting reduction of basogranulin output over time under frozen conditions both, the fresh and frozen samples showed similar trends. The data is non-parametric and thus to compare the two measurements taken from the same individual, the Wilcoxon matched pairs signed-rank test was used, to determine the distribution of the data, Spearman's rank correlation coefficient was used. A) p =0.125, rs = 0.8; B) p = 0.250, rs = -0.5 ; C) p = 0.167, rs = -1

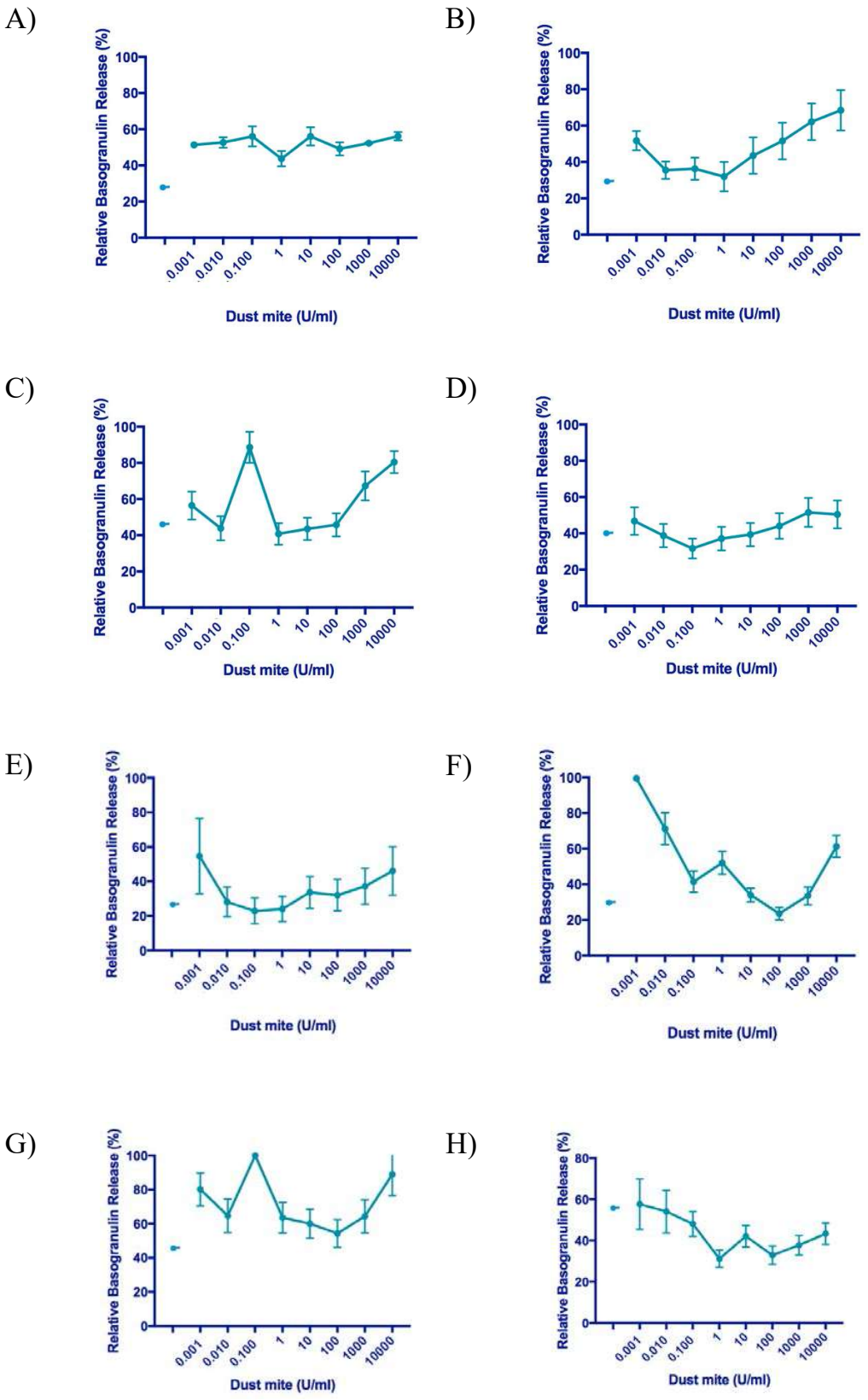

Figure 52: Net percentage of basogranulin release from activated basophils in response to increasing concentrations of house dust mite in eight house mite sensitive subjects. 17 subjects were screened, spontaneous release is shown in blue, lines indicate SEM from triplicate values

A)

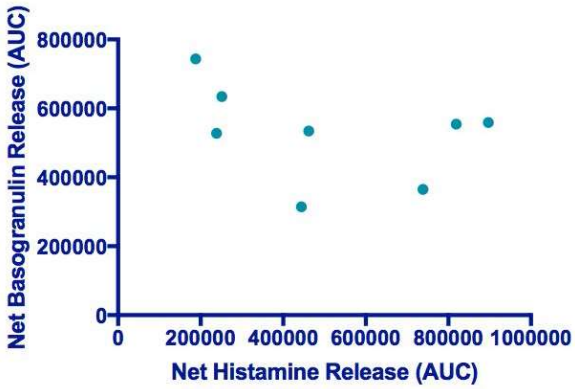

B)

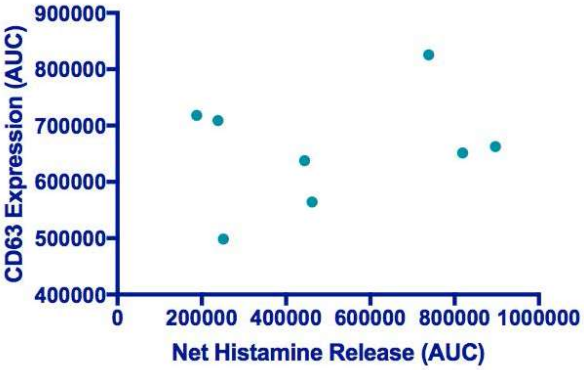

C)

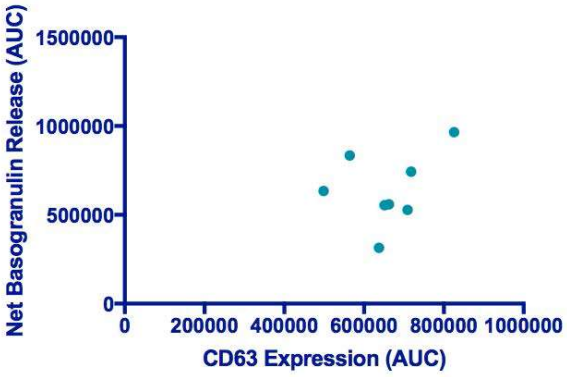

Figure 53: Relative degree of A) net basogranulin and histamine release, B) histamine release and CD63 expression, and C) basogranulin release and CD63 expression (all expressed as area under the curve) in response to a range of dilutions of dust mite in eight allergic subjects. Wilcoxon matched pairs signed rank test and Spearman rank correlation coefficient was run on each. A) p = 0.844, p = 0.664 (SC), r^2 = -0.190; B) p = 0.195, p = 0.522 (SC), r^2 = 0.267 ; C) p = 0.945, p = 0.582 (SC), r^2 = 0.238

A)

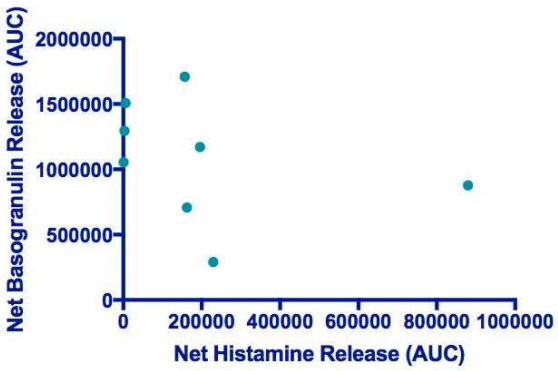

B)

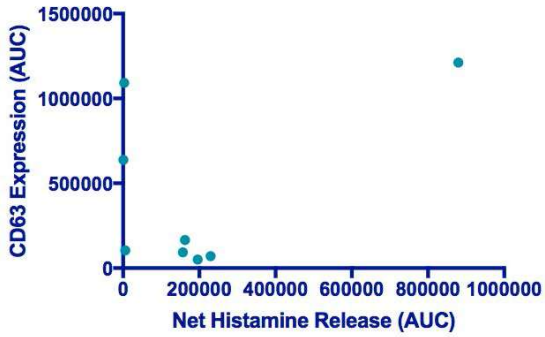

C)

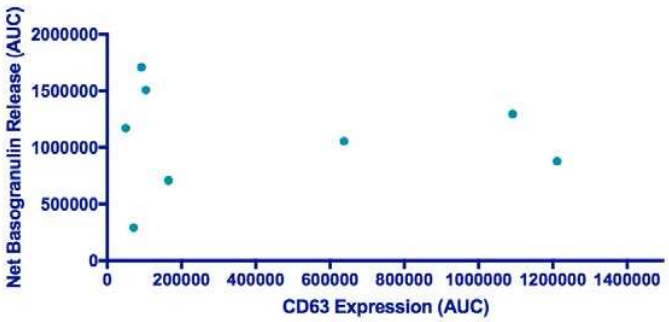

Figure 54: Relative degree of A) net basogranulin and histamine release, B) histamine release and CD63 expression, and C) basogranulin release and CD63 expression (all expressed as area under the curve) in response to a range of dilutions of grass pollen in eight allergic subjects. Wilcoxon matched pairs signed rank test and Spearman rank correlation coefficient was run on each. A) p = 0.016 *, p = 0.197 (SC), r^2 = -0.524; B) p = 0.460, p = 0.619 (SC), r^2 = -0.214 ; C) p = 0.039 *, p = 0.882 (SC), r^2 = - 0.071

3.3 Integration of an acoustofluidic device to measure basophil activation

3.3.1 Creation of controls using anti-CD63 outside of the device

To explore the use of CD63 as a marker of activation within the acoustofluidic device, controls were first sought by testing the anti-CD63 Alexa Fluor 647, alongside the nuclear stain DAPI, on large basophil populations adhering to slides by cyto-centrifugation. In Figure 55 when controls were visually compared by high purity basophil samples with either buffer (A), FcεRI (B) or FMLP (C); it was observed that larger CD63 expression was present on basophils incubated with FcεRI . The negative control, allowed the background CD63 expression to be removed from all images, so that when tested within the device, false positive results could be determined. This created a range that would describe the basophil population as negative. The anti-FcεRI based on other basophil activation tests, typically activates a higher population of basophils than FMLP and thus by using the two controls a range of positive fluorescent values were determined. This enabled any new morphology of the basophils to be observed.

Figure 56 demonstrates the different channels used (DAPI and Alexa Fluor 647) and how these were edited to remove background noise and channel leaking. Separate channels were imaged alone A) DAPI nuclear staining, B) anti-human CD63 Alexa Fluor 647 and C) demonstrated the overlay of both DAPI and Alexa Fluor 647 to determine basophil activation on slide.

3.3.2 Use of anti-CD63 integration into the acoustofluidic device

For activation studies, imaging was performed within the device. When using enriched basophil populations, the negative control was successfully established using DAPI staining in Figure 55. These images demonstrate that the device has successfully bound cells in the reflector layer. However, these experiments were hindered by the inability to produce quality images with using an objective of more than 25 x magnification. Images taken within the device using the FITC (to label anti-CD63) and DAPI stain were able to identify the basophils bound to the reflector layer of the device (slide coated with anti-CD203c). When comparing images of positive basophil controls collected outside of the device, to those within the device; it was evident that basophil activation had been achieved (Figure 57). Although the images within the device differ by microscope and magnification, basophil morphology observed is somewhat similar. This proposes that if experiments continued, basophil activation could be observed within the device.

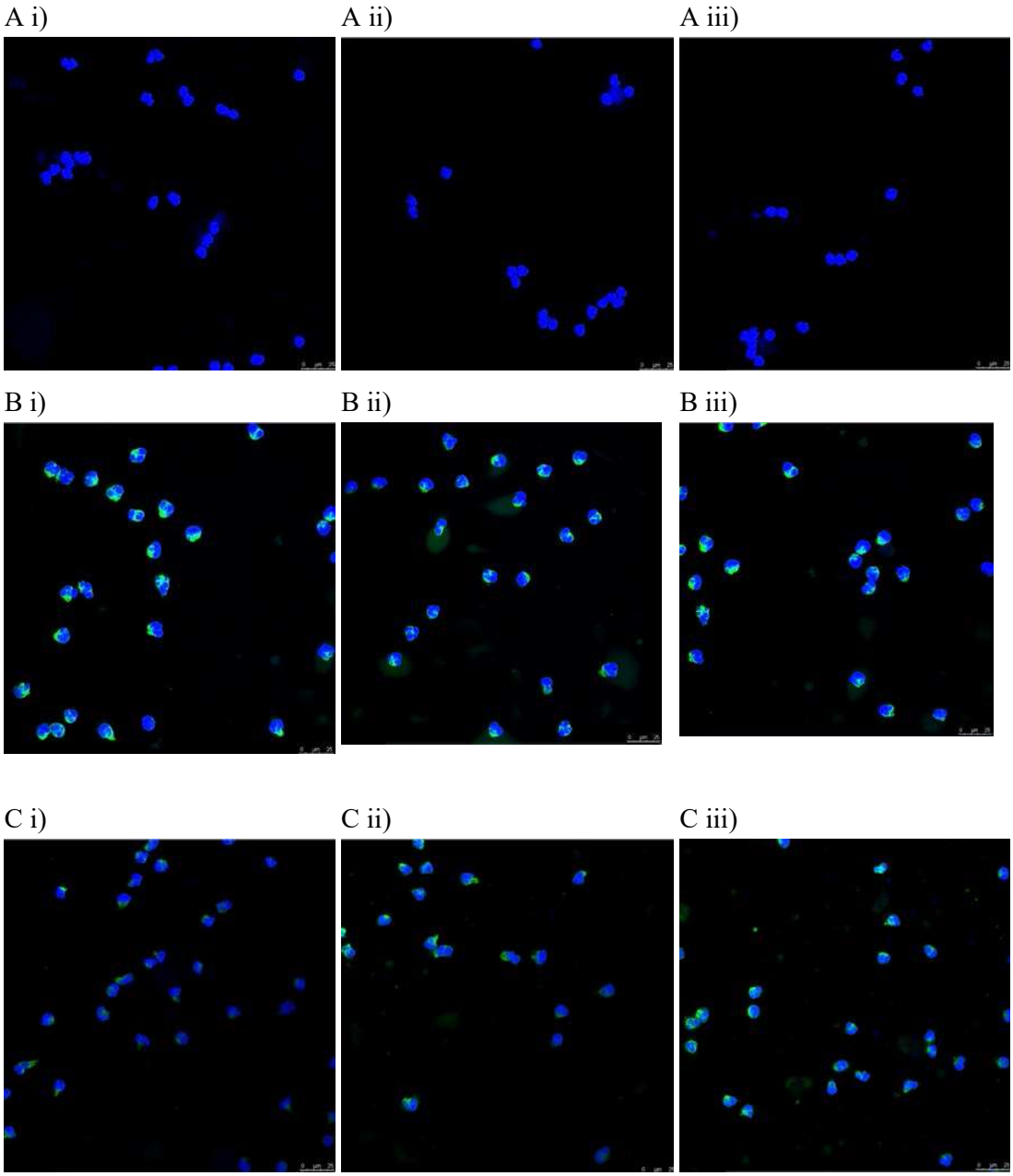

Figure 55: Initial testing of CD63 Alexa Fluor 647 using RoboSep buffer as a negative control (A) and positive controls anti-FcεRI (B) and FMLP (C)

The images depict the nucleus of basophils (blue) and CD63 expression (green) to determine activated cells when either resting (A) or stimulated (B, C). From these images, the mean fluorescence density can be determined and thus a value can be obtained for the threshold of activation in basophils when using CD63 as a marker of activation.

A)

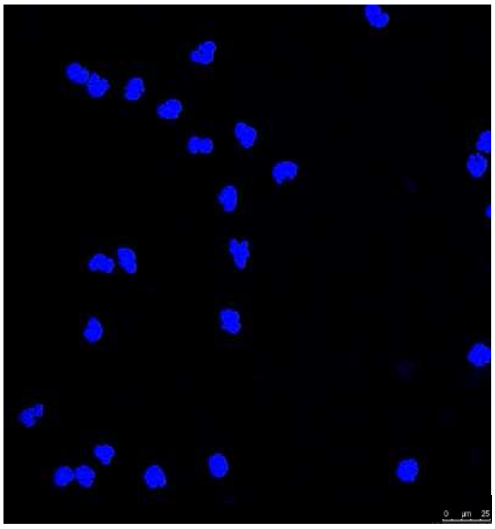

B)

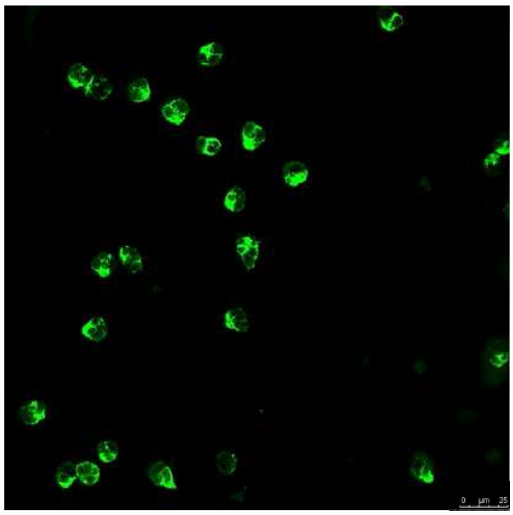

C)

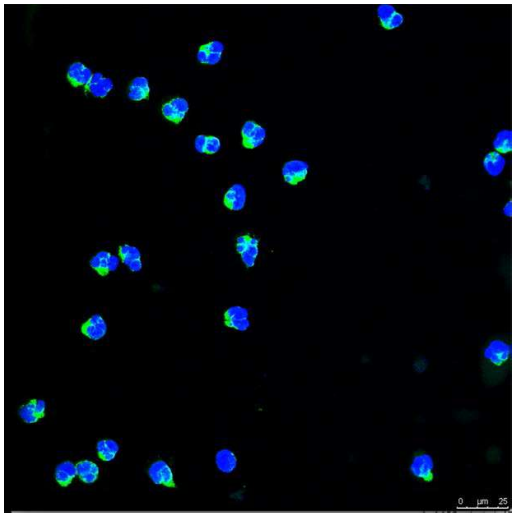

Figure 56: Confocal imaging of basophils when activated with anti-FcεRI with 63X glycerol objective A) DAPI nuclear staining, B) anti-human CD63 Alexa Fluor 647 C) Overlay of both DAPI and Alexa Fluor 647 to determine basophil activation on slide

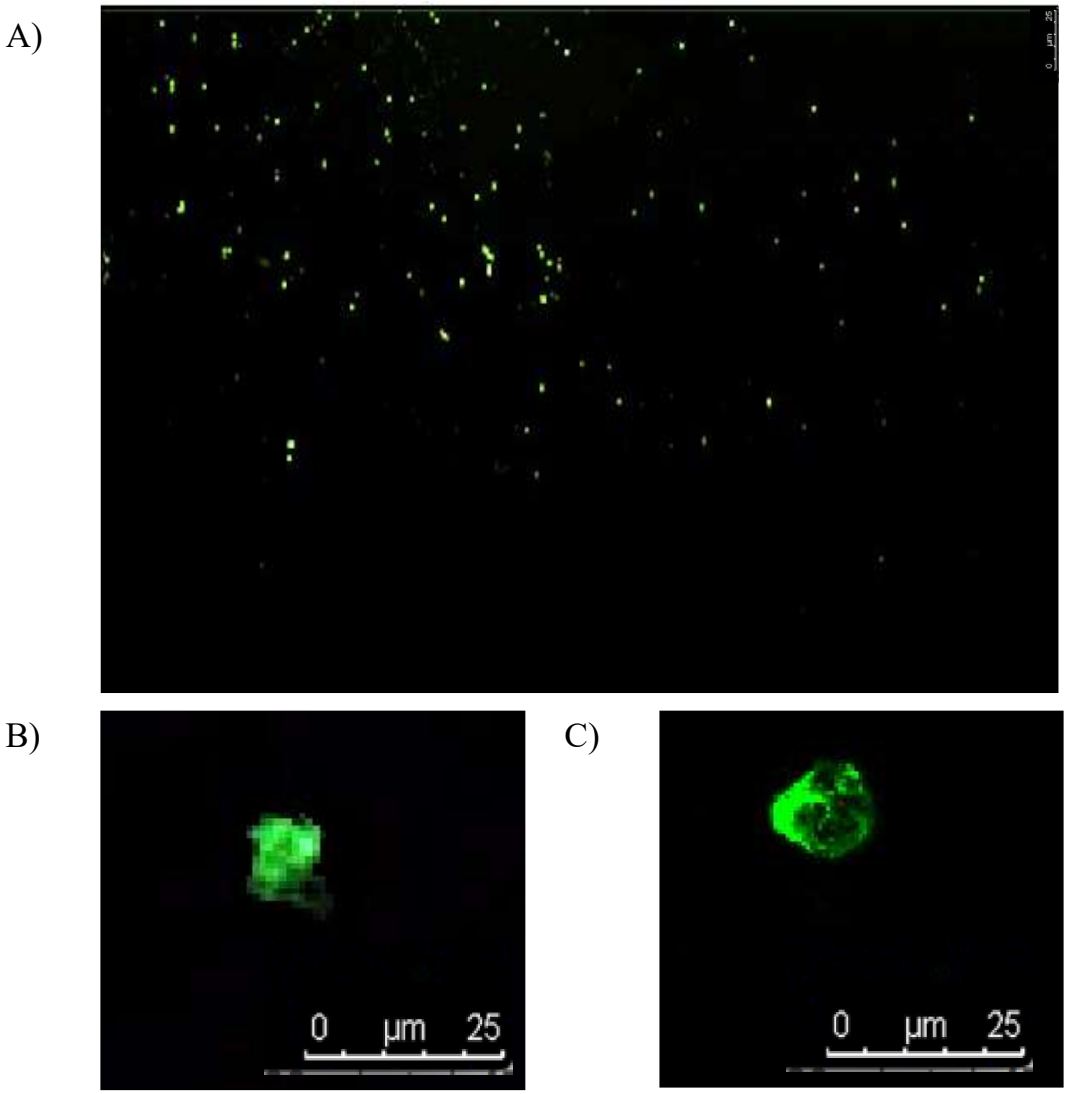

Figure 57: Basophils activated with anti-FcεRI observed using Alexa Fluor 647 tagged CD63 at A) 10X objective within the device B) 25X magnification within the device C) 25X magnification; slides were removed from the device and imaged

Chapter 4: Discussion

A novel microfluidic protocol has been created; which combines both the isolation of basophils from whole blood and the measurement of their activation through the imaging of cells detected by an antibody specific for CD63. Our approach has been developed through evaluation of two different microfluidic means for enriching basophil populations in blood samples, as well as the assessment of established procedures involving density gradient separation negative immune-selection and FACS. While further evaluation of the prototype is required, the preliminary studies indicate that the device constructed can be adapted to measure the activation of basophils *in situ* by immunofluorescent staining. The studies provide a conceptual framework that should allow development of rapid more effective means for establishing allergic sensitivity.

4.1 Basophil isolation within the acoustofluidic device

The novel basophil isolation method employed for extracting basophils from whole blood represents the first successful application of acoustofluidic separation of basophils. Other microfluidic devices that have been investigated for separation of blood cells include paper-based analytical devices (Songjaroen *et al.*, 2012), pinched flow coupled shear modulated inertial microfluidics (Asgar *et al.*, 2001) and trapezoid based spiral sorters (Wu *et al.*, 2012a), though none of these microfluidic devices have been investigated for means of purifying basophils specifically. Flow cytometry on chip had the potential to provide a solution to our research, however these devices already been developed and characterised with mouse melanoma cells (Schmida *et al.*, 2012). Therefore, in this study, we have applied and tested two different microfluidic devices in order to enable the integration of basophil activation into clinical allergy diagnosis in clinic.

By pursuing the basophil isolation step, prior to activation, it is hypothesised that increased sensitivity will be observed in comparison to current methods in clinic. This is based on comparative studies, which found that isolated basophils' increased sensitivity would prove beneficial in allergy diagnosis where grades of activation observed are markedly lower (De Weck *et al.*, 2008). Therefore, isolated cells not only increase the sensitivity, but also may potentially enable accurate diagnosis of allergy that may otherwise be missed in whole blood basophil activation tests currently conducted in the laboratory.

Two different microfluidic methods were explored, the spiral sorter and the acoustofluidic device. An advantage of the acoustofluidic system is that the label-free approach using anti-CD203c can bind

basophils irrespective of weight or size. Despite the microfluidic spiral sorter offering a label free approach, the effectiveness of cell sorting was based on size, and thus inefficient sorting was observed when blood was introduced to this system Figure 32. Basophils are estimated to be 10 – 16 μm in size (publication dependant), whereas other leukocytes are expected to range from 8 - 20 μm in size, therefore size-based separation could not be achieved. In addition, due to their percentage within blood (>1%), basophils are at a disadvantage for size based sorting as other leukocytes of similar size are much more abundant e.g. neutrophils (60%) or lymphocytes (30%) (Sarrafzadeh *et al.*, 2014). The spiral sorter encountered leaking at flow rates higher than 10 ml/h, despite the device being adapted to withstand larger pressure. This proved inefficient; as it took the same time as density gradient centrifugation, however current techniques could process much larger volumes of blood. The spiral sorter is a closed device, which proved problematic, when it came to cleaning the device, unlike the acoustofluidic device, which could simply be de assembled. Due to the spiral sorter chips being commercially bought, the manufacturer had not cleaned the device thoroughly and thus polymer fibres loosened when liquid was flown through and blocked the outlets. When caused, this would require a water and soap suspension to be syringed through the channel to try to remove the fibre. However, due to the fineness of the outlets, these would easily break and thus the device would be rendered unusable. Such factors were taken into consideration when deciding upon which device to move forward with. The finite decision was made on the basis that in order to determine and analyse the cells flowing through the outlets within the spiral sorter using Image J, a faster camera was required that would only be able to focus on one outlet at a time. Therefore, the spiral sorter experiments were not pursued further. Had these experiments been revisited, the samples from each outlet could be collected and cell count analysed via visually by Kimura on a haemocytometer and analysed by FACS, rather than the application of Image J. In addition, the whole blood could have been lysed prior to entry into the device.

Supplementary studies were employed to explore the effect of erythrocyte-depleted blood on basophil function (Figure 29). Saponin concentrations typically used in FACS have ranged from 1 to 5% (Ryan and Wu, 2004), but we have investigated the erythrocyte depletion solution employed by Holmes et al (2009) using the ratio of whole blood: erythrocyte depletion buffer: quench solution 1-18-3. These findings are (to some extent) at odds with those of Holmes et al; whereby basophil function was diminished when basophil activation was assessed by net histamine release (Holmes *et al.*, 2009a). Wilcoxon paired signed-rank test was run on each of the data sets to test the hypothesis that the use of saponin affected the basophil's ability to release histamine. The low P values concluded that the median difference between whole blood and saponin is not due to chance and that saponin does have

a detrimental effect on basophil ability to release histamine. In addition, Spearman's rank correlation coefficient test determined that the p values were non-significant, despite coming from the same donor. This was further reinforced by both donors having inverse r^2 values. Therefore, despite samples being tested within the same system, with the same stimulus, and from the same donor, when incubated with saponin, the samples are statistically incomparable. These results are however, in accordance with the previous research from Vuorte et al; that saponin impairs basophil function possibly by altering the integrity of the basophils (Vuorte *et al.*, 2001).

Our findings are broadly in harmony with those of researchers such as Ide et al; who observed that the degranulation responses in eosinophils were reduced in cells same treated with ammonium chloride, than those treated with hypotonic shock solution to deplete erythrocytes (Ide *et al.*, 1994). Unlike the saponin samples tested, ammonium chloride incubated and hypotonic shock treatment when compared were found to have statistically significant correlation, ($p = 0.042$ *) and an r^2 value of 1 as depicted in Figure 30. This suggests that either method could be used, as the data demonstrates that when the same conditions are used with each lysis agent, the results correlate. Wilcoxon matched pair signed-rank tests demonstrated large P values (0.625 – 0.875) and thus the overall means do not differ between groups. However, our studies did not examine the survival and morphology of these cells, which the literature found that ammonium chloride (155 mM); had marked effect on both morphology and cellular function, suggesting this agent can cause cellular damage. Erythrocyte depleted blood by hypotonic shock treatment was thus employed to reduce the incidence of non-specific cell binding and increase the likelihood of basophil adhesion within the device. The addition of this method enabled the basophil isolation protocol to be reduced by approximately 60%, as it replaced the dependency of the expensive negative immunomagnetic separation step with methods using solutions that are available in all laboratories.

The sensitivity of the device could be improved further by re suspending the lysed pellets in plasma. In a study by Morgan et al; it was shown that when basophils were centrifuged in Tyrode's solution, significantly more histamine was released than when centrifuged in plasma ($p = <0.003$ non-atopic, $p = <0.005$ atopic) (Morgan *et al.*, 1983). This implied that density mediums could lead to the increased release of histamine and the inactivation or loss of FcεRI receptors. When using 1X PBS to re suspend cells in our experiments, PBS did not contain magnesium or calcium ions which affects basophil releasability. Thus by keeping the cells in cooled plasma 4 °C, cells would be in their natural environment, however due to temperature would be dormant. Basophil plasma could be obtained from blood samples prior to the lysis by allowing separation to occur; this could then be collected and stored

on ice. Therefore, by using plasma, it would have the ability to significantly increase basophil releasability for all basophil activation tests. For these tests, platelets would need to remain unstimulated, as stimulated platelets have been shown to express lamp 2 (CD63), which may provide false positives. One pitfall would be if the device were to be used for cancer patients; their unstimulated platelets express significantly elevated levels in comparison to healthy patients (3.79 ± 1.48% *vs* 33.9 ± 5.6%) and thus would create false positives in the CD63 fluorescent output of the device (Kannan *et al.*, 1995).

The acoustofluidic device was optimised initially using basophils isolated by negative immunomagnetic separation. Initial optimisation was achieved by running these cells through the device for each subject from 10 ml/h – 50 ml/h for ten minutes as shown in Figure 35. The data demonstrates that the standard error was subject dependent and not flow rate dependent. This was validated by running the non-parametric Kruksal-Wallis test to compare the means of basophil adhesion at each flow rate, which was found to be significant p = <0.0001. This indicates the populations have different distributions at each flow rate. Based on this, 30 ml/h was the flow rate that produced the overall highest basophil adherence when indirectly measured (80%, Figure 35 F). The pattern observed in these studies was non-conventional in that it was hypothesised that as the flow rate increased, the more binding opportunities and thus the larger the basophil adherence. However, at flow rates of 40 – 50 ml/h little basophil adherence was obtained (less than 5%), suggesting that the flow rate was too fast for the basophils to adhere. The flow rate of 30 ml/h was decided to be the best flow rate to obtain optimal basophil adherence.

The acoustofluidic device demonstrated its ability to adhere basophils in both enriched and erythrocyte depleted samples (Figure 40). Maximum binding experiments were performed over a 30-minute period within the device. A ten-fold difference in basophil adherence to the slide was observed in enriched samples; approximately 60,000 basophils in comparison to erythrocyte depleted samples, which reached 6,000 basophils bound. The raw data is depicted along with the standard error of mean in Figure 41. Erythrocyte depleted samples achieved 39% mean adherence, whereas enriched samples had a mean adherence of 72.5%. Each time point was compared for enriched basophils and erythrocyte depleted blood using Wilcoxon paired signed-rank test, P = <0.0001 ****. Both erythrocyte depleted and basophil enriched samples showed significant correlation (p = 0.043 *) and thus determined that both methods would produce essentially the same pattern of basophil adhesion. This indicates that the device's performance is subject dependent and not dependent upon the number of basophils entering the device.

Despite achieving 72.5 % mean basophil adherence in these experiments, it was observed that the current in house antibody coating method might be the limiting factor for basophil adherence. With this method, the orientation of the antibodies on the surface of the slide was uncertain, thus causing inefficient binding of cells to its surface. Such possibilities of binding include tail on, head on, side on or flat on; therefore, it is of great interest as to how this can be improved. A collaboration with the Karlsruhe Institute of Technology allowed us to compare the IH slides with those created by dip-pen nanolithography (DPN) slides. With this technique, a uniform pattern is printed with anti-CD203c, creating an optimal binding area. Basophil binding experiments were evaluated over a 30-minute period by flow cytometric methods and determined that approximately 60,000 basophils were bound when employing DPN slide and 30,000 when using IH slides. When the DPN slide was employed within the acoustofluidic device at optimal conditions, it was found that a mean capture rate of 92% basophil adherence could be achieved (Figure 43). In comparison, IH slides had a lower mean capture rate of 62%. Spearman's rank correlation coefficient determined that there was good correlation between IH and DPN slides, r^2 = 0.771, though not significant (p = 0.051). Results indicate that the uniform distribution of antibody on DPN slide may attribute to the small range observed across samples (8%). In addition, DPN slide indicates the possibility that imaging may be plausible in the device, as the basophil binding area is known. In order to determine the absolute maximal binding, further experiments could be conducted over a longer time to reach the binding plateau. Although, it must be taken into consideration that this will involve multiple syringe changes and thus a higher incidence error will be introduced into the device, as observed. Had time permitted, an alternative to using the DPN slides would have been to optimise the IH slides by using recombinant antibody fragments - f(ab) fragments targeted against anti-CD203c instead of pure anti-CD203c. This would result in predominantly tail on binding and thus increase the chance of cells binding to the slides. Recombinant fragments have been engineered to increase binding affinity and specificity; an advantage which would have massive benefit to the current IH slides. Such orientation could be achieved using either covalent or non-covalent immobilisation methods. The covalent coupling approach to slide surfaces has been achieved by utilising the carbohydrate moiety of the Fc antibody to generate aldehydes. Such aldehydes are then reactive and thus orientate the covalent antibody coupling on animated or hydrazine functionalised dendrimers on surfaces of slides (Ho *et al.*, 2010). Stronger non-covalent immobilisation could be achieved using streptavidin biotin interaction. The biotinylation method determines whether antibodies are immobilised in an organised, orientated fashion, or at random. Cho et al compared such techniques and determined that as immobilisation increased in both populations, the antibodies adopted a tail-on orientation, however the site-specific biotinylated antibodies became orientated faster (Cho *et al.*, 2011).

In terms of efficiency, the acoustofluidic device enables an ease of use and each run of the device can achieve 94% capture in whole blood and take just ten minutes (Figure 38). This is faster than current techniques; such as the negative immunomagnetic separation, which takes approximately two hours. It must be taken into consideration that the device is reusable and thus needed to be cleaned between tests. Alternatively, further work could create a disposable device for ease of use in clinic. Currently, the slides are disposable and the steel carrier layer of the device could be autoclaved to be sterilised so that this can be re-used in clinic. It is possible that if other materials were evaluated and compared in terms of conductivity and cost, then the device would become disposable.

Inter-subject variation was observed when using the acoustofluidic device for basophil isolation. This Issue could be addressed by making small changes to the device to resolve the variability introduced by the tightness of screws (Figure 16). Further models have been designed to use magnets, thus creating a strong and reproducible tightness of device. This will prevent leaking, slide breakages and large resonance peak variance, thus eliminating the need to adjust the voltage to compensate the difference in pressure. Therefore, this model could be employed and optimised using the current protocol to increase basophil adherence, whilst reducing the variance.

The acoustofluidic device significantly reduces costs associated with both basophil isolation and activation. Efficient coating of the slides through dip pen nanolithography (DPN slide) enabled an evenly distributed layer of anti-CD203c for the basophils to bind. IH slide not only increased the surface area for basophils to bind, but also additionally reduced the amount of antibody required by >100 fold Figure 43. The problematic imaging of basophils when using the DPN slide, was overcome by performing the imaging studies with anti-CD63 Alexa Fluor 647. This enabled the fluorescent identification of basophils within the carrier layer that could not be previously found due to the uneven distribution of antibody across the target region of the slide. This issue was not encountered when imaging DPN slide as the target area for binding is already known. Due to time constraints further imaging studies were not conducted. Basophils were identified in the initial imaging studies using anti-CD63; therefore, we can conclude that cells identified are in fact basophils based on the rationale that CD63 is a cell surface marker present exclusively in basophils. The utilisation of DPN slide almost doubled the number of basophils bound within the device in comparison to the in-house printed slides (IH slide) based on both FACS analysis and imaging studies conducted. Furthermore, the microscopy studies using anti-CD63 calculated that approximately 23,500 basophils were bound over a ten-minute period. Therefore, results present that improved basophil adherence to slide by approximately 50%, by achieving up to 94% capture. In order to further validate this work; a direct comparison of basophil

purification would need to be conducted between the EasySep technique and the acoustofluidic device. This analysis would provide a basis for why the acoustofluidic technique is superior to current methods using multiple donors with differing basophil counts. This would enable the identification of contaminating cells using toluidine blue on a haemocytometer, in addition to using the CCR3 positive cells identification by using FACS.

Specifying basophils' contribution to human disease is problematic due to difficulties in the isolation process. We have created a platform for efficient basophil separation from whole blood, thus once bound; these cells can be employed for alternate uses other than that of basophil activation. For example, mRNA analysis to investigate whether new unique basophil specific proteins in human can be found. Such research, has been hindered by the inability to extract large basophil numbers as very little mRNA is present in circulating basophils. In addition, CD203c has been identified as a marker that is expressed on a major sub population of immature cells, and also as a marker of identified basophil precursors from cord blood (Reimer *et al.*, 2006). Therefore, the device could alternatively be used for identifying premature basophil precursors from cord blood to enhance current basophil research.

By pursuing the basophil isolation step, prior to activation, it is hypothesised that increased sensitivity will be observed in comparison to current methods in clinic. This is based on comparative studies, which found that isolated basophils Increased sensitivity would prove beneficial in allergy diagnosis where grades of activation observed are markedly lower (De Weck *et al.*, 2008). Therefore, isolated cells not only increase the sensitivity, but may potentially enable accurate diagnosis of allergy that may otherwise be missed in whole blood basophil activation tests currently conducted in the laboratory. Here we have proven that the microfluidic platform has the potential to remove the need for highly trained staff to perform repetitive tasks and meet the clinical demand for a rapid turnaround for accurate results. The acoustofluidic device has eliminated many of the errors currently encountered for both the isolation and activation of basophils when using traditional methods.

4.2 Means of measuring basophil activation *in vitro*

Measurements of basophil activation are dependent on the method employed. In the present studies, it was found that there were a number of ways to measure the degree of basophil activation as determined by either the measurement of the expression of surface markers or the measurement of secreted mediators. An understanding of the relative merits of different means for assessing basophil activation is of strategic importance to this project. The methods applied in these proof of principle experiments involved FACS, enzyme immunoassay and dot blot assays respectively.

Flow cytometry was explored to measure basophil activation by identifying cells that were both CCR3 and CD63 positive. As mentioned, CD63 is a protein that is anchored to the intracellular granules of basophils and is rapidly up-regulated upon activation (Ebo *et al.*, 2008). Therefore, CD63 was used as a marker of activation, which has been highlighted in numerous studies to have 97% accuracy and a 95% positive predictive value (Santos *et al.*, 2014). Due to the accuracy of this technique, flow cytometry was later used to assess basophil numbers in the isolation experiments. To ensure our protocol was in line with current research, experiments were performed to compare the effect of IL-3 on basophil activation. Flow cytometric studies determined that blood samples incubated with IL-3 significantly increased the percentage of basophil activation measured in respect to samples measured without. Spearman's correlation coefficient showed significance p = 0.001 ** - p = 0.023 *, with the exception of A) p = 0.273, F) p = 0.0057 and G) p = 0.076. Samples generally correlated well, as expected with r^2 values accounting for the majority of the distribution seen (r^2 = 0.691 - r^2 = 0.922), with the exception of A) r^2 = 0.252; G) r^2 = 0.571. Such a result concludes that basophils are primed by IL-3 (Figure 45). These findings are in harmony with MacGlashan whereby IL-3 primed basophils by inducing increased Syk expression in calcium dependent pathways by 38% (MacGlashan *et al.*, 2008b).

Consistently throughout the basophil activation studies both anti-FcεRI and FMLP were used as positive controls. Activation testing when anti-FcεRI in comparison to anti-IgE has been reported previously to have increased the sensitivity of the basophil activation test *via* flow cytometry when used (De Weck and Sanz, 2002). In addition, anti-FcεRI antibody has been reported to identify more responders within the population than anti-IgE antibody. Therefore, for all basophil activation tests in this thesis, anti-FcεRI was used as a positive control (as well as FMLP) in order to achieve our goal of successfully comparing techniques of basophil activation. Subjects' responses to positive controls anti-FcεRI and FMLP were compared using flow cytometric analysis and found that percentage CD63 expression was much higher in anti-FcεRI (Figure 47). In addition, when comparing atopic to non-atopic subjects, atopic subjects had a much higher elicitation of basophil activation upon anti-FcεRI stimulation, whereas FMLP

stimulation resulted in a much larger range of basophil activation in the non-atopic population. Such observations are in agreement with a study that when comparing basophil activation against controls in atopic and non-atopic patients, that atopic patients had significantly increased releasability to anti-FcεRI, and no difference observed with FMLP (Marone *et al.*, 1986). These results suggest that there are major differences in signal-response coupling leading to histamine release in human basophils. This is in agreement with Knol *et al*, who concluded that the differences observed could be due to the availability of the calcium dependent (anti-FcεRI) and independent (receptor specific, FMLP) activation pathways (Knol *et al.*, 1991a).

When deciding upon the secreted mediators to measure within this project, the availability of the mediators had to be taken into consideration. Basogranulin is a murine proteoglycan localised to the cytosolic granules of basophils (Mochizuki *et al.*, 2003a). Basogranulin can be indirectly measured by monoclonal antibody BB1 when a dot blot is performed and visualised by chemiluminescent substrate. Before tests could be performed, a new protocol was required and later optimised. This was due to new variables introduced such as a new dot blot apparatus, and the original protocol not being run for many years within the lab. Therefore, factors had to be explored such as standards for the basogranulin assay. Originally, bronchoalveolar lavage was used as a standard, until basophil isolation kits were available. This enabled the testing of BB1 antibody dilutions to determine what dilution would be the best for measuring basogranulin when performing the dot blot assay, this was decided to be 1/3 dilution as depicted in Figure 49. Once lysates of purified basophils were available, these were tested within the assay and compared to the BAL sample being used, that which was able to produce the best standard curve was chosen to be used in all future experiments and replaced the use of BAL fluid. The basogranulin measurement assay was accomplished using erythrocyte depletion agent distilled water. In comparison to whole blood, it was found that erythrocyte depleted samples had a higher basogranulin measurement. This is in line with current research, that has been reported the presence of detergents can have major effects on the detection of basogranulin and thus enhance its detection (Fawzy, 2011). It can be concluded that the dot blot assay for the measurement of basogranulin was successfully implemented due to the low spontaneous values and reproducible results achieved. When comparing fresh lysate samples and freeze-thawed lysate samples (stored at – 20°C) it was determined that chemiluminescent output was lost over time. A full evaluation was not conducted, although this observation is in agreement with Mochizuki *et al* who found that samples stored at– 80°C had a higher basogranulin measurement than samples stored at – 20°C (Mochizuki *et al.*, 2003b). Thus, basogranulin can be considered a reliable marker for basophil activation measurement. This hypothesis was tested

by employing the basogranulin assay to measure basophil activation in eight house dust mite allergic and eight grass pollen allergic subjects Figure 52.

The second secreted mediator to measure basophil activation was histamine. Although other pre formed mediators have a longer half-life than histamine, such as tryptase (1.5 – 2.5 hours (Schwartz *et al.*, 1989b)), histamine can be successfully measured *in vitro* by employing a competitive enzyme immunoassay. The sensitivity of the immunoassay is manufacturer dependent, which for consistency the same Neogen Life Sciences kit was used for all histamine measurement assays. An advantage of this is that the measurements were in ng/ml; coincidentally, the same sensitivity for commercially available tryptase assays. One disadvantage is the 96-well plate requires hand pipetting and thus due to the low μl volumes required, the potential for both equipment errors and human error is introduced across the assay. This is demonstrated in Figure 48; whereby up to 20% standard error of mean is observed. One reason for this is that the colour change observed was reported to be optimal at 30 minutes, however in some cases, this was too long and therefore the measurements were inaccurate. In order to decrease the error, incubation times with the enzyme conjugate and horse radish peroxidase could be incubated for set periods of time and measured determine an optimal time to stop the reaction, outside of what is reported in the manufacturer's instructions i.e. 10 minutes – 30 minutes at 2 minute intervals.

For these studies newly formed mediators such as leukotriene C_4 were not taken into consideration. While a commercial kit is available, the current ELISA protocol to measure newly formed mediators is lengthily e.g. Cayman Chem (Denver, Colorado, USA) LTC_4 96 well ELISA Kit, which despite producing sensitive measurements in pg/ml, requires 18 hours' incubation. Therefore, due to the number of patients required for testing to determine what mediator should be measured within the microfluidic device, this method was not facilitated. Had time and materials been available, the measurement of leukotriene C_4 could have been used as a potential measurement of basophil activation. When downsizing the assay to microfluidic scale, the incubation time would have been significantly reduced.

Although allergy research is continually moving forward, the bell shaped curve exhibited in response to increasing allergen concentrations is not yet completely scientifically explained. The bell shaped curve observed emphasises the importance of testing serial dilutions of suspected allergens in clinic to determine whether activation (if any) is observed for diagnosis. These conclusions are in agreement with Kleine-Tebbe *et al;* who concluded that multiple allergen concentrations of at least four logs are required to be tested in order to observe an individuals' response to allergen (Kleine-Tebbe *et al.*, 2006). The underlying mechanisms were not explored in these studies – current literature suggests that

tyrosine kinase syk plays a major role. Further studies into syk's involvement in the inter-subject basophil releasability observed are imperative to the understanding of why the bell shaped curve is observed in some subjects, but not others. Syk is regulated through three different mechanisms, for example both controls FMLP and anti-FcεRI have been shown individually to down regulate syk expression (MacGlashan *et al.*, 2008a). Therefore syk not only to correlates to histamine release, but additionally has been shown to play a role in the non-responder basophil healthy donor population (up to 20% of donors) (Kepley *et al.*, 2000; Laven-Phillips and MacGlashan, 2000). Other studies have identified the activation of the SHIP phosphorylation pathway to contribute to the descending portion of the bell-shaped curve in basophils in activation studies. A negative association between basophil releasability and SHIP activation was observed in non-responders and has indicated that SHIP may be responsible for the dampening of IgE-mediated signalling (Gibbs *et al.*, 2006). In order to explore tyrosine kinase signalling, lyn and syk expression could be explored in both responder and non-responder populations in these studies. This could be achieved by performing SDS page and western blot to separate the proteins across a nitrocellulose membrane similar to those conducted by Laven-Phillips et al. The nitrocellulose membrane could be incubated with either antihuman p72 syk or antihuman p53/56 lyn (Laven-Phillips and MacGlashan, 2000). This would enable the proteins to later be visualised by enhanced chemiluminescent blotting agents for quantification. The intensity of each band could then be measured by densitometric analysis, which would allow for the comparison of basophil activation measured by histamine release, basogranulin release and CD63 expression to be compared to the level of lyn and syk expression. Non-parametric statistical analysis could then be performed, to determine the correlation between tyrosine kinase expression and basophil activation.

One desirable goal of comparing techniques for measuring basophil activation, (enzyme immunoassay for the measurement of histamine release, basogranulin dot blotting procedure and flow cytometric methods), is to work towards the development of an acoustofluidic protocol for basophil activation measurement. Furthermore, comparator studies have not been conducted previously. Therefore, for the first time, when comparing the area under the curve in atopic subjects in response to increasing doses of grass pollen and dust mite allergen; we hypothesised that CD63 flow cytometric methods would show the have the strongest relationship between its comparator's histamine and basogranulin. Basophil granyulocytes contain secretory lysosomes where both histamine and CD63 are located. Thus, CD63 expression has been suggested to be correlated to histamine, which indicates its potential to be a more reliable marker of basophil activation (Knol *et al.*, 1991b). Allthough histamine release occurs upon allergen sensitisation, histamine is also released by piecemeal degranulation (MacGlashan, 2010). Piecemeal degranulation, unlike the rapid IgE-mediated anaphylatic degranulation, is the slow

secretory process whereby mediator release occurs over a peiod of hours or days (Dvorak *et al.*, 1995). Therefore, CD63 is a more precise marker of anaphylactic degranulation in IgE-mediated events. The significant correlation between CD63 and basogranulin observed suggests that these mediators are stored together, which is generally compatible with the literature. However, these findings disagree with studies by Mochizuki *et al* who found that quantitative analysis found that there was an invariably lower basogranulin percentage released in respect to total cell content than histamine, which indicated that the two mediators were not released together (Mochizuki *et al.*, 2003b). One disadvantage of this study is that results are reflective of atopic patients, in a real-world scenario it is likely that for a handful of these tests the release observed will be completely dissociated in individual patients (Sanz *et al.*, 2001). Such conclusions are drawn as basophil activation is induced by a limited number of aggregated IgE receptors, once over the threshold, basophils are hypothesised to become independent of the concentration of extracellular IgE (Saini *et al.*, 1999).

However, the strongest correlation between the three methods was not demonstrated in the CD63 activation studies, as hypothesised. Due to intersubject variation and the introduction of human error by hand pipeting, our comparator studies were non conclusive, producing non-significant results. CD63-mediated fluorescence, has been previously hypothesised to be due to platelets bound to the activated basophils (Knol *et al.*, 1993). Alternative studies have found that the platelets contribution to fluorescence is negligible and thus this phenomenon has been proven to be more theoretical than in practice (Sainte-Laudy, 1998). Thus, due to non-conclusive results, we based our decision on the literature and the results that produced the lowest standard error. Therefore, it was decided that CD63-mediated fluorescence would be integrated into the device as a measure of basophil activation in these studies. It must be emphasised that basophil activation tests are not primary diagnostic measures in clinic, and used as complementary tests to skin prick testing to determine a patient's sensitivity to allergen. Thus by making the test more accessible in clinic, and removing the need for specialist equipment, this research provides the means for basophil activation tests to be used as a primary diagnostic tool in allergy clinics.

4.3 Development of an acoustofluidic device to measure basophil activation

The acoustofluidic experiments conducted created the foundation for the development of a protocol for basophil isolation from whole blood, and allowed the the exploration into the device's potential to measure basophil activation. The acoustofluidic device has already proven itself easier, faster and more efficient than current basophil isolation methods. As this device is a prototype, further studies are required to develop a protocol for basophil activation within the device before it can be tested in clinics as a means to investigate allergic sensitivity and for the prediction of symptom severity in patients.

Slides were imaged outside of the device to obtain high quality images of activation. Initial imaging using anti-CD63 tagged Alexa Fluor-647 provided evidence to suggest that basophil activation could be imaged within the device when basophils were stimulated with either anti-FcεRI when compared to the control slides created. If time had permitted, further images would be obtained to enable a statistical analysis of subjects' basophil activation against controls when using Alexa Fluor 647 tagged anti-CD63. Further characterisation of basophil activation within the device could be achieved by using atopic subject samples and measuring their basophil activation in response to increasing allergen concentrations. In order to achieve this, feasibility studies must first be conducted to determine whether multiple devices could be run alongside each other to measure basophil activation in response to different allergens at different concentrations. This would allow for an improved turnaround time as the measurements could be obtained simultaneously. If this testing confirms the hypothesis that the device is able to predict allergy sensitivity that either matches or excels current methods in clinic, this device could be integrated into the clinical setting. As previously mentioned, basophil activation tests are not commonly used in clinic due to costs, training and organisation of equipment and staff. Typically, CD63 flow cytometry is used for basophil activation testing and many hospitals share this equipment and thus timings need to be accurate and scheduled efficiently to ensure that the equipment is booked on the day of patient visit. The device overcomes the need for scheduling of staff and expensive equipment as the syringe pump, oscillope and amplified could be run in any lab, and imaged on a fluorescent microscope. The device does not require excessive training and thus any clinic member could be trained to run this device and perform the test once venesection was performed. Therefore, this device overcomes the pitfalls of why basophil activation testing is not utilised in clinic. In addition, waiting times for allergic sensitivity confirmation would be reduced as subjects would need to provide a blood sample and would not be required to spend hours in the clinic receiving skin prick tests. This would result in more patients being seen per day and a significant reduction in the time from

suspected allergy to confirmation, which is currently longer than one year. This would result in a better quality of life for those with suspected allergy, as the suspected allergens would not have to be avoided for a long time. The current protocol turnaround time is less than one hour, provided staff are available, patients could receive confirmation of allergic sensitivity the same day as their visit. This is much faster than the current processes run in the allergy clinics. Therefore, this device if further characterised has the potential to be easier, faster and more efficient than current allergy testing performed. Results obtained with the device should be compared to the other basophil activation tests explored through the measurement of mediator release and basophil surface expression markers. Once optimised, the activation protocol would allow for patient samples from the clinic to be tested within the device and enable a true comparison to current allergy diagnostic methods applied. This would enable the evaluation of the acoustofluidic device's ability to predict allergic sensitivity. Such data would determine the whether the integration of the device into allergy testing clinic is plausible.

In the present studies with the acoustofluidic device, measurement of basophil activation was conducted using human blood samples. This contrasts with studies in other microfluidic devices which have performed their evaluation of basophil activation testing through the measurement of histamine (Kurita *et al.*, 2002) and acridine orange (Chen *et al.*, 2010). Devices within studies utilise animal cell lines such as KU812 (Kurita *et al.*, 2002) and RBL-2H3 (Chen *et al.*, 2010). Therefore, this study has bypassed the dependency on cell lines by performing basophil isolation in the first step of the protocol to overcome the issue of low basophil numbers *in vitro*. This holds a major advantage for our device, as it is able to bypass the current issues within basophil research as to whether animal models are able to accurately predict allergic sensitivity in human disease (Mestas and Hughes, 2004). Such questions have arisen due to the differences in the human and mouse genome, and therefore indicate the possibility of significant differences in immune system and inflammatory response, which could produce a false result. In addition, cell lines have been reported to elicit a low degree of degranulation (Blom *et al.*, 1992). Therefore, through the characterisation of the acoustofluidic device using human blood, this device offers itself to have the potential to be more reliable than devices currently available for basophil activation. Here we have provided the evidence to indicate that the microfluidic platform has the potential to remove the need for highly trained staff to perform repetitive tasks and meet the clinical demand for a rapid turnaround for accurate results. The acoustofluidic device has overcome many of the errors currently encountered for both the isolation and activation of basophils when using traditional methods.

Chapter 5: References

Abe, Y., Ogino, S., Irifune, M., Imamurai, F., Ukui, H., Wada, H. and Histamine Content, S.a.D.I.H.N.M. (1993) Histamine content, synthesis and degradation in human nasal mucosa. *Clinical and Experimental Allergy,* 23, 132 - 136.

Ainslie, K.M., Garanich, J.S., Dull, R.O. and Tarbell, J.M. (2005) Vascular smooth muscle cell glycocalyx influences shear stress-mediated contractile response. *Journal of Applied Physiology,* 98, 242-249.

Arock, M., Schneider, E., Boissan, M., Tricottet, V. and Dy, M. (2002) Differentiation of human basophils: an overview of recent advances and pending questions. *Journal of Leukocyte Biology* 71, 557 - 564.

Asgar, A., Bhagat, S., Hou, H.W., Li, L.D., Lim, C.T. and Han, J. (2001) Pinched flow coupled shear-modulated inertial microfluidics for high-throughput rare blood cell separation. *Lab on a Chip,* 1, 1 - 9.

Auslander, D., Eggerschwiler, B., Kemmer, C., Geering, B., Auslander, S. and Fussenegger, M. (2014) A designer cell-based histamine-specific human allergy profile. *Nature Communications,* 5, 1 - 8.

Balachandar, K., Balaji, V., Prem Kumar, D. and Arun Kumar, S. (2016) Design and simulation of MEMS based micromotors. *International Journal of Chemical Sciences,* 14, 1105 - 1112.

Becker, H. and Locascio, L.E. (2002) Polymer microfluidic devices. *Talanta,* 56, 267 - 287.

Berroa, F., Lafuente, A., Javaloyes, G., Ferrer, M., Moncada, R., Goikoetxea, M.J., Urbain, C.M., Sanz, M.L. and Gastaminza, G. (2014) The usefulness of plasma histamine and different tryptase cut-off points in the diagnosis of peranaesthetic hypersensitivity reactions. *Journal of Clinical and Experimental Allergy,* 44, 270 - 277.

Bhagat, A.A., Kuntaegowdanahalli, S.S. and Papautsky, I. (2008) Continuous particle separation in spiral microchannels using Dean flows and differential migration. *Lab on a chip,* 8, 1906 - 1914.

Blom, T., Huang, R., Aveskogh, M., Nilsson, K. and Hellman, L. (1992) Phenotypic characterization of KU812, a cell line identified as an immature human basophilic leukocyte. *European Journal of Immunology,* 22, 2025 - 2032.

Bodger, M.P., Morris, C.M., Kennedy, M.A., Bowen, J.A., Hilton, J.M. and Fitzgerald, P.H. (1989) Basophils (Bsp-1. *Blood,* 73 (3), 777-781.

Bodger, M.P., Mounsey, G.L., Nelson, J. and Fitzgerald, P.H. (1987) A monoclonal antibody reacting with human basophils, *Blood,* 69, 1414-1418.

Boone, T.D., Fan, Z.H., Hooper, H.H., Ricco, A.J. and Tan, H. (2002) Plastic advances in microfluidic devices. *Journal of Analytical Chemistry,* 1, 78A - 86A.

Brockow, K., Romano, A., Blanca, M., Ring, J., Pichler, W. and Demoly, P. (2002) General considerations for skin test procedures in the diagnosis of drug hypersensitivity. *Allergy,* 57, 45 - 51.

Brooks, C.R., Van Dalen, C.J., Hermans, I.F., Gibson, P.G., Simpson, J.L. and Douwes, J. (2017) Sputum basophils are increased in eosinophilic asthmacompared with non-eosinophilic asthma phenotypes. *Allergy,* 72, 1583 - 1586.

Brunner, T., Heusser, C.H. and Dahinden, C.A. (1993) Human Peripheral Blood Basophlh Primed by Interleukin 3 (IL-3) Produce II-4 in Response to Inmunoglobulln E Receptor Stimulation. *Journal of Experimental Medicine,* 17, 605 - 611.

Carugo, D., Octon, T., Messaoudi, W., Fisher, A.L., Carboni, M., Harris, N.R., Hill, M. and Glynne-Jones, P. (2014) A thin-reflector microfluidic resonator for continuous- flow concentration of microorganisms: a new approach to water quality anal- ysis using acoustofluidics. *Lab on a Chip,* (14), 3830-3842.

Chatterjee, A. (2011) *Size-dependent separation of multiple particles in spiral microchannels*, Master of Science in Electrical Engineering, University of Cincinnati.

Chen, Q.L., Hoa, H.P., Cheung, K.L., Kong, S.K., Suenb, Y.K., Kwanc, Y.W., Lid, W.J. and Wong, C.K. (2010) A fluorescence-based centrifugal microfluidic system for parallel detection of multiple allergens. *Progress in Biomedical Optics and Imaging - Proceedings of SPIE,* 7565, 1605 - 7422.

Chirumbolo, S. (2011) Basophil Activation Test in Allergy: Time for an Update? *Nanomedicine*, 1-17.

Cho, I.-H., Park, J.-W., Lee, T.G., Lee, H. and Paek, S.-H. (2011) Biophysical characterization of the molecular orientation of an antibody-immobilized layer using secondary ion mass spectrometry. *Analyst,* 136, 1412 - 1419.

Cho, J.L., Ling, M.F., Adams, D.C., Faustino, L., Islam, S.A., Afshar, R., Griffith, J.W., Harris, R.S., Ng, A., Radicioni, G., Ford, A.A., Han, A.K., Xavier, R., Kwok, W.W., Boucher, R., Moon, J.J., Hamilos, D.L., Kesimer, M., Suter, M.J., Medoff, M.D. and Luster, A.D. (2016) Allergic asthma is distinguished by sensitivity of allergen- specific CD4+ T Cells and airway structural cells to type 2 inflammation. *Scientific Translational Medicine,* 8, 1 - 20.

Church, M.K. and Levi-Schaffer, F. (1997) Updates on cells and cytokines. *Journal of Allergy and Clinical Immunology,* 99, 155 - 160.

D'ambrosio, C., Akin, C., Wu, Y., Magnusson, M.K. and Metcalfe, D.D. (2003) Gene expression analysis in mastocytosis reveals a highly consistent profile with candidate molecular markers. *Journal of Allergy and Clinical Immunology,* 112, 1162 -1179.

Dannhauser, D., Rossi, D., Memmolo, P., Causa, F., Finizio, A., Ferraro, P. and Netti, P.A. (2017) Label-free analysis of mononuclear human blood cells in microfluidic flow by coherent imaging tools. *Journal of Biophotonics,* 10, 683 – 689.

De Weck, A.L. and Sanz, M.L. (2002) Flow cytometric cellular allergen stimulation test (FAST / Flow CAST): technical and clinical evaluation of a new diagnostic test in allergy and pseudo- allergy. *Journal of Allergy and Clinical Immunology International,* 14, 204 - 205.

De Weck, A.L., Sanz, M.L., Gamboa, P.M., Aberer, W., Bienvenu, J., Blanca, M., Demoly, P., Ebo, D.G., Mayorga, L., Monneret, G. and Sainte- Laudy, J. (2008) Diagnostic tests based on human basophils: more potentials and perspectives than pitfalls. *International Archives of Allergy and Immunology,* 146, 177 - 189.

Demoly, P., Adkinson, N.F., Brockow, K., Castells, M., Chiriac, A.M., Greenberger, P.A., Khan, D.A., Lang, D.M., Park, H.S., Pichler, W., Sanchez-Borges, M., Shiohara, T. and Thong, B.Y. (2014) International consensus on drug allergy. *Allergy,* 69, 420 - 437.

Doh, I. and Cho, Y.H. (2005) A continuous cell separation chip using hydrodynamic dielectrophoresis (DEP) process. *Sensors and Actuators,* 121, 59 - 65.

Douaiher, J., Succar, J., Lancerotto, L., Gurish, M.F., Orgill, D.P. and Hamilton, M. (2014) Development of mast cells and importance of their tryptase and chymase serine proteases in inflammation and wound healing. *Journal of Advances in Immunology,* 122, 211 - 252.

Du Toit, G., Roberts, G., Sayre, P.H., Bahnson, H.T., Radulovic, S., Santos, A.F., Brough, H.A., Phippard, D., Basting, M., Feeney, M., Turcanu, V., Sever, M.L., Lorenzo, M.G., Plaut, M. and Lack, M. (2015) Randomized trial of peanut consumption in infants at risk for peanut allergy. *The New England Journal of Medicine,* 372, 803 - 813.

Dvorak, A.M., Macglashan, D.W.J., Morgan, E.S. and Lichtenstein, L.M. (1995) Histamine distribution in human basophil secretory granules undergoing FMLP-stimulated secretion and recovery. *Blood,* 86, 3560 - 3566.

Ebo, D.G., Bridts, C.H., Hagendorens, M.M., Aerts, N.E., De Clerck, L.S. and Stevens, W.J. (2008) Basophil activation test by flow cytometry: present and future applications in allergology. *Cytometry Part B: Clinical Cytometry,* 74, 201 - 210.

Ebo, D.G., Bridts, C.H., Mertens, C.H., Hagendorens, M.M., Stevens, W.J. and De Clerck, L.S. (2012) Analyzing histamine release by flow cytometry (HistaFlow): a novel instrument to study the degranulation patterns of basophils. *Journal of Immunological Methods,* 375, 30 - 38.

Fawzy, A. (2011) *Biochemical and molecular approaches to the identification and characterisation of novel markers of human basophils*, Doctor of Philosophy, University of Southampton.

Fiorini, G.S. and Chiu, D.T. (2005) Disposable microfluidic devices: fabrication, function, and application. *BioTechniques* 38, 429 - 446.

Fleischer, D.M. (2015) Pitfalls in food allergy diagnosis: serum IgE testing. *The Journal of Pediatrics,* 166, 8 - 10.

Fukuda, S., Yasu, T., Predescu, D.N. and Schmid-Schönbein, G.W. (2000) Mechanisms for Regulation of Fluid Shear Stress Response in Circulating Leukocytes. *Circulation Research,* 86, e13-e18.

Gandhi, N.A., Bennett, B.L., Graham, N.M.H., Pirozzi, G., Stahl, N. and Yancopoulos, G.D. (2016) Targeting key proximal drivers of type 2 inflammation in disease. *Nature,* 15, 35 - 50.

Gell, P.G.H. and Coombs, R.R.A. (1963) The classification of allergic reactions underlying disease in Clinical Aspects of Immunology. *Blackwell Science*.

Gibbs, B.F. (2005) Human basophils as effectors and immunomodulators of allergic inflammation and innate immunity. *Clinical and Experimental Medicine,* 5, 43 - 49.

Gibbs, B.F., Papenfuss, K. and Falcone, F.H. (2008) A rapid two-step procedure for the purification of human peripheral blood basophils to near homogeneity. *Clinical and Experimental Allergy,* 38, 480 - 485.

Gibbs, B.F., Rathling, A., Zillikens, D., Huber, M. and Haas, H. (2006) Initial FcεRI-mediated signal strength plays a key role in regulating basophil signaling and deactivation. *Journal of Allergy and Clinical Immunology,* 118, 1060 - 1067.

Gilbert, H.S. and Ornstein, L. (1975) Basophil assessment by toluidine blue staining. *Blood,* 46, 279 - 286.

Glynne-Jones, P., Boltryk, R.J. and Hill, M. (2012) Acoustofluidics 9: Modelling and applications of planar resonant devices for acoustic particle manipulation. *Lab on a Chip,* 12 (8), 1417-1426.

Glynne-Jones, P., Boltryk, R.J., Hill, M., Harris, N.R. and Baclet, P. (2009) Robust acoustic particle manipulation: a thin-reflector design for moving particles to a surface. *Acoustical Society of America,* 126 (3), EL75–EL79.

Gómez, E., Campo, P., Rondón, C., Barrionuevo, E., Blanca-López, N. and Torres, M.J. (2013) Role of the basophil activation test in the diagnosis of local allergic rhinitis. *Journal of Allergy and Clinical Immunology,* 132, 975 – 976.

Gor'kov; (1962) On the forces acting on a small particle in an acoustical field in an ideal fluid. *Soviet Physics Doklady,* 6, 773.

Gossett, D.R., Weaver, W.M., Mach, A.J., Hur, S.C., Tse, H.T., Lee, W., Amini, H. and Di Carlo, D. (2010) Label-free cell separation and sorting in microfluidic systems. *Analyltical and Bioanalytical Chemistry,* 397 (8), 3249-3267.

Grattan, C.E.H. (2001) Basophils in chronic urticaria. *Society for Investigative Dermatology,* 1, 139 - 140.

Gruchalla, R.S. (2003) 10. Drug allergy. *Allergy and Clinical Immunology,* 111 (2), S548–S559.

Haisch, K., Gibbs, B., Körber, H., Ernst, M., Grage-Griebenow, E., Schlaak, M. and Haas, H. (1999) Purification of morphologically and functionally intact human basophils to near homogeneity. *Journal of Immunological Methods,* 226, 129 - 137.

Hamilton, R.G. (2016) *Laboratory diagnosis of human allergic disease*.

Han, X., Van Berkel, C., Gwyer, J., Capretto, L. and Morgan, H. (2012) Microfluidic Lysis of Human Blood for Leukocyte Analysis Using Single Cell Impedance Cytometry. *Analytical Chemistry,* 84 (2), 1070-1075.

Hanania, N.A., Wenzel, S., Rose´, K., Hsieh, H.J., Mosesova, S., Choy, D.F., Lal, P., Arron, J.R., Harris, J.M. and Busse, W. (2013) Exploring the effects of omalizumab in allergic asthma an analysis of biomarkers in the EXTRA study. *American Journal of Respiratory Critical Care Medicine,* 187, 804 - 811.

Ho, J.A., Hsua, W.L., Liao, W.C., Chiua, J.K., Chen, M.L., Chang, H.C. and Lic, C.C. (2010) Ultrasensitive electrochemical detection of biotin using electrically addressable site-oriented antibody immobilization approach via aminophenyl boronic acid

Author links open overlay panel. *Biosensors and Bioelectronics,* 26 (3), 1021 - 1027.

Hoffmann, H.J., Santos, A.F., Mayorga, C., Nopp, A., Eberlein, B., Ferrer, M., Rouzaire, P., Ebo, D.G., Sabato, V., Sanz, M.L., Pecaric-Petkovic, T., Patil, S.U., Hausmann, O.V., Shreffler, W.G., Korosec, P. and Knol, E.F. (2015) The clinical utility of basophil activation testing in diagnosis and monitoring of allergic disease. *Allergy,* 70, 1393 - 1405.

Holmes, D., Pettigrew, D., Reccius, C.H., Gwyer, J.D., Van Berkel, C., Holloway, J., Davies, D.E. and Morgan, H. (2009a) Leukocyte analysis and differentiation using high speed microfluidic single cell impedance cytometry. *Lab on a chip,* 9, 2881 - 2889.

Holmes, D., Pettigrew, D., Reccius, C.H., Gwyer, J.D., Van Berkel, C., Holloway, J., Davies, D.E. and Morgan, H. (2009b) Leukocyte analysis and differentiation using high speed microfluidic single cell impedance cytometry. *Lab on a Chip,* 9 (20), 2881-2889.

Ide, M., Weiler, D., Kita, H. and Gleich, G.J. (1994) Ammonium chloride exposure inhibits cytokine-mediated eosinophil survival. *Journal of Immunological Methods,* 168, 187 - 196.

Idoate, M.A., Echeveste, J., Gil, P., Sanz, M.L. and Ferrer, M. (2013) Expression of the basophil-specific antibodies 2D7 and BB1 in patients with cutaneous mastocytosis. *Journal of Investigational Allergology Clinical Immunology,* 23, 392 - 393.

Irani, A.M.A., Huang, C., Xia, H.Z., Kepley, C., Nafie, A., Fouda, E.D., Craig, S., Zweiman, B. and Schwartz, L.B. (1998) Immunohistochemical detection of human basophils in late-phase skin reactions. *Journal of Allergy and Clinical Immunology,* 101, 354 - 362.

Jacobi, H.H., Johansson, O., Liang, Y., Nielsen, H.V., Thygesen, C., Hansen, J.B. and Poulsen, L.K. (2000) Histamine immunocytochemistry: a new method for detection of basophils in peripheral blood. *Journal of Immunological Methods,* 237, 29 - 37.

Jacobs, C.R., Yellowley, C.E., Davis, B.R., Zhou, Z., Cimbala, J.M. and Donahue, H.J. (1998) Differential effect of steady versus oscillating flow on bone cells. *Biomechanics,* 31, 969-976.

Jogie-Brahim, S., Min, H., Fukuoka, Y., Xia, H. and Schwartz, L.B. (2004) Expression of alpha-tryptase and beta-tryptase by human basophils. *Journal of Clinical Immunology,* 113, 1086 - 1092.

Jörg, L., Pecaric-Petkovic, T., Reichenbach, S., Coslovsky, M., Stalder, O., Pichler, W. and Hausmann, O. (2018) Double-blind placebo-controlled trial of the effect of omalizumab on basophils in chronic urticaria patients. *Journal of Clinical and Experimental Allergy,* 48, 196 - 204.

Kalesnikoff, J., Huber, M., Lam, V., Damen, J.E., Zhang, J., Siraganian, R.P. and Krystal, G. (2001) Monomeric IgE stimulates signaling pathways in mast cells that lead to cytokine production and cell survival. *Immunity,* 14, 801 - 811.

Kannan, K., Divers, S.G., Lurie, A.A., Chervenak, R., Fukuda, M. and Holcombe, R.F. (1995) Cell surface expression of lysosome-associated membrane protein-2 (lamp2) and CD63 as markers of in vivo platelet activation in malignancy. *European Journal of Haematology,* 55, 145 - 151.

Katz, H.R., Stevens, R.L. and Austen, K.F. (1985) Heterogeneity of mammalian mast cells differentiated in vivo and in vitro. *Journal of Allergy and Clinical Immunology,* 76 (2), 250 - 259.

Kepley, C.L., Youssef, L., Andrews, R.P., Wilson, B.S. and Oliver, J.M. (2000) Multiple defects in Fc RI signaling in Syk-deficient nonreleaser basophils and IL-3-induced recovery of Syk expression and secretion. *Journal of Immunology,* 165, 5913 - 5920.

Khan, F.M., Ueno-Yamanouchi, A., Serushago, B., Bowen, T., Lyon, A.W., Lu, C. and Storek, J. (2012) Basophil activation test compared to skin prick test and fluorescence enzyme immunoassay for aeroallergen-specific Immunoglobulin-E. *Allergy, Asthma & Clinical Immunology* 8(1).

Kikuchi, Y. and Kaplan, A.P. (2001) Mechanisms of autoimmune activation of basophils in chronic urticaria. *Journal of Allergy and Clinical Immunology,* 107, 1056 - 1062.

Kimura, I., Moritani, Y. and Tanizaki, Y. (1973) Basophils in bronchial asthma with reference to reagin-type allergy. *Clinical and Experimental Allergy,* 3 (2), 195-202.

Kleine-Tebbe, J., Erdmann, S.M., Knol, E.F., Macglashan, D.W.J., Poulsen, L.K. and Gibbs, B.F. (2006) Diagnostic tests based on human basophils : Potentials, pitfalls and perspectives. *International Archives of Allergy and Immunology,* 141, 79 - 90.

Knol, E.F., Koenderman, L., Mul, F.P.J., Verhoeven, A.J. and Roos, D.J. (1991a) Differential activation of human basophils by anti-IgE and formyl-methionyl-leucylphenylalanine. Indications for protein kinase C-dependent and -independent activation pathways. *European Journal of Immunology,* 21, 881 - 885.

Knol, E.F., Kuijpers, T.W., Mul, F.P.J. and Roos, D.J. (1993) Stimulation of human basophils results in homotypic aggregation. *Journal of Immunology,* 151, 4926 - 4933.

Knol, E.F., Mul, F.P., Jansen, H., Calafat, J. and Roos, D.J. (1991b) Monitoring human basophil activation via CD63 monoclonal antibody. *Journal of Allergy and Clinical Immunology,* 345, 328 - 338.

Konstantinou, G.N., Asero, R., Maurer, M., Sabroe, R.A., Schmid-Grendelmeier, P. and Grattan, C.E.H. (2009) EAACI/GA LEN task force consensus report: the autologous serum skin test in urticaria. *Allergy,* 64, 1256 - 1268.

Koplina, J.J., Martina, P.E. and Allen, K.J. (2011) An update on epidemiology of anaphylaxis in children and adults. *Current Opinion in Allergy and Clinical Immunology,* 11, 492 – 496.

Kovacs, G.S. (1961) A simple direct method for absolute basophil and eosinophil counts from the same blood sample. *Folia Haematologica,* 5, 166 - 175.

Kumar, R., Bonicelli, A., Sekula-Neuner, S., Cato, A.C.B., Hirtz, M. and Fuchs, H. (2016) Click-chemistry based allergen arrays generated by polymer pen lithography for mast cell activation studies. *Small Journal,* 1, 1 - 9.

Kurita, R., Hayashi, K., Horiuchi, T., Niwa, O., Maeyamac, K. and Tanizawa, K. (2002) Differential measurement with a microfluidic device for the highly selective continuous measurement of histamine released from rat basophilic leukemia cells (RBL-2H3). *Lab on a Chip,* 2, 34 - 38.

Laven-Phillips, S.E. and Macglashan, D.W.J. (2000) The tyrosine kinases p53/56lyn and p72syk are differentially expressed at the protein level but not at the messenger RNA level in nonreleasing human basophils. *American Review of Respiratory Disease,* 23, 566 - 571.

Lee, K.H., Kim, S.B., Lee, K.S. and Sung, H.J. (2011) Enhancement by optical force of separation in pinched flow fractionation. *Lab on a chip,* 11, 354 – 357.

Lenshof, A., Evander, M., Laurell, T. and Nilsson, J. (2012) Acoustofluidics 5: Building microfluidic acoustic resonators. *Lab on a Chip,* (12), 684-685.

Liew, W.K., Williamson, E. and Tang, M.L. (2009) Anaphylaxis fatalities and admissions in Australia. *Allergy and Clinical Immunology,* 123, 434 - 442.

Lighthill, S.J. (1978) *Sound Vibrations,* 61, 391-418.

Lim, C.T. and Zhang, Y. (2007) Bead-based microfluidic immunoassays: the next generation. *Biosensors and Bioelectronics,* 22 (7), 1197-1204.

Lipworth, B., Newton, J., Ram, B., Small, I. and Schwarze, J. (2017) An algorithm recommendation for the pharmacological management of allergic rhinitis in the UK: a consensus statement from an expert panel. *Primary Care Respiratory Medicine,* 27, 1 - 8.

Liu, Y., Barua, D., Liu, P., Wilson, B.S., Oliver, J.M., Hlavacek, W.S. and Singh, A.K. (2013) Single-cell measurements of IgE-mediated FcεRI signaling using an integrated microfluidic platform. *PloS One,* 8, 1 - 12.

Lorentz, A., Schwengberg, S., Sellge, G., Manns, M.P. and Bischoff, S.C. (2005) Human Intestinal Mast Cells Are Capable of Producing Different Cytokine Profiles: Role of IgE Receptor Cross-Linking and IL-4. *The American Association of Immunologists,* 174, 6751 - 6756.

Lozzo, R.V. and Schaefer, L. (2015) Proteoglycan form and function: a comprehensive nomenclature of proteoglycans. *Matrix Biology,* 42, 11 - 55.

Macglashan, D.W.J. (2010) Expression of CD203c and CD63 in human basophils: relationship to differential regulation of piecemeal and anaphylactic degranulation processes. *Clinical and Experimental Allergy,* 40, 1365 - 1377.

Macglashan, D.W.J., Ishmael, S., Macdonald, S.M., Langdon, J.M., Arm, J.P. and Sloane, D.E. (2008a) Induced loss of Syk in human basophils by non-IgE-dependent stimuli. *Journal of Immunology,* 180, 4208-4217.

Macglashan, J.D.W., Ishmael, S., Macdonald, S.M., Langdon, J.M., Arm, J.P. and Sloane, D.E. (2008b) Induced Loss of Syk in Human Basophils by Non-IgE-Dependent Stimuli. *Immunology,* 180, 4208-4217.

Mandralis, Z.I., Feke, D.L. and Adler, R.J. (1990) *Fluid and Particle Separation,* 3, 115-121.

Mark, D., Haeberle, S., Roth, G., Von Stettenzab, F. and Zengerle, R. (2010) Microfluidic lab-on-a-chip platforms: requirements, characteristics and applications. *Chemical Society Reviews,* 31, 1153 – 1182.

Marone, G., Giugliano, R., Lembo, G. and Ayala, F. (1986) Human basophil releasability. II. Changes in basophil releasability in patients with atopic dermatitis. *Journal of Investigative Dermatology,* 87, 19 - 23.

Mayorga, C., Sanz, M.L., Gamboa, P.M., Garcia, B.E., Caballero, M.T. and Garcia, J.M. (2010) In vitro diagnosis of immediate allergic reactions to drugs: an update. *Journal of Investigational Allergology Clinical Immunology,* 20, 103 - 109.

Mertes, P.M., Demoly, P. and Malinovsky, J.M. (2012) Hypersensitivity reactions in the anesthesia setting/allergic reactions to anesthetics. *Allergy and Clinical Immunology,* 12 (4), 361-368.

Mertes, P.M., Malinovsky, J., Jouffroy, L., Sfa*, W.G.O.T.S.A., Aberer, W., Terreehorst, I., Brockow, K. and Demoly, P. (2011) Reducing the Risk of Anaphylaxis During Anesthesia: 2011 Updated Guidelines for Clinical Practice. *Investigational Allergology Clinical Immunology,* 21 (6), 442-453.

Mestas, J. and Hughes, C.C. (2004) Of mice, not men: differences betweenmouse and human immunology. *Journal of Immunology* 172, 2731 - 2738.

Metcalfe, D.D., Bland, C.E. and Wasserman, S.I. (1984) Bicochemical and funcational characterisation of proteoglycans isolated from basophils of patients with chronic myelogenous leukemia. *Journal of Immunology,* 132 (4), 1943 - 1950.

Miyara, M., Yoshioka, Y., Kitoh, A., Shima, T., Wing, K., Niwa, A., Parizot, C., Taflin, C., Heike, T., Valeyre, D., Mathian, A., Nakahata, T., Yamaguchi, T., Nomura, T., Ono, M., Amoura, Z., Gorochov, G. and Sakaguchi, S. (2009) Functional delineation and differentiation dynamics of human CD4+ T cells expressing the FoxP3 transcription factor. *Immunity,* (30), 899 - 911.

Mochizuki, A., Mceuen, A.R., Buckley, M.G. and Walls, A.F. (2003a) The release of basogranulin in response to IgE-dependent and IgE-independent stimuli: Validity of basogranulin measurement as an indicator of basophil activation. *Journal of Allergy and Clinical Immunology,* 112, 102 - 108.

Mochizuki, A., Mceuen, A.R., Buckley, M.G. and Walls, A.F. (2003b) The release of basogranulin in response to IgE-dependent and IgE-independent stimuli: Validity of basogranulin measurement as an indicator of basophil activation. *Allergy and Clinical Immunology,* 112 (1), 102-108.

Morgan, D., Moodley, I., Phillips, M.J. and Daies, R.J. (1983) Plasma histamine in asthmatic and control subjects following exercise: influence of circulating basophils and different assay techniques. *Thorax,* 38, 771 - 777.

Muraro, A., Werfel2, T., Hoffmann-Sommergruber, K., Roberts, G.,et al. (2014) EAACI Food Allergy and Anaphylaxis Guidelines: diagnosis and management of food allergy. *Allergy,* 69, 1008 - 1025.

Murphy, K., Travers, P. and Walport, W. (2008) *Janeways Immunobiology*. Garland Science.

Neuman-Sunshine, D.L., Eckman, J.A., Keet, C.A., Matsui, E.C., Peng, R.D. and Lenehan, P.J. (2012) The natural history of persistent peanut allergy. *Annals of Allergy, Asthma and Immunology,* 108, 326 - 331.

Nivedita, N. and Papautsky, I. (2013) Continuous separation of blood cells in spiral microfluidic devices. *Biomicrofluidics,* 7 (5), 1 - 12.

Nopp, A., Johansson, S.G.O., Ankerst, J., Bylin, G., Cardell, L.O., GrçNneberg, R., Irander, K., Palmqvist, M. and ÖMan, H. (2006) Basophil allergen threshold sensitivity: a useful approach to anti-IgE treatment efficacy evaluation. *Allergy,* 61, 298 - 302.

Ohnmacht, C. and Voehringer, D. (2009) Basophil effector function and homeostasis during helminth infection. Blood 2009; 113:2816–25. *Blood,* 113, 2816-2825.

Pallaoro, M., Fejzo, M.S., Shayesteh, L., Blount, J.L. and Caughey, G.H. (1999) Characterization of genes encoding known and novel human mast cell tryptases on chromosome 16p13.3. *Journal of Biochemistry,* 274, 3355 - 3362.

Pirmohamed, M., Breckenridge, A.M., Kitteringham, N.R. and Park, B.K. (1998) Adverse drug reactions. *British Medical Journal,* 316 (Fortnightly review), 1295-1298.

Prussin, C. and Metcalfe, D.D. (2006) 5. IgE, mast cells, basophils, and eosinophils. *Allergy and Clinical Immunology,* 117 (2 Suppl Mini-Primer), S450-456.

Reimer, J.M., Magnusson, S., M. Juremalm, M., Nilsson, G., Hellman, L. and Wernersson, S. (2006) Isolation of transcriptionally active umbilical cord blood-derived basophils expressing FceRI, HLA-DR and CD203c. *Allergy,* 61, 1063 - 1070.

Reynolds, D.S., Stevens, R.L., Gurley, D.S., Lane, W.S., Austen, K.F. and Serafin, W.E. (1989) Isolation and Molecular Cloninogf Mast Cell CarboxypeptidaseA. *Journal of Biological Chemistry,* 264 (33), 20094-20099.

Ryan, W.L. and Wu, J., (2004) *Lysing Reagent and Method of Lysing Red Blood Cells for Hematology*. Organisation, E.P.

Sabroe, R.A., Francis, D.M., Barr, R.M., Black, A.K. and Greaves, M.W. (1998a) Anti-FcεRI autoantibodies and basophil histamine releasability in chronic idiopathic urticaria. *Journal of Allergy and Clinical Immunology,* 102 (4), 651-658.

Sabroe, R.A., Francis, D.M., Barr, R.M., Black, A.K. and Greaves, M.W. (1998b) Anti-FcεRI autoantibodies and basophil histamine releasability in chronic idiopathic urticaria. *Journal of Allergy and Clinical Immunology,* 102, 651 - 658.

Sabroe, R.A., T, S.P., Statb, C., Francis, D.M., Barr, R.M., Kobza Black, A. and Greaves, M.W. (1999) Chronic idiopathic urticaria: Comparison of the clinical features of patients with and without anti-FcεRI or anti-IgE autoantibodies. *Journal of the American Academy of Dermatology,* 40 (3), 443-450.

Saini, S.S., Macglashan, D.W.J., Sterbinsky, S.A., Togias, A., Adelman, D.C., Lichtenstein, L.M. and Bochner, B.S. (1999) Down-regulation of human basophil IgE and FC epsilon RI alpha surface densities and mediator release by anti-IgE-infusions is reversible in vitro and in vivo. *JOurnal of Immunology,* 162, 5624 - 5630.

Sainte-Laudy, J. (1998) Application of flow cytometry to the analysis of activation of human basophils. Immunologic validation of the method. *Allergie et Immunologie,* 30, 41 - 43.

Salter, B.M., Nusca, G., Tworek, D., Oliveria, J.P., Smith, S.G., Watson, R.M., Scime, T., Obminski, C., Sehmi, R. and Gauvreau, G.M. (2016) Expression of activation markers in circulating basophils and the rela- tionship to allergen-induced bron- choconstriction in subjects with mild allergic asthma. *Journal of Allergy and Clinical Immunology,* 137 (3), 936 - 938.

Sampson, H.A. (1999) Food allergy. part 2: diagnosis and management. *Journal of Allergy and Clinical Immunology,* 103, 981 - 989.

Santos, A.F., Douiri, A., Bécares, N., Wu, S., Stephens, A., Radulovic, S., Chan, S.M., Fox, A.T., Du Toit, G., Turcanu, V. and Lack, G. (2014) Basophil activation test discriminates between allergy and tolerance in peanut-sensitized children. *Journal of Allergy and Clinical Immunology,* 134, 645 - 652.

Santos, A.F., Douiri, A., Bécares, N., Wu, S.Y., Stephens, A., Radulovic, S., Chan, S.M.H., Fox, A.T., Du Toit, G., Turcanu, V. and Lack, G. (2014) Basophil activation test discriminates between allergy and tolerance in peanut-sensitized children. *Journal of Allergy and Clinical Immunology,* 134, 645 - 652.

Sanz, M.L., Sanchez, G., Gamboa, P.M., Vila, L., Uasuf, C., Chazot, M., Dieguez, I. and De Weck, A.L. (2001) Allergen-induced basophil activation: CD63 cell expression detected by flow cytometry in patients allergic to Dermatophagoides pteronyssinus and Lolium perenne. *Journal of Clinical and Experimental Allergy,* 31, 1007 - 1013.

Sarrafzadeh, O., Rabbania, H., Talebib, A. and Yousefi-Banaem, H. (2014) Selection of the best features for leukocytes classification in blood smear microscopic images. *Proceedings of SPIE - The International Society for Optical Engineering*.

Sato, S., Tachimoto, H., Shukuya, A., Kurosaka, N., Yanagida, N. and Utsunomiya , T. (2010) Basophil activation marker CD203c is useful in the diagnosis of hen's egg and cow's milk allergies in children. *International Archives of Allergy and Immunology,* 152, 54 - 61.

Schmida, L., Weitzb, D.A. and Franke, T. (2012) Sorting drops and cells with acoustics: Acoustic microfluidic fluorescent activated cell sorter. *Lab on a Chip,* 1, 1 - 8.

Schneider, T.W., Schessler, H.M., Shaffer, K.M., Dumm, J.M. and Younce, L.A. (2001) Surface Patterning and Adhesion of Neuroblastoma X Glioma (NG108-15) Cells. *Biomedical Microdevices,* 3 (4), 315-322.

Schulman, E.S., Kagey-Sobotka, A., Macglashan Jr, D.W., Adkinson Jr, N.F., Peters, S.P., Schleimer, R.P. and Lichtenstein, L.M. (1983) Heterogeneity of human mast cells. *Journal of Immunology,* 131 (4), 1936-1941.

Schwartz, L.B. (2006) Diagnostic value of tryptase in anaphylaxis and mastocytosis. *Journal of Immunology and Allergy of Clinics in North America,* 26, 451 - 463.

Schwartz, L.B., Austen, K.F. and Wasserman, S.I. (1981) Immunologic Release of β-Hexosaminidase and β-Glucuronidase from Purified Rat Serosal Mast Cells. *Journal of Immunology,* 123 (4), 1445-1450.

Schwartz, L.B., Irani, A.M., Roller, K., Castells, M.C. and Schechter, N.M. (1987) Quantitation of histamine, tryptase, and chymase in dispersed human T and TC mast cells. *Journal of Immunology,* 138 (8), 2611-2615.

Schwartz, L.B., Min, H., Ren, S., Xia, H., Hu, J., Zhao, W., Moxley, G. and Fukuoka, Y. (2003) Tryptase precursors are preferentially and spontaneously released, whereas mature tryptase Is retained by HMC-1 Cells, mono-mac-6 cells, and human skin-derived mast cells. *Journal of Immunology,* 170, 5667 - 5673.

Schwartz, L.B., Yunginger, J.W. and Miller, J.S. (1989a) The time course of appearance and disappearance of human mast cell tryptase in the circulation after anaphylaxis. *83,* Journal of Clinical Investigation (1551 - 1555).

Schwartz, L.B., Yunginger, J.W. and Miller, J.S. (1989b) The time course of appearance and disappearance of human mast cell tryptase in the circulation after anaphylaxis. *Journal of Clinical Investigation,* 83, 1551 - 1555.

Sekula-Neuner, S., Maier, J., Oppong, E., Cato, A.C.B., Hirtz, M. and Fuchs, H. (2012) Allergen Arrays for Antibody Screening and Immune Cell Activation Profiling Generated by Parallel Lipid Dip-Pen Nanolithography. *Small Journal*, 1-7.

Settipane, R.A. and Charnock, D.R. (2006) Epidemiology of Rhinitis: Allergic and Nonallergic *Nonallergic Rhinitis*. 12.

Shamji, M., Layhadi, J.A., Scadding, G.W., Cheung, D.K.M., Calderon, M.A., Turka, L.A., Phipphard, D. and Durham, S.R. (2015) Basophil expression of diamine oxidase: A novel biomarker of allergen immunotherapy response. *J Allergy Clin Immunol,* 135 (4), 913-921.

Shiratori, I.E.A. (2005) Down-regulation of basophil function by human CD200 and human herpesvirus-8 CD200. *Journal of Immunology,* 175, 4441-4449.

Simons, F.E., Frew, A.J., Ansotegui, I.J., Bochner, B.S., Golden, D.B. and Finkelman, F.D. (2007a) Risk assessment in anaphylaxis: current and future approaches. *Journal of Allergy and Clinical Immunology* 120, S2–24. .

Simons, F.E.R., Frew, A.J., Ansotegui, I.J., Bochner, B.S., Golden, D.B.K., Finkelman, F.D. and Walls, A.F. (2007b) Risk assessment in anaphylaxis: current and future approaches. *The Journal of Allergy and Clinical Immunology,* 120, S2-24.

Siracusa, M.C., Kim, B.S., Spergel, J.M. and Artis, D. (2013) Basophils and allergic inflammation. *Journal of Allergy and Clinical Immunology* 132 (4), 789-788.

Sollier, E., Murray, C., Maoddi, P. and Di Carlo, D. (2011) Rapid prototyping polymers for microfluidic devices and high pressure injection. *Lab Chip,* 11, 3752-3765.

Songjaroen, T., Dungchai, W., Chailapakul, O., Henrye, C.S. and Laiwattanapaisa, W. (2012) Blood separation on microfluidic paper-based analytical devices. *Lab on a Chip,* 12, 3392 - 3398.

Stevens, R.L., Fox, C.C., Lichtenstein, L.M. and Austen, K.F. (1988) Identification of chrondroitin sulphate e-proteoglycans and heparin proteoglycans in the secretory granules of human-lung mast cells. *Proceedings of the National Academy of Sciences of the USA,* 85 (7), 2284 - 2287.

Stone, H.A., Stroock, A.D. and Ajdari, A. (2004) Engineering Flows in Small Devices. *Annual Review of Fluid Mechanics,* 36 (1), 381-411.

Stone, K.D., Prussin, C. and Metcalfe, D.D. (2010) IgE, mast cells, basophils, and eosinophils. *Journal of Allergy and Clinical Immunology,* 125, S73 - S80.

Takabayashi, T., Kato, A., Peters, A.T., Suh, L.A., Carter, R. and Norton, J. (2012) Glandular mast cells with distinct phenotype are highly elevated in chronic rhinosinusitis with nasal polyps. *Journal of Allergy and Clinical Immunology* 130 (2), 410 - 420.

Tanno, L.K., Calderon, M.A., Li, J., Casale, T. and Demoly, P. (2016) Updating Allergy and/or Hypersensitivity Diagnostic Procedures in the WHO ICD-11 Revision. *Journal of allergy and clinical immunological practices,* 4 (4), 650-657.

Thong, B.Y. and Tan, T.C. (2011) Epidemiology and risk factors for drug allergy. *British Journal of Clinical Pharmacology,* 71 (5), 684-700.

Tsujimura, Y., Obata, K., Aori Mukai, K., Shindou, H., Yoshida, M., Nishikado, H., Kawano, Y., Minegishi, Y., Shimizu, T. and Karasuyama, H. (2008) Basophils Play a Pivotal Role in Immunoglobulin-G-Mediated but Not Immunoglobulin-E-Mediated Systemic Anaphylaxis. *Immunity,* 28 (4), 581-589.

Uzzaman, A. and Cho, S.H. (2012) Classification of hypersensitivity reactions. *Allergy & Asthma Proceedings,* 33, 96 - 99.

Von Pirquet, C. (1906) Allergie. *Munchen Med Wchnschr,* 53, 1457 - 1458.

Wao (2011) *WAO White Book on Allergy*. World Allergy Organisation.

Warner, J.O., Kaliner, M.A., Crisci, C.D., Giacco, S.D., Frew, A.J., Gh, L., Maspero, J., Moon, et al. (2006) Allergy Practice Worldwide: A Report by the World Allergy Organization Specialty and Training Council. *Allergy and Clinical Immunology,* 18 (1).

Wasserman, S.I. (1983) Mediators of hypersensitivity. *Journal of Allergy and Clinical Immunology,* 72 (2), 101-115.

Whitesides, G.M. (2006) Overview the origins and the future of microfluidics. *Nature,* 442, 368 - 373.

Wood, R.A., Kim, J.S., Lindblad, R., Nadeau, K., Henning, A.K., Dawson, P., Plaut, M. and Sampson, H.A. (2016) A randomized, double-blind, placebo-controlled study of omalizumab combined with oral immunotherapy for the treatment of cow's milk allergy. *Journal of Allergy and Clinical Immunology,* 137 (4), 1103 - 1110.

Wu, L., Guan, G., Hou, H.W., Bhagat, A.A. and Han, J. (2012a) Separation of leukocytes from blood using spiral channel with trapezoid cross-section. *Analytical Chemistry,* 84, 9324 - 9331.

Wu, L., Guan, G., Hou, H.W., Bhagat, A.A. and Han, J. (2012b) Separation of leukocytes from blood using spiral channel with trapezoid cross-section. *Anal Chem,* 84 (21), 9324-9331.

Xia , N., Hunt, T.P., Mayers, B.T., Alsberg, E., Whitesides, G.M., Westervelt, R.M. and Ingber, D.E. (2006) Combined microfluidic-micromagnetic separation of living cells in continuous flow. *Biomed Devices,* 8, 299–308.

Yu, Q., Zhang, Y., Chen, H., Zhou, F., Wu, Z., Huang, H. and Brash, J.L. (2010) Protein Adsorption and Cell Adhesion/Detachment Behavior on Dual-Responsive Silicon Surfaces Modified with Poly(N-isopropylacrylamide)-block-polystyrene Copolymer. *Langmuir,* 26 (11), 8582-8588.

Zhang, C.Z. and Andreas Manz, A. (2003) High-Speed Free-Flow Electrophoresis on Chip. *Analytical Chemistry,* 75 (21), 5759–5766.